Evaluating the Optimal *In Vitro* Transport Conditions for PBPK Modeling of OAT1 Involvement in Renal Drug Clearance

by

Aaron O. Buaben

Submitted in partial fulfilment of the requirements
for the degree of Master of Science

at

Dalhousie University
Halifax, Nova Scotia
April 2018

TABLE OF CONTENTS

LIST OF TABLES

LIST OF FIGURES

ABSTRACT

Predicting pharmacokinetics of drug transporter substrates using PBPK modeling requires accurate transport kinetics *in vitro*. It is unclear what effect incubation time has on transport kinetics under initial *zero-trans* conditions. In this study, the influence of incubation time on OAT1 transport kinetics and its influence on PBPK predictions was examined. The *in vitro* intrinsic uptake clearance (CL_{int}) of *para*-aminohippurate (PAH) by OAT1 stably expressed in CHO cells was determined at different time points, from initial-rate to steady-state, under *zero*-trans or equilibrium exchange conditions. The Simcyp Simulator was used to simulate PAH pharmacokinetics using the different CL_{int} values obtained. The data show that transport kinetics and inhibition potency are both influenced by the *in vitro* incubation time used. This results in modest to large differences in PBPK predictions in the involvement of OAT1 in pharmacokinetics and DDIs.

LIST OF ABBREVIATIONS USED

A-B	Apical-to-basolateral
ABC	ATP-binding cassette
ADME	Absorption, distribution, metabolism and excretion
AhR	Aryl hydrocarbon receptor
AUC	Area under the plasma concentration-time curve
B-A	Basolateral-to-apical
BCRP	Breast cancer resistance protein
Caco-2	Human colon epithelial cancer cell line
CAR	Constitutive androstane receptor
CHO	Chinese hamster ovary
Ci	Curie
CIPTEC	Conditionally immortalized human proximal tubular epithelial cells
CL_{int}	Intrinsic clearance
Da	Dalton
2-D	Two-dimensional
3-D	Three-dimensional
DDI	Drug-drug interaction
DMPS	2,3-dimercapto-1-propanesulfonic acid
ER	Efflux ratio
FXR	Farnesoid X receptor
^{3}H	Tritium

HEK293	Human embryonic kidney 293 cell line
IC_{50}	Half maximal inhibitory concentration
$I_{u,max}$	Maximum, unbound plasma concentration of inhibitor
IVIVE	In vitro-to-in vivo extrapolation
J_{max}	Maximal rate of transport
α-KG	α-ketoglutarate
K_i	Inhibition constant
K_m	Michaelis constant
LC-MS	Liquid chromatography-mass spectrometry
LLC-PK1	Lewis-lung cancer porcine kidney 1 cell
MDCK	Madin-Darby canine kidney cell
MRP	Multidrug resistance-associated proteins
NaDC	Sodium dicarboxylate co-transporter
NME	New molecular entity
NPT	Sodium phosphate co-transporter
NSAIDs	Non-steroidal anti-inflammatory drugs
OAT	Organic anion transporter
OATP	Organic anion transporting polypeptide
PAH	*p*-Aminohippuric acid
PBPK	Physiologically based pharmacokinetic
P_i	Inorganic phosphate
PK	Pharmacokinetics
PTCPGK	Proximal tubule cell number per gram kidney

PXR	Pregnane X receptor
RAF	Relative activity factor
REF	Relative expression factor
RPT	Renal proximal tubular cell
SLC	Solute carrier
SNP	Single nucleotide polymorphism

ACKNOWLEDGEMENTS

I would like to thank my supervisor, Dr. Ryan Pelis, for his patient guidance, motivation and advice he provided me throughout my time as his student. I have been extremely lucky to have a supervisor who not only cared about my work but also cared about my general well-being. I would never forget the kind gesture he extended to me by picking me up from the airport when I first arrived in Halifax and making sure I had a place to stay. As my mentor, he responded to my questions and challenged me to think outside the box. Most importantly, he has taught me more than I can give him credit for. My time with Dr. Pelis has been a great learning experience.

I am grateful to my advisory committee, Dr. Kerry Goralski and Dr. Melanie Kelly, for the thoughtful feedback given to me throughout my research and during the writing of my thesis. I would also like to extend my appreciation to Dr. Kerry Goralski, once again, and Dr. Christopher McMaster for their willingness to read these countless pages and examine my thesis.

Completing this work would have been all the more difficult were it not for the friendship and support provided me by Luisa Vaughan, Sandi Leaf and Cheryl Bailey, in the department of Pharmacology. I am grateful to them for helping me with all the necessary administrative tasks.

I would also like to say a big thank you to my lovely wife for all the support during my time away from home. I couldn't have achieved this without her support.

Finally, I would like to thank Dr. Pelis and the department of Pharmacology for providing the funding which allowed me to undertake this research, as well as contributing to my monthly stipend.

CHAPTER 1 INTRODUCTION

1.1 Introduction

The kidneys play an important role in the elimination of many therapeutic drugs from the body that are negatively charged at physiologic pH, that is, organic anions – henceforth referred to as anionic drugs. Importantly, many clinically relevant therapeutic drugs, including antibiotics, chemotherapeutics, antiviral agents and nonsteroidal anti-inflammatory drugs (NSAIDs) are anionic drugs (Rizwan & Burckhardt, 2007). For many small molecular weight anionic drugs, their urinary excretion is mediated via tubular secretion by transporters that are localized in the basolateral and apical membranes of renal proximal tubule cells (RPTs) (Pelis & Wright, 2011). Tubular secretion is an important determinant of anionic drug half-life and systemic concentration, is a site of drug-drug interactions (DDIs), and for potentially hazardous drugs, may favour their accumulation into RPTs, leading to nephrotoxicity (George et al., 2017; Morrissey et al., 2013). Of the top 200 prescribed drugs that are predominately eliminated by the kidney, >90% are actively secreted by transporter-mediated tubular secretion (Morrissey et al., 2013), underscoring the importance of renal transporters in drug elimination. DDIs involving drug metabolism has been widely recognized for years. DDIs involving transporters is becoming more recognized, and is gaining greater interest from pharmaceutical companies and regulatory agencies for safety testing during drug development (Bickel et al., 2013; Kirby et al., 2012; Konig et al., 2013).

Transport proteins involved in renal tubular secretion belong to one of two major protein families – namely, the solute carrier (SLC) and ATP binding cassette (ABC) families. SLC transporters that interact with therapeutic drugs facilitate membrane transport from energy derived from electrochemical gradients, and include transport mechanisms involving co-transport, exchange and facilitated diffusion. Depending on the prevailing electrochemical gradients, SLC transporters can facilitate cellular substrate uptake or efflux. On the other hand, ABC transporters always support cellular substrate efflux, as they are ATPases that hydrolyze intracellular ATP to ADP as their energetic mechanism (Otani et al., 2017; Pelis & Wright, 2014). SLC and ABC transporters work in parallel (opposing membranes) and series (same membrane) of renal epithelial cells to support tubular secretion of drugs from blood to the glomerular filtrate – of interest to my studies are renal transporters that handle anionic drugs, so this is where I will primarily focus (**Figure 1.1**). The major renal transporters involved in tubular anion drug secretion include, organic anion transporters 1, 2 and 3 (OAT1, OAT2 and OAT3), organic anion transporting polypeptide 4C1 (OATP4C1), the multidrug resistance-associated proteins 2 and 4 (MRP2 and MRP4), and the breast cancer resistance protein (BCRP). The first step in tubular secretion, which involves uptake of anionic drugs from blood into RPTs, is mainly mediated by SLC transporters, including OAT1, OAT2, OAT3 and OATP4C1 (Otani et al., 2017; Pelis & Wright, 2014). Subsequent efflux of drug from RPTs into the tubular filtrate largely involves ABC transporters, including MRP2 and MRP4 (Smeets et al., 2004), and BCRP (Huls et al., 2008), and possibly P-glycoprotein as well. SLC transporters, such as the sodium-phosphate co-transporters (NPT1 and NPT4), may contribute to efflux of some anionic drugs from RPTs (Ivanyuk et al., 2017; Jutabha et

al., 2010). There are also several other apically-located SLC transporters that have been implicated in efflux of anionic drugs into the tubular filtrate, but because of limited evidence of their importance in renal anionic drug elimination from the body, they are not discussed here.

Like drug metabolizing enzymes, drug transporters interact with ligands having diverse physicochemical properties, making these transporters a DDI liability. (Astorga et al., 2011; Konig et al., 2013; Mao & Unadkat, 2015). In this case, a ligand could be a translocated substrate or a non-translocated substrate, both of which could compete as inhibitors with other ligands for the ligand binding region. Consequently, renal tubular secretion of one drug (victim drug) could be altered when its transporter-mediated translocation across the membrane is influenced by another drug (perpetrator) (Konig et al., 2013). Due to increasing reports of clinically relevant transporter-mediated DDIs, the US Food and Drug Administration (FDA) and European Medicines Agency (EMA) have developed protocols to guide the evaluation of the interaction of new molecular entities (NMEs) with relevant transporters (European Medicines Agency, 2012; US Food Drug Administration, 2017). Of the top 200 prescribed drugs that undergo renal tubular secretion, many are ligands of renal anionic drug transporters: OAT1 (28%), OAT3 (41%), MRP2 (22%) and MRP4 (19%) (Morrissey et al., 2013). These statistics highlight the importance of these transporters in renal drug disposition and DDIs.

Discussed in this literature review are the expression and localization of the major transporters important for renal elimination of anionic drugs from the body, their mechanisms and energetics of transport, their role in pharmacokinetics (PK) and DDIs,

techniques used to evaluate the interaction of NMEs with transporters and how *in vitro* transport kinetic data are used to guide clinical drug development.

1.2 Transepithelial Secretion of Organic Anions in the Human Kidney

Renal tubular secretion of anionic drugs consists of two steps involving the concerted activity of SLC and ABC drug transporters (**Figure 1.1**) (Moller & Sheikh, 1982; Otani et al., 2017; Russel et al., 2002). The first step is uptake across the basolateral membrane (also known as the peritubular membrane) from blood-to-cell, a process mediated in large part by OAT1 and OAT3. OATP4C1 and OAT2 have also been implicated in basolateral drug uptake, although less is known about their clinical relevance to PK (Lepist et al., 2014; Toyohara et al., 2009). The second and final step is efflux across the apical membrane (also known as the brush border membrane) from cell-to-tubule lumen (i.e., glomerular filtrate), a process thought to be mediated primarily by the ABC transporters, MRP2, MRP4 and BCRP (Ivanyuk et al., 2017; Morrissey et al., 2013; Nigam et al., 2015). SLC transporters including the Na-phosphate transporters (NPT1, NPT4) and the organic anion transporter 4 (OAT4) may also contribute to apical efflux of anionic drugs (Ivanyuk et al., 2017; Jutabha et al., 2010). Transport experiments with single perfused proximal tubules and kidney slices suggest that basolateral uptake is the rate-limiting step in active tubular anionic drug secretion (Chatsudthipong & Dantzler, 1991; Chatsudthipong & Dantzler, 1992; Watanabe et al., 2009). Preloading the tubules with α-ketoglutarate (α-KG), a preferred counter ion for OAT anion exchange,

resulted in increased tubular uptake of *p*-aminohippurate (PAH), but most importantly a three to six-fold increase in the net tubular secretion rate of PAH (Chatsudthipong & Dantzler, 1991; Chatsudthipong & Dantzler, 1992). Studies in rats have further shown that for minimally metabolized anionic drugs, their renal clearance and fraction excreted in urine can be predicted from the tissue uptake clearance determined from uptake studies conducted with kidney slices (Watanabe et al., 2009).

1.3 Basolateral Uptake Transporters in the Human Kidney

1.3.a Expression and Localization

In humans, OAT1, OAT2 and OAT3 localize to the basolateral membrane of RPT cells of the kidney cortex (Breljak et al., 2016; Hosoyamada et al., 1999; Motohashi et al., 2002; Pelis & Wright, 2014; Wright & Dantzler, 2004). In comparison to OAT1 and OAT3, the expression of OAT2 in the renal cortex appears to be relatively low (El-Sheikh et al., 2008; Rizwan & Burckhardt, 2007; Wright & Dantzler, 2004), and its subcellular localization is apparently species-dependent (Pelis & Wright, 2014; Wright & Dantzler, 2004). In humans, OAT2 localizes to basolateral membranes of RPT cells (Breljak et al., 2016; Enomoto et al., 2002; Pelis & Wright, 2014), but in rats and mice, it is expressed in apical membranes (Brzica et al., 2009; Ljubojevic et al., 2007; Pelis & Wright, 2014). Studies indicate that OAT1 is more widely distributed along the length of the proximal tubule than OAT3 (Motohashi et al., 2002; Wright & Dantzler, 2004).

However, other studies have shown that OAT1, OAT2 and OAT3 have a similar localized distribution – namely, that they are mostly in S1 and S2 segments of the renal proximal tubule, but not in S3 segments in the outer stripe or other nephron segments (Breljak et al., 2016).

There are conflicting reports regarding the mRNA expression levels of OAT1, OAT2 and OAT3 in the human kidney cortex. Using kidney cortex from 7 donors, Motohashi et al. (Motohashi et al., 2002) showed a 3-fold higher expression of OAT3 than OAT1, and levels of OAT2 were only 5-10% that of OAT1, i.e. OAT3 > OAT1 > OAT2. Another study using kidney cortex from 8 human donors showed that the expression of OAT3 was highest, and levels of OAT2 and OAT1 were approximately equal, i.e., OAT3 > OAT1 ≈ OAT2 (Cheng et al., 2012). A third study using kidney cortex obtained from 57 human donors revealed that OAT1 transcripts were more abundant (~ 3-fold) than OAT3; that is, OAT1 > OAT3 (Morrissey et al., 2013). The larger number of samples analyzed in this study provide a more robust data set on the expression of these transporters. However, it is important to note that mRNA levels do not necessarily reflect functional protein levels of these transporters. When kidney cortex samples were analyzed for OAT2 mRNA (qPCR) and protein (immunoblotting) levels, mRNA levels showed large inter-individual variability (~17-fold), whereas protein levels were less variable (3-fold) (Cheng et al., 2012), indicating that mRNA and protein levels are not necessarily reflective of each other.

OATP4C1, a relatively novel uptake transporter, is expressed in the kidney, however, there is no direct evidence of its subcellular localization in human kidney (Bleasby et al., 2006). Consequently, there are discrepancies in literature regarding its

subcellular localization in human kidney. Mikkaichi et al reported that in rat kidney, Oatpc4c1 localizes to the basolateral membrane of RPT cells (Mikkaichi et al., 2004). Toyohara et al subsequently showed that human OATP4C1 localizes to the basolateral membrane of RPT cells in transgenic rats (Toyohara et al., 2009). Consistent with the basolateral expression of OATP4C1, Toyohara and colleagues demonstrated in a renal failure model that uremic toxin plasma concentrations were decreased in human OATP4C1-transgenic rats, when compared to wild-type rats, suggesting a role of OATP4C1 in basolateral uptake of uremic toxins and subsequent efflux by an apically expressed transporter (Toyohara et al., 2009). In contrast to these findings, Kuo et al showed that rat Oatp4c1 is expressed in the apical membrane of RPT cells, where it may be involved in reabsorption of substrates from the tubular filtrate (Kuo et al., 2012).

1.3.b Mechanism and Energetics of Transport

Cellular uptake of anionic drugs by OAT1 and OAT3 at the basolateral membrane occurs by a tertiary active process involving Na^+-K^+-ATPase and the Na^+-dicarboxylate co-transporters 1 (NaDC1) and 3 (NaDC3) (**Figure 1.2**) (Breljak et al., 2016; Pelis & Wright, 2014; Russel et al., 2002). The rate of PAH uptake in OAT1-expressing oocytes did not change upon replacement of extracellular sodium with lithium or choline, indicating that OAT1 and OAT3 -mediated uptake is sodium-independent (Sekine et al., 1997; Sweet et al., 2003). Although OAT1 and OAT3 are Na^+-independent anion exchangers, uptake of substrate mediated by both is indirectly coupled to the inwardly-directed Na^+ gradient maintained by Na^+-K^+-ATPase (Pritchard, 1988; Sekine et al.,

1997; Sweet et al., 2003). In this mechanism, OAT-mediated substrate uptake occurs in exchange for intracellular α-ketoglutarate (α-KG, Kreb's cycle intermediate), the most abundant dicarboxylate in renal tubule cells, and the preferred physiological counter ion of OAT1 and OAT3 (Chatsudthipong & Dantzler, 1992; Kaufhold et al., 2011; Pritchard & Miller, 1993). Kaufhold et al demonstrated that although the dicarboxylate succinate accumulates intracellularly via NaDC3, it may not be the preferred counter ion for OAT1 and OAT3-mediated exchange as it has a low affinity for OAT1 and OAT3 (Kaufhold et al., 2011). The high intracellular α-KG concentration and hence its steep outwardly-directed gradient is maintained through intracellular metabolic generation as well as the activity of NaDC3 and NaDC1, which occur at the basolateral and apical membranes, respectively (Pritchard, 1995; Russel et al., 2002; Wright & Dantzler, 2004). The Na^+ gradient generated by Na^+-K^+-ATPase provides the energy to support the influx of α-KG into tubule cells on NaDC1 and NaDC3 via Na^+-αKG cotransport (El-Sheikh et al., 2008; Wright & Dantzler, 2004). Static-head experiments with rat basolateral membrane vesicles has shown that the exchange of the monocarboxylate PAH for the dicarboxylate α-KG is 1:1, and therefore, in the case of PAH/α-KG the translocation process is electrogenic (Aslamkhan et al., 2003). In support of this conclusion, exchange of PAH for the dicarboxylate glutarate in current-clamped *Xenopus* oocytes expressing OAT1 was accompanied by a net entry of positive charge (Aslamkhan et al., 2003). A different study using current-clamped *Xenopus* oocytes showed that the exchange of extracellular glutarate (dicarboxylate) for intracellular α-KG (dicarboxylate) resulted in a lack of voltage change, suggesting that dicarboxylate/dicarboxylate exchange is electroneutral (Burckhardt et al., 2000). Overall, the results of these studies show that the stoichiometry

of OAT1 is 1:1, and can be either electroneutral or electrogenic depending on the translocated molecules at the *cis*- and *trans*-face of the transporter. The stoichiometry of the other OATs remains unknown.

OAT2, like OAT1 and OAT3, is a sodium-independent organic anion/dicarboxylate exchanger. Uptake of PAH into *Xenopus* oocytes expressing OAT2 was not influenced by replacement of extracellular sodium with lithium, choline or mannitol (Kobayashi et al., 2005). In contrast to OAT1 and OAT3, glutarate and α-KG failed to *trans*-stimulate cGMP uptake into OAT2-expressing HEK293 cells (Henjakovic et al., 2015). However, preload experiments demonstrated that the dicarboxylates fumarate or succinate can serve as counter ions for OAT2-mediated estrone-3-sulfate transport (Kobayashi et al., 2005).

OATP4C1 mediates the unidirectional uptake of its substrates, albeit its energetics of transport are not clearly understood (Kuo et al., 2012; Leuthold et al., 2009; Mikkaichi et al., 2004). There are discrepancies in the literature regarding the effect of pH on OATP4C1-mediated transport. Mikkaichi et al reported a pH-independent effect on OATP4C1-mediated transport. However, Leuthold and colleagues demonstrated a pH-dependent effect on OATP4C1-mediated transport of thyroxine or estrone-3-sulfate (Mikkaichi et al., 2004; Leuthold et al., 2009). Extracellular sodium does not affect OATP4C1-mediated transport, indicating that OATP4C1-mediated transport occurs in a Na^+-independent manner (Mikkaichi et al., 2004). Unlike other members of the OATP family, OATP4C1 has two potential ATP binding sites (Walker motif A) (Mikkaichi et al., 2004). However, according to results from an ATP-depletion assay in Madin-Darby canine kidney (MDCK) cells expressing OATP4C1, ATP depletion did not have a

significant effect on triiodothyroxine uptake, suggesting that ATP may not be a direct driving force for OATP4C1-mediated transport (Mikkaichi et al., 2004).

1.3.c Ligand Selectivity

The renal tubular organic anion secretory system is important for transporting a broad range of physiologically, toxicologically and pharmacologically relevant molecules with diverse physicochemical properties. Several clinically relevant drugs, including NSAIDs, loop and thiazide diuretics, antivirals, beta lactam antibiotics, angiotensin converting enzyme inhibitors and methotrexate are ligands of OATs (**Table 1.1**) (Ahn & Bhatnagar, 2008; Burckhardt & Burckhardt, 2011; Otani et al., 2017; You, 2008). OATs display broad ligand selectivity because they contain multiple ligand binding regions with distinct structural differences (Astorga et al., 2011; Pelis & Wright, 2014). Generally, OAT1 has a higher affinity for small molecular weight, hydrophilic anionic drugs while OAT3 mostly transports bulky amphipathic anionic drugs, including, glucuronide conjugates (Ivanyuk et al., 2017; Pelis & Wright, 2014). Although OAT1 and OAT3 have overlapping ligand selectivity in many cases, there are many cases where they differ. For example, the affinity of PAH (a diagnostic marker of renal plasma flow) for OAT1 is approximately 10 times greater than that of OAT3 (Cha et al., 2001; Hosoyamada et al., 1999). Cidofovir, is a relatively specific substrate of OAT1 (Uwai et al., 2007), whereas bumetanide is relatively specific for OAT3 (Hasannejad et al., 2004).

Ligands of OATs exist primarily as anions at physiological pH, however, neutral and basic (cationic) molecules may also interact with these transporters. OAT1 and OAT3 transport the weak base cimetidine, as well as the neutral creatinine (Ahn et al., 2009; Cha et al., 2001; Nigam et al., 2015; Vallon et al., 2012; Wright & Dantzler, 2004). OAT2 also transports creatinine and is suggested to play a substantial role in its tubular secretion (Lepist et al., 2014; Shen et al., 2015). While OAT1 has a fairly restricted ability to transport cations, OAT3 tends to interact more with cations and zwitterions, yet, both are known to be important for anionic drug transport (Varma et al., 2017).

Homology models of mammalians OATs have proven useful in identifying amino acid residues that contribute to homolog-specific selectivity and have improved understanding of the molecular basis of ligand interactions with OATs. Based on the homology model of OAT1, the amino acids tyrosine at position 230 (tyr230), arginine at position 466, lysine at position 431 and phenylalanine at position 438 are implicated in ligand binding and translocation (Perry et al., 2006). Consistent with the multi-selectivity of OATs, mutation of tyr230 in OAT1 eliminates PAH transport but not cidofovir transport, indicating the OAT1 contains multiple ligand-binding regions (Perry et al., 2006).

Structural differences in the ligand binding regions as well as distinct physicochemical characteristics of ligands influence the binding preferences of OATs. There is evidence that cysteine residue at position 440 (cys440) of OAT1 is more accessible from the extracellular space than the homologous cys428 of OAT3 (Astorga et al., 2011). Studies showed that OAT1 was more sensitive to inhibition with membrane-impermeable thiol-reactive agents than OAT3 (Astorga et al., 2011). However, after

mutation of cys440 to alanine, OAT1 was less sensitive to inhibition (Astorga et al., 2011). Studies examining the inhibitory effect of the clinically important heavy metal chelator 2,3-dimercapto-1-propanesulfonic acid (DMPS) and its structural congeners revealed that molecular size is an important determinant for binding to OAT1 and OAT3. Removal of a single thiol group from DMPS attenuated its inhibition potency towards OAT1 and OAT3, whereas removal of both thiol groups effectively eliminated the inhibitory effect on both transporters (Astorga et al., 2011).

Whereas the ligand selectivity of OAT1 and OAT3 appear conserved across species (for the most part), OAT2 shows significant species-dependent ligand selectivity (El-Sheikh et al., 2008; Ljubojevic et al., 2007). For example, salicylate, a classical substrate for rat *Oat2*, is not transported by human OAT2 (Rizwan & Burckhardt, 2007).

The ligand selectivity of OATP4C1 has not been characterized in detail. OATP4C1 substrates include cardiac glycosides (digoxin, ouabain) and methotrexate. It also transports sitagliptin (Chu et al., 2007; Mikkaichi et al., 2004; Yamaguchi et al., 2010).

1.4 Apical Efflux Transporters in the Human Kidney

1.4.a Expression and Localization

Several transporters in the ABC family have been implicated in mediating the apical efflux of anionic drugs from cell-to-glomerular filtrate. MRP2 and MRP4 are the major multidrug resistance-associated proteins expressed in the human kidney, where they localize to apical membranes of RPTs (Denk et al., 2004; Robertson & Rankin, 2006; van Aubel et al., 2002; van de Water et al., 2005). Two studies have examined the mRNA expression levels of MRP2 and MRP4 relative to one another. One study showed the mRNA expression of MRP4 to be approximately five times higher than that of MRP2 (Smeets et al., 2004). The other study suggested equal expression level of both transporters in the kidney cortex (Morrissey et al., 2013).

BCRP is localized to the apical membrane of RPTs in human kidney but it is expressed at lower levels than in rodent kidneys (Huls et al., 2008). Studies reported low mRNA expression levels of BCRP in human kidney but failed to detect the transporter protein itself (Doyle & Ross, 2003; Maliepaard et al., 2001). Consistent with its low expression levels in human kidney, another study confirmed the low mRNA expression of BCRP and, unlike previous findings, established that low levels of the BCRP protein are expressed in the human kidney (Huls et al., 2008). Aside from ABC transporters (MRP2, MRP4 and BCRP) that localize to apical membrane of RPTs, several SLC transporters (NPT1, NPT4 and OAT4) have been localized to apical membranes and may

play a role in apical efflux, albeit, much less is known about their involvement in the renal tubular anionic drug secretory system (Babu et al., 2002; El-Sheikh et al., 2008).

1.4.b Mechanism and Energetics of Transport

ABC transporters, including MRP2, MRP4 and BCRP are primary active efflux pumps which utilize energy derived from ATP hydrolysis to drive efflux of substrates from RPTs into the tubule lumen (Otani et al., 2017; Pelis & Wright, 2014; Robertson & Rankin, 2006). An understanding of the mechanism and energetics of transport mediated by these efflux transporters comes from homology models and the basic structure of ABC transporters. The basic structure of ABC transporters comprises membrane-spanning domains (consisting of transmembrane α-helices, TMHs) and cytoplasmic nucleotide-binding domains (NBDs), which contain characteristic sequence motifs that bind and hydrolyse ATP (Jani et al., 2014; P. Jones & George, 2014; Linton & Higgins, 2007). The TMHs form a channel which contains multiple ligand-binding sites, and through which substrates are translocated across the membrane. Substrate translocation is a multistep process which begins with substrate binding to an inward-facing conformation of the transporter, accessible from the cytoplasm, followed by conformational changes in the transporter that allow substrate to be released on the extracellular side of the membrane (Jani et al., 2014; Jones & George, 2014; Linton & Higgins, 2007; Slot et al., 2011). The processes that follow substrate binding are obligatorily coupled to the binding of ATP to the nucleotide binding site on the transporter, and its hydrolysis to ADP and inorganic phosphate (*Pi*).

OAT4 is an organic anion exchanger, and has been shown to use glutarate, chloride (Cl^-) or urate as counter ions to facilitate anionic drug transport (Hagos et al., 2007; Ekaratanawong et al., 2004; Noguchi et al., 2015). Studies suggest that OAT4 may participate in both tubular secretion and/or reabsorption of anionic drugs from the tubular filtrate depending on the prevailing electrochemical gradients (Ekaratanawong et al., 2004; Hagos et al., 2007). The efflux of olmesartan from T-REx-OAT4-293 cells (tetracyline-inducible human OAT4-expressing cell line) was stimulated by an inwardly-directed gradient of Cl^- at high extracellular Cl^- concentration, whereas the OAT4-mediated uptake was enhanced by an outwardly-directed Cl^- gradient at lower extracellular Cl^- concentrations (Noguchi et al., 2015). Similarly, both the uptake and efflux of PAH in mouse proximal tubular cells expressing OAT4 was *trans*-stimulated by glutarate (Ekaratanwong et al., 2004). Because, for some anionic drugs, OAT4 displays different substrate recognition characteristics on the intracellular versus the extracellular side, OAT4-mediated transport has been proposed to occur in an asymmetric manner (Hagos et al., 2007). In this way, OAT4 solely facilitates excretion into urine or the reabsorption of anionic drugs from the tubular filtrate. Intracellular hydrochlorothiazide *trans*-stimulated urate uptake in OAT4-expressing human embryonic kidney cells (HEK293-OAT4). However, extracellular hydrochlorothiazide had no significant effect on urate uptake via OAT4. This suggests little interaction of hydrochlorothiazide with OAT4 from the extracellular side and represents a one-way efflux of hydrochlorothiazide via anion drug/ urate exchange (Hagos et al., 2007). On the other hand, OAT4 may solely facilitate reabsorption of anionic drugs from urine. Studies revealed that OAT4 is involved in the cellular uptake, but not efflux, of estrone-3-sulfate and levocetirizine

(Noguchi et al., 2017; Ekaratanawong et al., 2004). NPT1 and NPT4 operate via electrogenic facilitated diffusion driven by the inside negative membrane potential (Jutabha et al., 2010; Uchino et al., 2000).

1.4.c Ligand Selectivity

ABC transporters have broad ligand selectivity because they possess multiple ligand binding sites formed by the TMHs (Mao & Unadkat, 2015). Ligands that interact with MRPs are primarily amphiphilic anionic drugs with an approximate molecular weight between 300 and 1000 Da (Keppler, 2011). MRP2, sometimes referred to as "the apical conjugate export pump", is largely involved in the transport of conjugated anionic drugs, including glucuronide and glutathione conjugates (Konig et al., 1999). However, some unconjugated anionic drugs, including methotrexate and PAH are substrates as well (Konig et al., 1999). PAH, a model substrate of the renal tubular organic anion secretory system is a low-affinity substrate of MRP2 (Leier et al., 2000; van Aubel et al., 2000). However, MRP2 interacts with conjugated ligands with a higher affinity than unconjugated ligands, and hence, may be more important in the elimination of anionic drug conjugates than unconjugated anionic drugs. Estradiol-17*ß-D*-glucuronide is transported with much greater affinity (Km = 7.2 μM), by MRP2, than PAH (1.9 mM), which is unconjugated (Konig et al., 1999; van Aubel et al., 2002). MRP2 has been reported to contain two similar, but not identical, ligand-binding sites. That is, aside from the site from which substrate is transported, a second binding site (allosteric) exists on MRP2 that regulates the affinity of the transport site for the substrate. Estradiol-17*ß-D*-

glucuronide appears to bind to both sites, but this is not the case for all ligands that bind to MRP2 (Slot et al., 2011).

MRP4, on the other hand, supports the efflux of small hydrophilic anionic drugs from RPTs into urine (Otani et al., 2017). Although MRP4, like MRP2, interacts with a broad range of anionic conjugates, its affinity for ligands and its expression in the human kidney differ markedly from that of MRP2. PAH is transported by MRP4 with much higher affinity (Km = 160 μM) than MRP2 (Km = 5 mM) (van Aubel et al., 2002), and may be more important than MRP2 in the efflux of small hydrophilic anionic drugs. Substantial differences in amino acid residues of the TMHs may account for marked differences in the ligand selectivity of these transporters. Mutational analyses of MRP2 revealed that substituting the tryptophan residue at position 1254 (Trp1254) with alanine or cysteine abolishes estradiol-17*β-D*-glucuronide transport, indicating that Trp1254 plays a crucial role in the selectivity of MRP2 for conjugated anionic drugs (Ito et al., 2001).

BCRP interacts with a diverse range of anionic drugs, including fluoroquinolones (Mulgaonkar et al., 2012), antiviral nucleosides (eg. lamivudine), chemotherapeutics (mitoxantrone, topotecan) and sulfated conjugates (Huls et al., 2008; Mao & Unadkat, 2015). Results from transport inhibition studies suggest that zidovudine and abacavir interact with BCRP at binding sites that are distinct from either prazosin or imatinib (Giri et al., 2009).

The clinical relevance of NPT1 and NPT4 is yet to be clarified; however, they interact with anionic drugs including PAH, benzylpenicillin, probenecid, diuretics and NSAIDs (Jutabha et al., 2003; Jutabha et al., 2010).

1.5 Involvement of Renal Drug Transporters in Pharmacokinetics and Drug-Drug Interactions

The kidney, aside from its numerous homeostatic functions, plays a vital role in eliminating from the body potentially toxic drugs and drug metabolites, and thus, is a major determinant in the disposition of xenobiotics, including many prescription drugs (Morrissey et al., 2013). When renal active tubular secretion of a drug is important, i.e., active secretion more than or equal to 25% of total clearance, or when there are concerns about renal toxicity, it is recommended to determine if the NME is a substrate of OAT1 and OAT3 (US Food and Drug Administration, 2017; European Medicines Agency, 2012). However, for all NMEs, it is required to test if they inhibit OAT1 and OAT3 activities. For some NMEs, other transporters (e.g. OATP4C1, MRP2, MRP4, BCRP) may be considered based on information concerning other drugs in the same therapeutic class, such as observed DDIs or new information in the literature. Of the top 200 prescribed drugs in the United States in 2010, at least 32% of them are renally eliminated, with transporter-mediated tubular secretion playing a major role (Morrissey et al., 2013). That is, their renal clearance is greater than glomerular filtration rate. Of the drugs predicted to undergo tubular secretion, 28% and 41% interact with OAT1 and OAT3, respectively, while 22% and 19% interact with MRP2 and MRP4, respectively (Morrissey et al., 2013). The relatively novel OATP4C1 interacted with 6% of these drugs (Morrissey et al., 2013). An interaction means that they were either a substrate and/or inhibitor when tested *in vitro*. These statistics highlight the potential importance of these transporters to PK.

The multi-selectivity of drug transporters increases the likelihood of DDIs. DDIs at renal tubular secretion occur when transporter-mediated uptake and/or efflux of one drug ("victim drug") is influenced by a second concomitantly administered drug ("perpetrator drug"). Such alteration of transport could occur via transport inhibition, direct stimulation of transport, or indirect stimulation through transcriptional induction (Konig et al., 2013; Muller & Fromm, 2011). Ultimately, for renal anionic drug transporters like OATs and MRPs, changes in their activity could influence the half-life, and area under the plasma concentration-time profile (AUC) of victim drugs through alterations in their renal clearance. The number of clinically-relevant DDIs resulting from direct stimulation or induction of transport proteins are few (Kis et al., 2010; Konig et al., 2013). Most transporter-mediated DDIs occur via inhibitory mechanisms (Kis et al., 2010; Konig et al., 2013). It should be noted that not all ligands of drug transporters are translocated – many bind and inhibit, but are not translocated substrates. Inhibition can occur by three distinct mechanisms, competitively, non-competitively or mixed-type, and DDI magnitude could be different depending on inhibition mechanism. A study that examined the mechanism by which drugs in a variety of classes inhibit OAT1 suggests that most inhibition (but not all) occurs via competition for a common ligand binding region (Hotchkiss et al., 2015). Kinetically, in the presence of a competitive inhibitor there is an increase in the Michaelis constant (K_m) associated with substrate transport without a change in the maximal transport rate (J_{max}). For non-competitive inhibition, the inhibitor binds to a distinct region (or irreversibly to the same region) resulting in a decrease in the J_{max} without affecting the K_m. The aforementioned study revealed that telmisartan and azilsartan are non-competitive inhibitors of OAT1. Mixed-type inhibition

results in a decrease in both the K_m and J_{max} values. Omeprazole and irbesartan inhibit OAT1 via mixed-type inhibition.

Given the complexity of mixed-type inhibition, I will focus on competitive and non-competitive inhibition mechanisms as examples of how they could differentially impact drug exposure. The first important thing to point out is that following administration, the concentration of both perpetrator and victim drug change with time, due to factors influencing their absorption, distribution, metabolism and elimination (ADME). For a perpetrator drug which is a reversible competitive inhibitor, its inhibition potential depends on the concentration of itself as well as the victim drug at the ligand binding region, and their respective affinities for binding. In contrast, inhibition potential of a non-competitive inhibitor, whether reversible or irreversible, depends solely on the concentration of itself at the ligand binding site, and is independent of the victim drug concentration. Therefore, a non-competitive inhibitor has more potential to cause DDIs of greater magnitude than a competitive inhibitor, assuming that both have similar inhibition potencies and that their concentrations are equivalent at the ligand binding region.

Inhibition of OATs at the basolateral membrane of RPTs decreases the cellular uptake of substrate drugs (Burckhardt & Burckhardt, 2011), and this may significantly reduce the renal clearance of drugs that undergo tubular secretion, potentially leading to overexposure and increased potential for systemic side effects. There are several clinically observed DDIs which have been attributed to inhibition of OAT1 and/or OAT3. Reduction in renal clearance of methotrexate and/or an increase in its AUC have been reported in combination therapy with several drugs including probenecid, NSAIDs and proton pump inhibitors (Aherne et al., 1978; Kremer & Hamilton, 1995; Santucci et al.,

2010). Inhibition of tubular secretion of methotrexate (OAT1- and OAT3-mediated) may have an important role in DDIs involving these perpetrator drugs (Chioukh et al., 2014; El-Sheikh et al., 2013; Iwaki et al., 2017; Maeda et al., 2014). The antidiabetic, sitagliptin is largely excreted into urine, a process in large part due to OAT3-mediated transport (Herman et al., 2005; Scheen, 2007). Inhibition of OAT3 by gemfibrozil (a carboxylic acid) may explain the clinically observed increase in plasma concentrations of sitagliptin following their co-administration (Chu et al., 2007; K et al., 2012). Similarly, inhibition of OAT3 by gemfibrozil and its metabolites explains the clinically relevant DDI in which the renal clearance of pravastatin was reduced by 40% (Kyrklund et al., 2003; Nakagomi et al., 2007). The urinary excretion of the radiopharmaceutical Tc-99m-mercaptoacetyl-triglycine (Tc-99m-MAG3) is mediated largely by OAT1 transport (Shikano et al., 2004). Clinically relevant DDIs which interfere with Tc-99m-MAG3 diagnosis of kidney function have been reported, following treatment with drugs that interact with OAT1. Co-administration of PAH (OAT1 substrate) or probenecid (OAT inhibitor) in healthy volunteers reduced Tc-99m-MAG3 renal clearance by 56% and 33% respectively, resulting in elevated plasma levels (Takahara et al., 2013).

For potentially hazardous drugs, tubular secretion may favour their accumulation in RPTs, leading to nephrotoxicity (George et al., 2017; Morrissey et al., 2013). Drugs that may accumulate in RPTs and cause direct cellular injury include chemotherapeutics (e.g., methotrexate), antivirals (e.g., cidofovir, adefovir, tenofovir) and antibiotics (e.g., cephalosporins) (Hagos & Wolff, 2010). Cidofovir and tenofovir are associated with dose-limiting nephrotoxicity, which results primarily from their intracellular accumulation mediated by OAT1 and/or OAT3 (Izzedine et al., 2005; Ortiz et al., 2005;

Ray et al., 2006). Inhibition of renal uptake transporters or development of prodrugs which lack the ability to be actively taken up into RPTs has been exploited to reduce the nephrotoxicity risk of potentially hazardous drugs. In clinical practice, probenecid, the classical OAT inhibitor, is administered with each dose of cidofovir to prevent cidofovir-associated nephrotoxicity (Cesaro et al., 2005; Izzedine et al., 2005; Yusuf et al., 2006). The superior renal safety profile of brincidofovir (CMX001) and tenofovir alafenamide, prodrugs of cidofovir and tenofovir, respectively, is likely due to their lack of transporter-mediated accumulation into RPTs in comparison to the active drugs cidofovir and tenofovir (Bam et al., 2014; Marty et al., 2013; Tippin et al., 2016).

There are also cases where perpetrator drugs can inhibit apical efflux of victim drugs mediated by ABC transporters thereby reducing their renal clearance and causing elevations in their intracellular concentration. NSAIDs, including ibuprofen, naproxen, sulindac and diclofenac, are potent inhibitors of MRP4, and by decreasing the apical efflux of MRP4 substrates, may cause a significant decrease in renal clearance of anionic drugs (El-Sheikh et al., 2007). Co-administration of diclofenac and tenofovir is associated with an increased risk of nephrotoxicity (Bickel et al., 2013), which results from inhibition of the apical efflux of tenofovir, via MRP4, by diclofenac.

Few DDIs are known to result from induction or direct stimulation of drug transporters. Drug transporters, such as OATP4C1, MRP2 and MRP4, have multiple ligand binding sites, and ligand binding to one site can influence binding of ligands to other sites via allosteric mechanisms (El-Sheikh et al., 2007; Yamaguchi et al., 2010; Zelcer et al., 2003). For example, bupropion and its metabolites were shown to stimulate digoxin transport by OATP4C1 *in vitro* (He et al., 2014). Renal tubular secretion

accounts for approximately 50% of urinary digoxin excretion, with OATP4C1 being the major basolateral uptake transporter and P-gp the apical efflux pathway (Mikkaichi et al., 2004). Co-administration of bupropion with digoxin leads to an 80% increase in renal digoxin clearance and a 40% decrease in its AUC (Kirby et al., 2012). This clinically-significant DDI could be due to the stimulatory effect of bupropion on OATP4C1-mediated digoxin uptake into RPT cells. Similarly, celecoxib and phenylbutazone stimulate methotrexate transport by MRP4 and MRP2, respectively, however, no clinically significant DDIs have been reported (Colebatch et al., 2012; El-Sheikh et al., 2007).

Drug transporters are regulated by ligand-activated nuclear receptors, including constitutive androstane receptor (CAR), farnesoid X receptor (FXR), aryl hydrocarbon receptor (AhR) and the pregnane X receptor (PXR) (Konig et al., 2013; Tirona, 2011). Few clinically relevant DDIs have resulted from induction of drug transporters, but those that have are mostly attributed to PXR agonism. This includes the antibiotic rifampin and the anti-epileptic carbamazepine, which influence the disposition of P-gp and MRP2 substrates (Giessmann et al., 2004; Greiner et al., 1999; Konig et al., 2013). For example, the oral bioavailability and AUC of digoxin was significantly lower during rifampin treatment (Greiner et al., 1999). Duodenal biopsies showed that P-gp expression in the small intestine increased by 3.5-fold during rifampin treatment. Similarly, co-administration of carbamazepine greatly decreased the oral absorption and increased the renal clearance of the β-adrenergic blocker talinolol (P-gp and MRP2 substrate) (Giessmann et al., 2004). Consistent with the reduced oral absorption of talinolol, duodenal biopsies revealed an increase in P-gp and MRP2 expression in the lower

duodenum following carbamazepine treatment. The increase in talinolol renal clearance may result from its increased apical efflux from RPTs, as a result of a carbamazepine-induced expression of P-gp and MRP2. *In vitro*, HMG-CoA reductase inhibitors induce OATP4C1 expression via activation of the AhR (Toyohara et al., 2009). For potentially nephrotoxic drugs that are actively secreted, induction of uptake and efflux transporters could modify nephrotoxic potential.

Genetic polymorphisms, which lead to variation in the expression and function of drug transporters among individuals, may account for variation in PK, and hence, pharmacodynamics and toxicity potential (Tirona, 2011). Polymorphisms in ABCC4 and ABCC2, genes encoding MRP4 and MRP2, respectively, have been linked to tenofovir-induced renal tubular damage (Izzedine et al., 2006; Rodriguez-Novoa et al., 2009). Heterozygous mutations in MRP2, replacing a highly conserved arginine by glycine at position 412, lead to reduced renal clearance and increased plasma steady-state levels of methotrexate, and increased potential for methotrexate-induced nephrotoxicity (Hulot et al., 2005; Rau et al., 2006). Consistent with these *in vivo* results, the G412 MRP2 mutant was unable to efflux methotrexate when expressed in Chinese hamster ovary (CHO) cells, whereas wild-type MRP2 could efflux methotrexate (Hulot et al., 2005). In humans the ABCG2 single nucleotide polymorphism (SNP) c.421C>A, which results in a glutamine to lysine substitution at position 141 (Gln141Lys), and low expression levels of BCRP, has been associated with delayed elimination of fluvastatin and simvastatin (Keskitalo et al., 2009; Miroševic Skvrce et al., 2013). This ABCG2 SNP has been associated with reduced ATPase activity, and impaired membrane localization of BCRP (Mizuarai et al., 2004). *In vitro*, glyburide uptake into HEK293 cells expressing the

polymorphic variant of ABCG2 (Gln141Lys) was greatly reduced (Pollex et al., 2010). In addition to polymorphisms in MRP2, MRP4 and BCRP, genetic variations in SLC22A11, the gene encoding the apically expressed OAT4, is associated with reduced renal clearance of torsemide (Vormfelde et al., 2006). Efforts to further understand genetic polymorphisms in renal anionic drug transporters could impact the optimization of drug therapy for individual patients. Thus, for renally cleared drugs with a high risk of systemic toxicity and/or nephrotoxicity, this understanding may allow genotyping of patients for transporter function prior to therapy, to avoid and predict adverse drug reactions.

1.6 Techniques for Studying Interactions of New Molecular Entities with Transporters

Evaluation of drug transporters during drug development has improved the understanding of their role in tissue distribution, efficacy and toxicity. Techniques used during drug development for studying the interaction of NMEs with transporters include cell and tissue-based assays, where the outcome is to input the data into static or mechanistic models to predict involvement of transporters in PK and DDIs.

1.6.a Cortical Slices and Primary Cells

Renal cortical slices and primary RPT cells have been used to characterize the renal uptake of drugs (Brown et al., 2008; Nozaki et al., 2007; Watanabe et al., 2009).

Such holistic *in vitro* systems contain an array of transporters that are involved in tubular secretion and provide a valuable system for assessing the interaction of drugs with renal transporters. Such systems also allow for studying inter-individual variability in active tubular anionic drug secretion. However, despite their usefulness, estimating kinetic parameters for individual transporters using primary cells and renal cortical slices is challenging. Also, their use is limited due to a lack of a consistent supply of sufficient fresh kidney tissue and a rapid decline in transporter expression (especially SLC uptake transporters) after isolation and culturing (Feng & Varma, 2016; Lash et al., 2006). Additionally, primary cells in culture stop dividing after a few passages, and the cell monolayers loose tight junctional integrity with time (Lash et al., 2006; Lepist & Ray, 2012).

Organotypic cell lines, such as conditionally immortalized human proximal tubular epithelial cells (CIPTEC), that maintain expression of uptake and efflux transporters have been developed, circumventing the limited availability of isolated human RPT cells (Schophuizen et al., 2013; Wilmer et al., 2010). Nevertheless, functional expression of anionic drug uptake transporters, mainly OAT1 and OAT3, tends to be lost in these systems (Hilgendorf et al., 2007).

1.6.b Cell-based Assays

Transfected cell lines are widely used in academia and the biopharmaceutical industry as alternatives to primary cells for identifying transporter substrates and inhibitors. These cell-based assays are functional assays where the transporter-mediated

flux of a substrate across the membrane is assessed either in the absence or presence of an inhibitor drug. Singly transfected cell lines are most suitable for kinetic characterization of an individual transporter. Namely, determining for transported substrates the Michaelis constant (K_m value) and the maximal transport rate (J_{max} value), and for inhibitors, the potency of inhibition (IC_{50} or K_i value for competitive inhibitors), and the inhibition mechanism (competitive, non-competitive or mixed-type). Polarized cell lines, stably expressing an uptake transporter at the basolateral membrane and an efflux transporter at the apical membrane have the advantage of assessing the interplay between uptake and efflux transporters in the transcellular transport of drugs (Lepist & Ray, 2012; Volpe, 2016). Typical cell lines used in cell-based assays include the non-polarized human embryonic kidney cells (HEK293) and CHO cells, and the polarized Madin-Darby canine kidney (MDCK) and Lewis-lung cancer porcine kidney cells (LLC-PK1) (Jia et al., 2016; Robey et al., 2011; van der Sandt et al., 2000). Cell-based assays discussed below are classified as uptake assays for uptake transporters, accumulation assays for efflux transporters, and bidirectional assays, which assess the combined impact of uptake and efflux to intracellular drug accumulation and transcellular transport (**Figure 1.3–A, B and E**).

1.6.c Cellular Uptake Assays for Uptake Transporters

NMEs that are substrates or inhibitors of an uptake transporter can be identified using cell-based uptake assays, which measure the intracellular accumulation of a compound in cells overexpressing that transporter (**Figure 1.3A**). Significantly higher

accumulation of a test compound, of at least two-fold, in transporter-expressing cells compared to control cells lacking the transporter indicates that the compound is a transported substrate (Brouwer et al., 2013). Inhibitors of uptake transporters reduce the uptake of probe substrates into the cells. Cellular uptake assays with transfected cell lines are used to identify and kinetically characterize substrates and inhibitors of OAT1, OAT2, OAT3 and OATP4C1, and for DDI predictions (Brouwer et al., 2013; Shin et al., 2010; Soars et al., 2014).

1.6.d Accumulation Assays for Efflux Transporters

Accumulation assays that assess efflux transporters are based on the premise that an efflux transporter, when expressed in a cell, reduces the intracellular accumulation of substrates (**Figure 1.3B**). A reduction in cell accumulation ratio between transfected and control cells indicates that a compound is a substrate of an efflux transporter. On the other hand, NMEs that inhibit an efflux transporter favour the accumulation of a probe substrate in transporter-expressing cells.

1.6.e Bidirectional Assays

Aside from conventional cellular uptake and accumulation assays, which are unidirectional, bidirectional assays are used to assess the combined influence of uptake and efflux transporters to transepithelial drug transport (Balimane et al., 2006; Xia et al.,

2007). Bidirectional assays are conducted in culture wells containing polarized cells (MDCK, LLC-PK1 or Caco-2 cells) grown on permeable supports (**Figure 1.3E**). When grown on permeable supports, a test compound is added to the apical compartment of one well and the movement of the compound across the epithelium in the apical-to-basolateral (*A-B*) direction is examined by sampling the basolateral compartment. In a separate well, the test compound is added to basolateral compartment and the movement of the compound across the epithelium in the basolateral-to-apical (*B-A*) direction is examined by sampling the apical compartment. Following the incubation, the cells can be rinsed and lysed to determine intracellular drug concentration. These experiments are routinely done in cells expressing specific transporters (uptake, efflux or both) in comparison to control cells not expressing transporters. The experiments can also be done in the presence versus absence of selective transport protein inhibitors. Compounds with efflux ratios *(B-A/A-B)* >2 are generally considered secreted substrates of the transporter(s) that are expressed. An inhibitor will cause a concentration-dependent decrease of the efflux ratio of a probe substrate. NMEs that are substrates or inhibitors of renal anionic drug transporters have been characterized using bidirectional assays in cells such as the human colon epithelial cancer cell line (Caco-2), which endogenously express MRP2, BCRP and P-gp, and transfected MDCK and LLC-PK1 cells (Cui et al., 1999; Giri et al., 2009; A. Poirier et al., 2014; Volpe, 2011).

1.6.f Membrane-based Assays

Membrane-based assays are used to assess interactions of compounds with the efflux transporters MRP2, MRP4, BCRP and P-gp. Membrane-based assays include ATPase activation assays (**Figure 1.3D**) and vesicular transport assays (**Figure 1.3C**).

ATPase activation assays (**Figure 1.3D**) are conducted using inside-out plasma membrane vesicles prepared from *Spodoptera frugiperda* (Sf9) insect cells or non-polarized transfected cells (typically HEK) over-expressing an ATP-dependent efflux transporter (Glavinas et al., 2007; Sarkadi et al., 1992; Shirasaka et al., 2006). Binding of a substrate to an ABC transporter expressed in the membranes leads to ATP hydrolysis, whereas inhibitors cause a decrease in ATP hydrolysis elicited by a known probe substrate. ATP hydrolysis is measured by examining the liberation of inorganic phosphate (P_i) using a colorimetric method (Sarkadi et al., 1992; Volpe, 2016). The measured absorbance is translated into concentration of P_i using a calibration curve produced from an inorganic phosphate standard. (Gallus et al., 2014; Kwak et al., 2010). ATPase activation assays are useful for high throughput screening of compounds during early drug discovery, whereas vesicular transport assays are typically used to confirm, based on these results, whether an NME is an ABC transporter ligand.

Vesicular transport assays (**Figure 1.3C**), unlike ATPase activation assays, measure the accumulation of substrate in inside-out membrane vesicles in the presence versus absence of ATP to allow for the identification of efflux transporter substrates and inhibitors. They also allow for determination of transport kinetic parameters (El-Sheikh et al., 2007; Glavinas et al., 2008; Kidron et al., 2012; Te Brake et al., 2016). Compounds

which are substrates of an efflux transporter accumulate inside the vesicles while inhibitors reduce the accumulation of probe substrates. Quantification of the accumulated substrate is possible using liquid scintillation counting, fluorescence detection or LC-MS. Vesicular transport assays are especially useful for compounds with poor membrane permeability, because access to the intracellular-facing ligand-binding site is difficult in intact cells. Membrane vesicles can be prepared from insect or mammalian cell lines including Sf9 insect cells, HEK293 and MDCK (Cui et al., 1999; Leier et al., 2000). Vesicular transport assays have been used to detect substrates and inhibitors of MRP2, MRP4 and BCRP (Jin & Di, 2008; Volpe, 2016).

1.6.g In Vivo Animal Models

In some cases, there are species differences in the expression and localization of renal anionic drug transporters, as well as their relative affinities for ligands, which often limits the translational value of animal studies. Expression and localization of OAT2 and OAT4 appear to be species-dependent. For example, OAT2 is expressed in basolateral membrane of RPTs but it localizes to the apical membrane in rodents (Burckhardt, 2012; Ljubojevic et al., 2007). OAT4, which is expressed in the apical membrane of human RPTs, is not present in rodents (Burckhardt, 2012). There are cases where relevant DDIs, which occur in humans, are not observed in animals due to interspecies differences in the affinities of renal anionic drug transporters for the victim drug. The reduction in renal clearance and increase in the plasma concentration of the antiulcer drug famotidine (OAT3 substrate) when co-administered with probenecid (OAT inhibitor) in humans,

does not occur in rats (Inotsume et al., 1990; Lin et al., 1988). The difference in transport activity between human OAT3 and rat Oat3 partly accounts for this observation. *In vitro* studies revealed that famotidine has an ~3-fold greater affinity for human OAT3, and is transported with a higher efficiency (J_{max} / K_m) than rat Oat3 (Tahara et al., 2005). Additionally, the organic cation transporter-1 (OCT1), which is expressed in rat kidney but not in human kidney, provides an alternative pathway for the active tubular secretion of famotidine in rats, thereby attenuating the effect of OAT3 inhibition (Tahara et al., 2005).

Despite their limited translational value in some cases, animal models have been used to support *in vitro* models in establishing the involvement of drug transporters in drug disposition. Knockout animal models have been used to link loss of renal anionic drug transporter function to altered drug PK (Vanwert et al., 2007; Vanwert et al., 2008). *Oat1* and *Oat3* knockout mice exhibit delayed elimination of methotrexate, benzylpenicillin, ciprofloxacin, PAH, furosemide and bendroflumethiazide (Eraly et al., 2006; Vanwert et al., 2007; Vanwert & Sweet, 2008; Vanwert et al., 2008), highlighting the contribution of OAT1 and OAT3 to the renal excretion of these drugs. Given that loop and thiazide diuretics act from within the tubular lumen where they are actively secreted, the delayed urinary excretion rate of furosemide and bendroflumethiazide in *Oat1* and *Oat3* knockout mice results in attenuation of their diuretic effect (Eraly et al., 2006; Vallon et al., 2008).

The role of BCRP in renal excretion of fluoroquinolones was established using *Bcrp* knockout mice, which show elevated plasma and kidney tissue levels of ciprofloxacin after oral and intravenous administration (Merino et al., 2006). When

clinically relevant concentrations of ciprofloxacin are administered to *Oat3*-knockout mice, the effect of transporter deletion is similar to the effect of probenecid co-administration (OAT3 inhibition) on fluoroquinolone disposition in humans (Vanwert et al., 2008).

1.7 Application of Transport Kinetic Data as a Guide in Clinical Development of Drugs

A key step in the drug development process is to assess the interaction of NMEs with relevant transporters, and to predict the likelihood and extent of transporter-mediated DDIs (Tweedie et al., 2013). Decision-making, therefore, relies mostly on *in vitro* data (mostly because of species differences), and its subsequent translation *in vivo*. Quantitative approaches used for predicting renal DDIs range from basic static models to more dynamic physiologically-based pharmacokinetic (PBPK) models (Feng & Varma, 2016; Scotcher et al., 2016).

Static models use *in vitro* inhibition potency (IC_{50} or K_i values) data and the anticipated maximum unbound plasma drug concentration ($[I_{u,max}]$), that is, $[I_{u,max}]/K_i$ ratio, to predict changes in renal clearance and victim drug exposure (AUC) due to inhibition of drug transporters caused by perpetrator drugs (US Food Drug Administration, 2017; Feng et al., 2013; Feng & Varma, 2016; Sager et al., 2015). The static model predicts that for victim drugs whose basolateral uptake is the rate-determining step of their renal clearance, as is the case for anionic drugs, inhibition of uptake by a perpetrator drug would cause an increase in the plasma AUC by: 1+

$[I_{u,max}]/K_i$ (Feng & Varma, 2016). Static models have been used for predicting the reduction in renal clearance for several clinical interactions involving anionic drug transporters (Feng et al., 2013; Maeda et al., 2014). The reduction in renal clearance of OAT substrates, including famotidine, acyclovir, oseltamivir carboxylate and ciprofloxacin, with probenecid co-administration was predicted reasonably well using the static model (Feng et al., 2013). A major limitation of the static model is that predictions of changes in overall drug exposure are based on steady-state assumptions, and is not useful for predicting changes in plasma concentration or exposure over time (Sager et al., 2015). Additionally, the static approach does not allow for predicting intracellular drug concentrations, and hence, does not provide insights into potential for nephrotoxicity.

PBPK models, in contrast to static models, provide a framework with comprehensive structural representation of the human body, which allows simulation of plasma and organ concentration-time profiles, in a mechanistic way (**Figure 1.4**). PBPK models incorporate parameters that represent properties of the drug and the biological system. System parameters are quantitative physiological data, such as organ size, tissue composition, blood flow rates, drug metabolizing enzyme abundances and polymorphic frequencies, etc. Drug-specific parameters include the drug's physicochemical properties and *in vitro* data, such as lipophilicity, molecular weight, tissue-to-plasma partition coefficient, plasma protein binding, and drug metabolizing enzyme and transport kinetic (i.e. maximal rate of transport, J_{max}, and Michaelis constant, K_m) and inhibition data (IC_{50} or K_i values). The ability of the dynamic PBPK approach to simultaneously model ADME processes is a major advantage over the static approach (Scotcher et al., 2016; Shardlow et al., 2013; Varma et al., 2015). However, it also makes PBPK modeling more

laborious since it requires considerable physiological and *in vitro* data. Model parameters are derived from both *in vitro* and physiological data through *in vitro*-to-*in vivo* extrapolation (IVIVE) (i.e. 'bottom-up) and/or empirical fitting to clinical data (i.e. 'top-down') (Feng & Varma, 2016; Scotcher et al., 2016).

IVIVE of transport kinetic data is performed using physiologically relevant scalars to extrapolate *in vitro* PK parameters to PK at the level of the tissue/organ. K_m and J_{max} values from *in vitro* transport assays are used to calculate intrinsic clearance values ($CL_{int} = J_{max}/K_m$) that are used along with IVIVE to model the contribution of renal transporters to urinary drug elimination. The mechanistic kidney model scales the CL_{int} *in vitro*-to-*in vivo* by taking into account the proximal tubule cell number per gram kidney (PTCPGK), the kidney weight, and the relative expression factor for the transporter in the *in vitro* test system versus the whole kidney (Scotcher et al., 2016). A major challenge with the mechanistic kidney model is the difficulty in scaling CL_{int} from *in vitro* systems to the level of the kidney (*in vivo)* since the number of PTCPGK is uncertain, and renal transporter REF values have to be generated in-house using semi-quantitative Western blotting or LC-MS/MS. The current data on the number of PTCPGK is based on indirectly calculated estimates from different literature sources, ranging from 30.9 to 209.2 million PTCPGK – this includes data from rabbit kidney (Scotcher et al., 2016). Calculated values of proximal tubule cell numbers from these studies are based on numerous assumptions, including approximations of the number of cells per millimeter length of proximal tubule, average length of proximal tubules per human kidney, kidney weight, volume of the proximal tubule epithelium, and the volume of a single proximal tubule cell (Cummings & Lash, 2000; Scotcher et al., 2016).

Stereological methods, which have been used to report the increase in proximal and distal tubule cell number in rat kidneys during diabetic renal growth (Nyengaard et al., 1993), may be a suitable approach for absolute quantification of proximal tubule cell number in the human kidney. Traditional stereological methods rely on two-dimensional (2-D) sections of tissue to extract information about three-dimensional (3-D) organization (Weibel, 1981). Confocal stereology, a contemporary approach which applies confocal microscopy to generate 3-D images of objects for subsequent characterization with stereological methods (Kubinova & Janacek, 2015), may offer a more precise approach to quantifying the number of PTCPGK.

Another difficulty with IVIVE is the lack of established data on absolute transporter protein abundances, which is required for calculating REF values for transporters in the human kidney (Brouwer et al., 2015). Expression levels of transporter mRNA in human kidney show significant inter-individual variability (Cheng et al., 2012; Nozaki et al., 2007), and moreover, protein and mRNA levels are not always reflective of each other, making data on mRNA expression unsuitable for determination of REF values. Semi-quantitative Western blotting has been used for determining REF values (Tucker et al., 2012). However, LC-MS/MS is the preferred technique for quantifying transporter protein abundances, mainly due to its quantitative precision (Badee et al., 2015). Among the organic anion transporters, data on OAT3 protein abundance has so far been reported (9.7 pmol/mg microsomal protein) (Nakamura et al., 2016). However, for IVIVE, the investigator needs to know the absolute abundance in the kidney vs. the individual test system, i.e., the *in vitro* batch an individual kinetic experiment is performed on.

A more empirical approach that circumvents the challenges of IVIVE is fitting *in vitro* data to clinical data, in order to determine optimal REF scalars (Varma et al., 2015). We have done this in the experimental portion of this thesis. For basolateral uptake transporters, CL_{int} values required for PBPK modeling can be refined using plasma-concentration time curves. This approach has been successfully used to describe the renal clearance of several drugs, in cases where IVIVE has failed to adequately describe their PK (Hsu et al., 2014; Posada et al., 2015). Renal DDIs for pemetrexed (OAT3 substrate), an antineoplastic drug, which is primarily eliminated in urine via active tubular secretion, has been predicted using this empirical approach. The renal clearance of pemetrexed was under-predicted by 2-fold when the bottom-up approach was used. However, when a REF value of 5.3, empirically determined from the plasma concentration-time curve was used to refine the $CL_{int,}$ the clinical PK data was adequately recovered (Posada et al., 2015). For efflux transporters, however, plasma-concentration time data are not sensitive to changes in CL_{int}. In such cases, data on intra-tubular or urine concentrations may be useful for empirical determination of optimal REF scalars for quantitative estimation of efflux CL_{int}.

Despite the challenges that make PBPK modeling labor-intensive, the support of regulatory agencies for this technique, as well as the availability of user-friendly software tools, have encouraged the widespread use of PBPK modeling in drug discovery. There are commercially available simulation software, such as the Simcyp Simulator and Gastroplus, which incorporate pre-defined virtual populations, population variability, and associated system parameters, as well as differential equations that describe ADME in the human body (Rostami-Hodjegan, 2012). Importantly, the use of PBPK modeling can

provide early insights into factors that influence clinical drug development, such as DDIs, and the influence of ethnicity, various disease states, and genetic polymorphisms on PK. An improved understanding of pathophysiological changes associated with different disease states, such as in renal impairment, has allowed the use of PBPK models for simulating drug disposition in such special populations. In chronic kidney disease patients, PBPK modeling has been applied to predict the effect of renal impairment on the PK of several anionic drugs (Hsu et al., 2014; Sayama et al., 2014). It is worth mentioning, that in 2013 and 2014, about 40% of new drugs approved had no dosing recommendations for severe renal impairment (Jadhav et al., 2015). In these patient groups, for which no clinical information is available, PBPK modeling may be of great advantage in guiding the design of clinical studies and establishing dosing recommendations (Rowland et al., 2011; Wagner et al., 2015).

PBPK models can also be used to predict intra-tubular drug concentrations, and therefore provide early information on potential adverse effects of drug therapy, such as nephrotoxicity. Since the PK of a drug dictates the potential for efficacy, simulated plasma or tissue concentrations can be linked to pharmacodynamic models. The clear distinction between drug and system parameters in PBPK models also makes it possible to explore and gain more insights into the effects of potential sources of inter-individual variability on PK (Tsamandouras et al., 2015; Vinks, 2013).

Prediction of DDIs using the PBPK approach aids in determining whether further clinical DDI studies are warranted, and how such studies should be designed. Several PBPK models have been described for prediction of renal transporter-mediated DDIs that involve probenecid (OAT inhibitor) and the OAT substrates, cidofovir, cefuroxime and

oseltamivir carboxylate (Hsu et al., 2014). Similarly, the potential DDI between pemetrexed and ibuprofen has been predicted by this mechanistic PBPK approach (Posada et al., 2015). Application of modeling and simulation to aid the design and timing of clinical DDI studies has resulted in improved planning and efficient use of resources, and has helped in providing mechanistic explanations for observed clinical DDIs (Shardlow et al., 2013).

In summary, transporter kinetic parameters determined *in vitro* can be used in both basic static and dynamic PBPK models to assess the likelihood of renal transporter-mediated DDIs. However, when there is a need to predict drug exposure profiles as well as time-based effects of co-administered medications on those profiles, PBPK models offer a great advantage.

Table 1. 1 Selected substrates and inhibitors of organic anion transporters						
	Basolateral transporters		**Apical transporters**			
	OAT1	**OAT3**	**OAT4**	**MRP2**	**MRP4**	**BCRP**
Anti-ulcer drugs						
cimetidine	S, I	S, I	I	-	-	S
famotidine	-	S, I		-	-	-
omeprazole	I	I		I		I
pantoprazole	I	I		-	-	S, I
rabeprazole				-	-	I
Anti-diabetic drugs						
glibenclamide	I	-		I	-	I
glimepiride				+	I	I
sitagliptin	-	S		-	-	
Statins						
atorvastatin	-	I		S, I	S, I	S
lovastatin				I	-	-
pravastatin	I	S, I	S, I	S*	S	S
rosuvastatin	-	S, I		S	S	S*
simvastatin	I	I		S, I	I*	S*, I
Diuretics						
acetazolamide	S, I*	I	I		-	I
bendroflumethiazide	S, I	S, I				
hydrochlorothiazide	S*, I*	S*, I	I	-	S, I*	S
furosemide	S*, I	S*, I*	I	S, I	S, I	S, I
torasemide	S, I	S, I	S, I		-	
bumetanide	S, I	S*, I*	S, I		S	I

Table 1. 1 Selected substrates and inhibitors of organic anion transporters						
	Basolateral transporters		**Apical transporters**			
	OAT1	**OAT3**	**OAT4**	**MRP2**	**MRP4**	**BCRP**
ACEIs/ ARBs						
captopril	S, I	S	I	-	S	-
enalapril		I		S	S	
irbesartan	I*	I	I	+	I	-
losartan	S, I	S, I	I	I+	I*	-
telmisartan	I	I	I	S, I	I	S, I
olmesartan	S, I	S*, I*	S, I	S, +	S, I	S
valsartan	I	S, I*	I	S	-	-
Anti-bacterial drugs						
amoxicillin	S, I	S*, I*			S	-
ampicillin		S*, I*		S	S	
carbenicillin	S, I	S, I				
cloxacillin	I*	S*, I*				
flucloxacillin	I	S*		-		-
penicillin	S, I	S*, I*	I	S, I	S	
piperacillin	S*, I*	S*, I*			S	
cefixime	S, I	S, I				
cefadroxil	S*, I	S*, I	I		I	
cefaclor	S, I	S, I	I		I	
cefotaxime	I	S*, I	I		S, I	
cefuroxime		S, I				
ceftriaxone	S, I*	S, I	I			
tetracycline	S*, I	S*	S	-	S	I
ciprofloxacin	I	S, I*			-	S
enoxacin	I	I			-	

Table 1. 1 Selected substrates and inhibitors of organic anion transporters						
	Basolateral transporters		**Apical transporters**			
	OAT1	**OAT3**	**OAT4**	**MRP2**	**MRP4**	**BCRP**
levofloxacin	I	I		I	I	
moxifloxacin	-	-				
norfloxacin	S	S, I			S	S
rifampicin	-	I		I	I	-
ketoconazole	I	I		-	I	I*
Antiviral drugs						
acyclovir	S*, I	S*, I	-		I	S
adefovir	S*, I	S, I		I	S*	-
cidofovir	S*, I	S		I	-	-
ganciclovir	S	I	-			-
lamivudine	S, I	I				S
lopinavir	I	I		S, I	I	I*
nelfinavir	I	I		-	S, I	I
ritonavir	-	I		S, I	I	I*
tenofovir	S*, I*	S, I		S	S*	
zidovudine	S*, I	S, I	S	-	S	S
Anti-neoplastic agents						
chlorambucil	I	I	I			
irinotecan		I		I		S
methotrexate	S	S*, I*	S	S	S*, I	S
mitoxantrone	I	-		+	+	S
tamoxifen				I	I	I
Immunosuppressant drugs						
cyclosporin	-	-		I	I	I

Table 1. 1 Selected substrates and inhibitors of organic anion transporters

	Basolateral transporters		Apical transporters			
	OAT1	**OAT3**	**OAT4**	**MRP2**	**MRP4**	**BCRP**
mycophenolic acid	I	S, I*		S, I*	S, I*	
NSAIDs						
acetylsalicylic acid	S, I	S, I	-	-	S, I	
celecoxib		I		I	I	I
diclofenac	S, I*	S, I	S, I	S, I	I	S, I
ibuprofen	S, I*	S, I*	I	I	I*	
indomethacin	S, I	S, I*	I	S, I*	I*	I
meloxicam		I				
naproxen	I*	I	I	I	I*	
mefenamic acid	I*	I*	I		S	
Uricosuric drugs						
probenecid	I*	S, I*	I	S, I+	I	I

Reference: *Ivanyuk et al., 2017.*

*Significant transport substrate – indicates a drug whose tubular secretion ≥ 25% of total clearance; predominantly through the transporter indicated.

*Significant inhibition – indicates that the IC_{50} or K_i of that drug for the transporter is within 10-fold of its unbound plasma concentration, [$I_{u,\,max}$]); and likely results in clinically relevant DDIs.

-*;* no interaction found, +*;* transport induction, *ACEIs;* angiotensin converting enzyme inhibitors, *ARBs;* angiotensin receptor blockers, *I*; transport inhibition, *I**; significant transport inhibition, *I*+; inhibition but induction of the expression, empty cells indicate no data. *NSAIDs;* non-steroidal anti-inflammatory drugs, *S*; substrate, *S**; significant transport substrate.

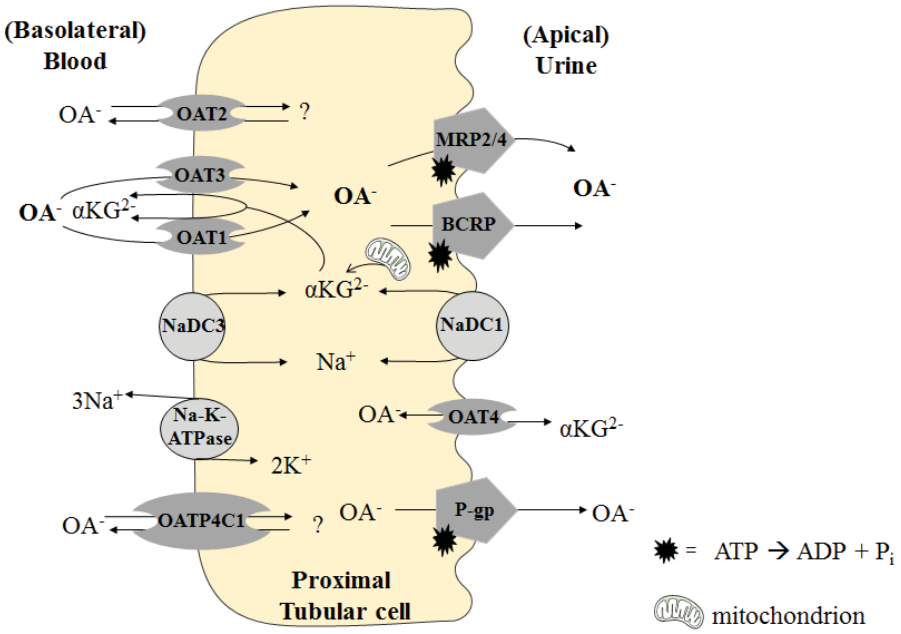

Figure 1. 1. Mechanism of tubular secretion of anionic drugs in the human kidney. SLC and ABC transporters localized at basolateral and apical membranes of proximal tubule cells act in combination to excrete drug substrates from blood into the glomerular filtrate, for final elimination in urine. OAT1 and OAT3 are known to work as anionic drug (organic anion, OA^-)/α-ketoglutarate exchangers, working via a tertiary active transport mechanism involving NaDCs and Na,K-ATPase. OAT2 and OATP4C1 are also anion exchangers, but the intracellular counter-anion that mediates uptake is unknown. MRP2, MRP4, BCRP and P-gp are ATP-dependent efflux transporters at the apical membrane, and OAT4 is an anion exchanger at the apical membrane that works as an exchanger with α-ketoglutarate as its counter-anion.

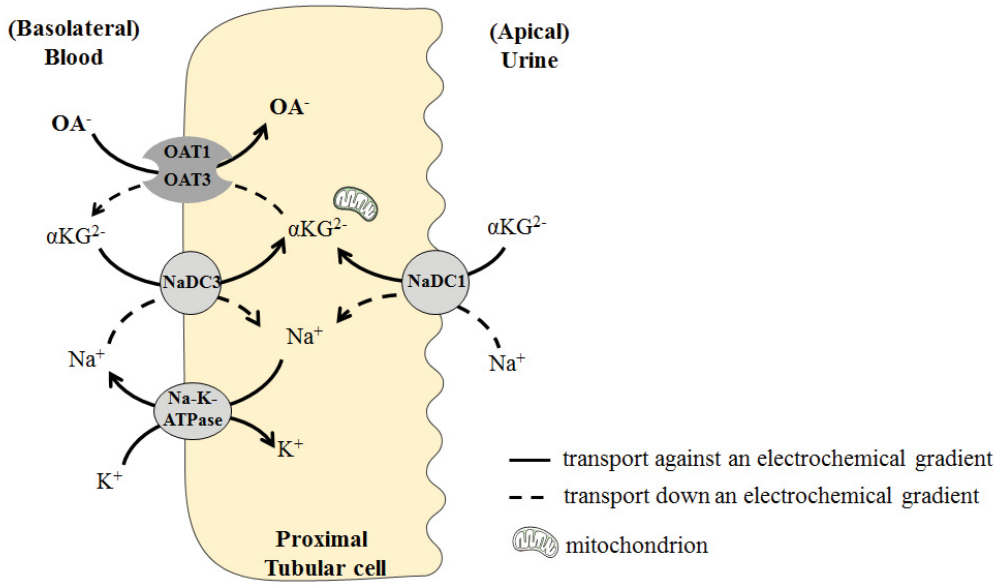

Figure 1. 2 Descriptive model of the tertiary active transport process involved in cellular uptake of anionic drugs by OAT1 and OAT3. The Na-K-ATPase maintains low intracellular sodium concentrations; the inwardly-directed sodium gradient provides energy to support influx of αKG into the tubule cells through Na^+-αKG co-transport by NaDC3 and NaDC1. Finally, intracellular αKG flows out in exchange for the anionic drug (OA^-) through OAT1 and OAT3.

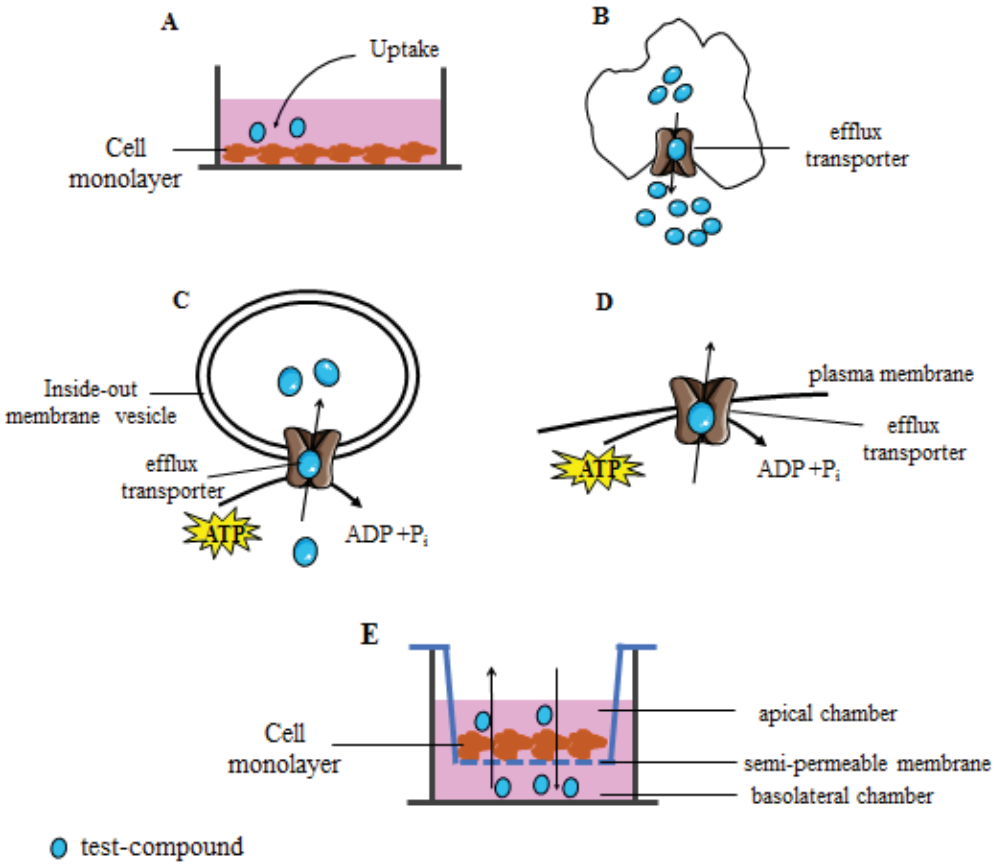

Figure 1.3. Frequently used in vitro transporter assays. A) Uptake assay – uptake transporters are usually studied with simple uptake assays which measure accumulation of substrate in transfected cells. **B) Accumulation assays for efflux transporters** – an efflux transporter reduces accumulation of substrate inside the cell. **C) Vesicular transport** – inside-out membrane vesicles prepared from transporter-expressing cells. This assay measures the accumulation of substrate in the vesicle in the presence versus absence of ATP. **D) ATPase assay** – compounds activate the ATPase activity of ABC transporters, leading to hydrolysis of ATP to form ADP and inorganic phosphate (P_i). The release of P_i is measured by a colorimetric method. **E) Bidirectional assays** – conducted in a transwell plate in which transfected cells form a distinct apical and basolateral membrane on a microporous filter membrane. Movement of test compound across the cell monolayer is measured in both the apical-to-basolateral and basolateral-to-apical directions. These assays are typically used to monitor for efflux transporter activity.

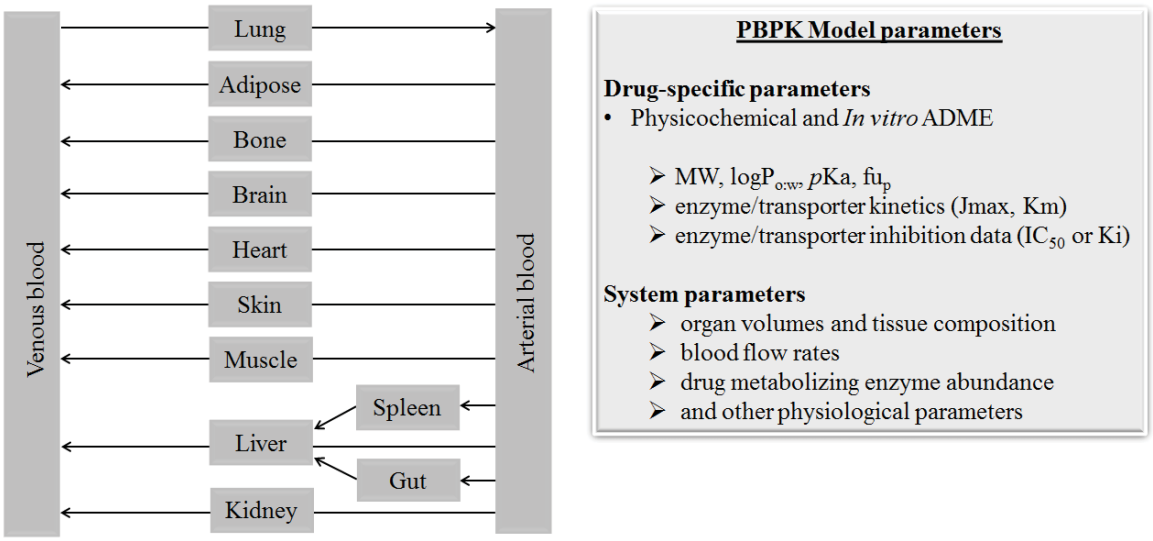

Figure 1.4 Schematic representation of a PBPK model. Compartments represent actual tissues and organs in the human body. Connecting arrows represent blood flow rates. MW; molecular weight, $P_{o:w}$; partition coefficient – octanol:water, pKa; acid dissociation constant, fu_p; unbound fraction of drug in plasma

CHAPTER 2 BACKGROUND

2.1 Rationale

The organic anion transporter 1 (OAT1) is localized in the peritubular membrane of renal proximal tubule cells, where it mediates the cellular uptake of numerous small molecular weight anionic drugs for their subsequent urinary excretion via tubular secretion (Pelis & Wright, 2011). Tubular secretion, mediated in part by OAT1, is an important determinant of plasma anionic drug concentration, is a site of wanted and unwanted DDIs, and for select drugs, such as cidofovir, their accumulation into proximal tubule cells mediated by OAT1 can be nephrotoxic (George et al., 2017; Morrissey et al., 2013). Of the top 200 prescribed drugs in the United States in 2010, 28% are known to interact with OAT1, highlighting the importance of OAT1 in renal drug disposition and DDIs (Morrissey et al., 2013).

The European Medicines Agency (EMA) and the US Food and Drug Administration (FDA) recognize the clinical significance of OAT1, and accordingly, in their guidance on drug interaction studies for the pharmaceutical industry they recommend determining *in vitro* if NMEs are substrates or inhibitors of OAT1 (as well as OAT3) (US Food and Drug Administration, 2017; European Medicines Agency, 2012). Due to a variety of technical issues associated with culturing human proximal tubule, and using them for studying the interaction of NMEs with a specific transport protein, cultured cells or *Xenopus laevis* oocytes with heterologous expression of transporters are typically used for these *in vitro* studies (Brouwer et al., 2013). Several criteria are used to decide

whether to test if NMEs are substrates of renal transporters. When the *in vivo* renal clearance of an NME is a substantial component of its total clearance, and there is evidence of its active tubular secretion, it is recommended to test if it is a substrate of OAT1 as well as the organic anion transporter 3 (OAT3) – under the assumption that the NME has the appropriate physicochemical properties to be an OAT substrate, i.e., a hydrophilic small molecular weight organic anion (Brouwer et al., 2013). Given the broad ligand selectivity of OAT1, and its potential involvement in DDIs, it is recommended for all NMEs to determine if they inhibit OAT1 and OAT3 transport activity (US Food and Drug Administration, 2017; European Medicines Agency, 2012).

Once an NME is determined an OAT substrate and/or inhibitor, the extent of its interaction with the transport protein is determined using *in vitro* kinetic transport studies. For substrates this entails determining the kinetic parameters of uptake, i.e., maximal transport rate (J_{max}) and the Michaelis constant (K_m), and for inhibitors, the inhibition potency of probe substrate uptake (IC_{50} or K_i value) (Brouwer et al., 2013). The kinetic parameters can then be used in either static or mechanistic models to predict the involvement of OATs in PK of NME substrates, and potential DDIs that may occur at the transporters due to inhibition caused by perpetrator drugs. Ultimately, the output of these models is used to guide the clinical development of NMEs (US Food and Drug Administration, 2017; European Medicines Agency, 2012). Thus, it is imperative that the kinetic parameters determined *in vitro* accurately reflect the kinetic interaction of drugs with renal transporters that occurs at the level of the proximal tubule cell *in vivo*.

In vitro kinetic parameters can be incorporated in PBPK models in order to mechanistically simulate the involvement of drug metabolizing enzymes and drug

transporters in PK. To date, several studies have incorporated *in vitro* transport kinetic parameters into PBPK models to simulate the PK of renal transporter substrates (Hsu et al., 2014; Posada et al., 2015; Scotcher et al., 2017; Ball et al., 2017; Hsueh et al., 2017). A requirement for accurate PK predictions using mechanistic PBPK modeling for transporters is the generation of *in vitro* kinetic parameters of transport that define the *in vitro* intrinsic substrate uptake clearance ($CL_{int,uptake} = J_{max}/K_m$), and knowledge of the relative expression level or activity (REF or RAF values) differences for the transport protein in the *in vitro* system compared to in the kidney *in vivo*. To date, retrospective PBPK modeling has been successful, but because REF/RAF values are unknown for transporters, it has required parameter estimation of these values for IVIVE of transport kinetic parameters and accurate PK predictions (Scotcher et al., 2016). However, without knowledge of expression level or activity differences of transporters from *in vitro*-to-*in vivo*, the accuracy of the *in vitro* kinetic data cannot be validated using PBPK modeling.

It is common practice prior to performing *in vitro* transport kinetic studies with uptake transporters such as OAT1 to determine the time course of transporter-mediated drug uptake into the cells, and to subsequently use an initial-rate time point (i.e., where drug uptake is linear over time) for subsequent kinetic studies (Zamek Gliszczynski et al., 2013). Historically, conducting kinetic studies at initial-rate time points, where transporter-mediated substrate flux into heterologous expression systems occurs predominantly from the transport medium, allows assessment of the kinetic interaction of NMEs with the extracellular-facing side of the transporter. With the increasing use of transport kinetic parameters in PBPK-IVIVE for predictive modeling, it is important that kinetic parameters determined *in vitro* accurately reflect the kinetic interaction of drugs

with transporters *in vivo*. Following administration *in vivo*, the concentration of drug substrates across transporter-expressing plasma membranes reach equilibrium at steady-state, and it is likely that such drugs interact with both intracellular and extracellular-facing sides of a transporter. Hence, for IVIVE, it is necessary to accurately characterize the kinetic interactions of NMEs with transporters. It is therefore, not clear if kinetic constants determined at an initial-rate time point are most appropriate for mechanistic PBPK modeling. Also, in *in vitro* systems it is possible, for exchangers like OAT1, that at longer incubation times as steady state is approached, the decrease in the inwardly-directed substrate concentration gradient impacts experimentally determined kinetic parameters, especially Jmax values. The lack of clearly established guidelines for selecting time points for kinetic characterization of transporters, whether initial-rate or steady state, partly accounts for the failure of the bottom-up mechanistic modeling approach to fully recover the observed clinical PK profiles, for some drugs.

2.2 Hypothesis

I hypothesize that transport kinetic parameters (especially J_{max} values) will be different depending on the time point chosen for *in vitro* transport kinetic studies with uptake transporters, such as OAT1 – the renal transporter of focus in this thesis. I anticipate that this will ultimately influence CL_{int} values in the *in vitro* uptake cultured cells systems that are used for PK modeling within the pharmaceutical industry. Ultimately, predictions of OAT1 involvement in PK using PBPK modeling is expected to differ depending on the time point chosen for determining substrate uptake *in vitro*.

2.3 Objectives

This study examined the effect of incubation time on the kinetics of PAH (a probe OAT1 substrate) transport mediated by OAT1 *in vitro*. The kinetic parameters obtained at different time points were then input into the Mechanistic Kidney model within the Simcyp Simulator to determine how the time point used influences PK predictions. Also examined was the effect of incubation time on the potency with which several drugs inhibit OAT1-mediated PAH transport. The data show that incubation time influences OAT1 transport kinetics, its potency of inhibition, and PBPK predictions of its involvement in drug disposition.

CHAPTER 3 MATERIALS AND METHODS

3.1 Reagents and Chemicals

[^{3}H]-PAH (40 Ci/mmol) was obtained from American Radiochemicals (St. Louis, MO). F12 Kaighn's modification medium, fetal bovine serum (certified, U.S. origin), 1% penicillin-streptomycin solution and hygromycin B were purchased from Thermo Fisher Scientific. All other chemicals were of the highest purity possible and were purchased from Sigma Aldrich (St. Louis, MO).

3.2 Cell Culture

Cloning of the human ortholog of OAT1 from human kidney and its stable expression in Chinese Hamster Ovary Flp-In cells (CHO-OAT1) was described previously (Ingraham et al., 2014) CHO-OAT1 cells were cultured in complete medium (F12 Kaighn's modification medium, 10% fetal bovine serum and 1% penicillin-streptomycin) supplemented with hygromycin B (200 μg/ml final concentration) in a humidified atmosphere of 5% CO_2:95% air at 37^{o}C. All cells were grown to confluence in 24-well flat bottom plates for transport experiments.

3.3 Transport Kinetic Studies

Transport kinetic studies were conducted under two different conditions, either zero-*trans* (where there was no substrate on the inside of the cells upon initiation of transport measurement) or equilibrium exchange (where the cells were pre-loaded with substrate prior to initiation of transport measurement). For zero-*trans* experiments, room temperature Waymouth's buffer (WB) containing [^{3}H]-labeled *p*-aminohippurate ([^{3}H]-PAH; 20 nM) with increasing concentrations of unlabeled PAH was used. The chemical composition of the WB was (in mM): 117 NaCl, 4.5 KCl, 20 $NaHCO_3$, 6 D-glucose, 1 $MgCl_2$, 1.5 $CaCl_2$ and 10 HEPES (pH 7.25). Zero-*trans* experiments involved aspirating the media, rinsing the cells quickly once with WB (0.4 ml), and then adding the transport solution (0.4 ml) to the wells for the amount of time indicated in the figure legends. Uptake was stopped by aspirating the transport buffer and rinsing the wells three times with ice-cold WB (0.4 ml). The cells were lysed in 0.5 N NaOH/1% SDS (0.4 ml) for 30 minutes on an orbital shaker and the lysates neutralized with 1 N HCl (0.2 ml). Radioactivity content was measured by liquid scintillation counting (Tri-Carb® 2910TR LSA; PerkinElmer). Several wells not used for transport were used for determining the number of cells per well with a hemocytometer.

For equilibrium exchange experiments, the cells were pre-treated for 30 minutes with increasing concentrations of unlabeled PAH (0-500 μM) diluted in Kaighn's medium lacking serum. The pre-treatment was conducted in a cell culture incubator at 37°C equilibrated with 5% CO_2. Following the pre-incubation period, the medium was aspirated and the cells rinsed rapidly twice with room temperature Kreb's solution prior

to measuring transport. The transport solution contained Kreb's and increasing concentrations of unlabeled PAH (0-500) that mimicked the pre-load composition, and [^{3}H]-PAH (20 nM). The Kreb's solution contained (in mM): 117 NaCl, 4.6 KCl, 20 $NaHCO_3$, 6 mM glucose, 1 mM $MgCl_2$, 1.5 mM $CaCl_2$ and 10 mM hydroxyethyl piperazineethanesulfonic acid (HEPES), pH 7.4. The transport buffer was pre-equilibrated with 95% air/5% CO_2 and maintained at either room temperature or at 37°C prior to transport measurement. Uptake was stopped, the cells lysed, and scintillation counting used for radioactivity detection as described above.

The kinetics of PAH transport was determined using an equation that describes the competitive inhibition of radiolabeled substrate uptake by unlabeled substrate:

$$J = \frac{J_{max}[* PAH]}{K_m + [PAH]} + C$$

J is the rate of PAH uptake from a concentration of unlabeled PAH equal to [PAH]. *[*PAH]* is the concentration of [^{3}H]-PAH in the transport solution. C is defined as the non-saturable component of uptake that is most likely due to factors such as nonspecific binding, incomplete rinsing, and passive diffusion – albeit, the non-saturable component of uptake for the hydrophilic organic anion PAH is minimal. J_{max} is the maximal transport rate, and K_m is the Michaelis constant – i.e., the PAH concentration resulting in half maximal transport.

3.4 Transport Inhibition Studies

All inhibition studies were conducted under zero-*trans* conditions at room temperature using a transport solution containing WB and [^{3}H]-PAH (20 nM). The incubation times are indicated in the figure legends. To examine inhibition potency, the transport solution contained increasing concentrations of OAT1 inhibitor (probenecid, furosemide, indomethacin, omeprazole or telmisartan). The concentration of drug to inhibit uptake by 50% (IC_{50} value) was determined by non-linear regression analysis using the following relationship:

$$J = \frac{J_{app}[* PAH]}{IC_{50} + [I]} + C$$

J is the rate of [^{3}H]-PAH uptake from a concentration of [^{3}H]-PAH in the transport solution equal to [$*PAH$]. IC_{50} is the inhibitor concentration [I] required to reduce substrate uptake by 50%. J_{app} is the apparent maximal transport rate, and C has the same meaning as noted above.

The recovery of inhibition caused by telmisartan, and the time-dependent inhibition caused by telmisartan were also examined – details of the methodology for those experiments are discussed in the Results section.

3.5 PBPK Modeling

The mechanistic kidney model within the Simcyp Simulator version 15 (Certara, Inc) was used for simulating the plasma concentration-time profile and renal tubule cell concentration-time profile of PAH. The simulated plasma concentration time-profile data was fit to the observed clinical data obtained in Prescott et al (Prescott et al., 1993) – the GetData Graph Digitizer 2.26 was used to extract the data from Figure 1A in Prescott et al. This particular data was obtained following intravenous administration of 10 mg · kg^{-1} PAH to 27 healthy male volunteers.

The input parameters for the Simcyp PBPK model are shown in **Table 3.1**. In this model, a blood:plasma partitioning ratio of 1, and a fraction unbound in plasma of 0.83 (Smith et al., 1945) was assumed. Using the full PBPK model, method 2, and a Kp scalar of 0.5, the predicted steady-state volume of distribution (V_{ss}) was 0.18 L · kg^{-1}, which approximates the observed V_{ss} of ~0.23 L · kg^{-1} (Prescott et al., 1993). Given that following intravenous administration the majority of PAH is eliminated in the urine unchanged, and only a small amount of PAH is excreted in the urine as acetyl-PAH (Prescott et al., 1993), no additional clearance pathways were included in the model other than OAT1 at the basolateral membrane and an efflux transporter at the apical membrane of renal tubule cells. Indeed, both the multidrug resistance-associated proteins 2 and 4, which are expressed in apical membranes of proximal tubule cells, transport PAH (Smeets et al., 2004). Although OAT3 is expressed on the basolateral membrane of renal tubule cells along with OAT1, PAH is a poor substrate of OAT3 (Zhang et al., 2004), therefore the model assumes that all PAH uptake into renal tubule cells is due exclusively

to OAT1. Since PAH is extremely hydrophilic, its passive diffusion clearance from blood-to-cell and from cell-to-tubule lumen was assumed to be negligible (zero).

The only parameter that was adjusted in the model was the intrinsic uptake clearance value ($CL_{int} = J_{max}/K_m$) that was obtained under zero-trans conditions at the various incubation time points (15 sec, and 1, 5, 10 and 30 min) or with equilibrium exchange conditions. To mechanistically model transporter involvement in PK requires knowledge of the protein`s absolute abundance (or activity) in the cultured cells and in the whole kidney. Namely, there is a need to know the REF, or the ratio of abundances *in vitro*-to-*in vivo* for proper extrapolation of its activity. Since there is no established data on absolute abundance of OAT1 in the kidney, the CL_{int} value obtained under zero-*trans* conditions at the 15 sec incubation time point (5.5 $\mu l \cdot min^{-1} \cdot$ million $cells^{-1}$) was used in the initial model, and the REF value was then adjusted using 'parameter estimation' within Simcyp, until the simulated data agreed reasonably well with the observed clinical data – this REF value was 7. That is, in order for the simulated data (using kinetic parameters obtained at 15 sec) to fit the observed data reasonably well, Simcyp estimated that there should be seven times more OAT1 protein in the human kidney per million cells compared to per million of the cultured cells. The REF for OAT1 was then fixed at a value of 7 when performing simulations using kinetic parameters obtained at the other time points under zero-*trans* conditions or with equilibrium exchange. Since tubular secretion of PAH requires the concerted activity of uptake mediated by OAT1, and efflux into the tubule lumen, a CL_{int} value of 2 and a REF value of 1 was arbitrarily set for efflux. This was considered reasonable since the intention was to only examine how changes in OAT1-

mediated CL_{int} values determined *in vitro* using different incubation conditions and times influence PK predictions for its prototypical substrate, PAH.

For the trial design, the healthy virtual human population within Simcyp was used. Ten trials with 10 subjects in each trial were performed, using males only, since the data extracted from Figure 1A in Prescott et al., (1993) was from males only. A 10 mg · kg^{-1} intravenous bolus of PAH was administered, and plasma was sampled over a 2-hour period.

3.6 Statistical Analysis

Data are reported as mean ± standard error of the mean. The number of observations (noted in the Legends) are the number of times the experiment was conducted in triplicate on a batch of cells at a different passage number. The effect of incubation time on J_{max}, K_m and CL_{int} values, and on the time-dependent inhibitory effect of telmisartan, was determined by One-Way Analysis of Variance followed by the Tukey's HSD test, where appropriate (see figure legends). Comparison of IC_{50} values at initial-rate versus steady-state was done using a two-tailed unpaired Student's *t*-test. Statistical significance was set at the $p < 0.05$ level. All non-linear regression and statistical analysis were done with GraphPad Prism (version 5.04; GraphPad Software, La Jolla, CA).

Table 3. 1 Physicochemical and *in vitro* pharmacokinetic parameters of *p*-aminohippuric acid

Parameter	Value	Method/Reference
Physicochemical properties		
Molecular weight	194.2	
Log$P_{o:w}$	-2.2	Experimental, https://www.drugbank.ca/drugs/DB00345 (Jan 2018)
pKa	3.83	
Compound type	Monoprotic acid	Experimental, https://www.drugbank.ca/drugs/DB00345 (Jan 2018)
Blood binding		
B/P	1	Assumed
fu_{plasma}	0.83	Measured, (Smith et al., 1945)
Distribution		
Full PBPK model		
Predicted V_{ss} (L/kg)	0.18	Method 2, (Rodgers & Rowland, 2007)
K_p scalar	0.5	Estimated based on IV PK profile
Observed V_{ss} (L/kg)	0.232	Measured, (Prescott et al., 1993)
Elimination		
Mechanistic Kidney Model		
$fu_{kidney,cell}$	1	Assumed
fu_{urine}	1	Assumed
Transport		
$CL_{PD,basal}$ ($\mu L.min^{-1}$. million $cells^{-1}$)	0	Assumed to be low based on physicochemical properties
$CL_{PD,apical}$ ($\mu L.min^{-1}$. million $cells^{-1}$)	0	Assumed to be low based on physicochemical properties

Table 3. 1 Physicochemical and *in vitro* pharmacokinetic parameters of *p*-aminohippuric acid

Parameter	Value	Method/Reference
$CL_{int,\ apical}$ ($\mu L.min^{-1}$. million $cells^{-1}$)	2	RAF/REF = 1; Assumed
$CL_{int,\ basal}$ ($\mu L.min^{-1}$. million $cells^{-1}$)	variable	RAF/REF = 7; Optimized by parameter estimation

B/P Blood:plasma ratio; $CL_{int,\ apical}$ in vitro intrinsic apical efflux clearance; $CL_{int,\ basal}$ in vitro intrinsic basolateral uptake clearance; CL_{PD} Passive diffusion clearance; $fu_{kidney,cell}$ Fraction unbound in kidney cells; fu_{plasma} Fraction unbound in plasma; fu_{urine} Fraction unbound in urine; *IV* Intravenous; K_p Partition coefficient; *PBPK* physiologically based pharmacokinetic; *pKa* Acid dissociation constant; $P_{o:w}$ Partition coefficient octanol:water; V_{ss} volume of distribution at steady-state.

CHAPTER 4 RESULTS

4.1 Time Course of PAH Uptake into CHO-OAT1

To establish initial-rate and steady-state time points the time course of PAH uptake (zero-*trans* at initiation of transport measurement) into CHO-OAT1 cells was examined. **Figure 4.1** shows the uptake of PAH at different incubation times using four different concentrations of PAH (0.02, 10, 50 or 100 μM). At all four PAH concentrations, uptake was near-linear for ~5 minutes, and approached steady-state at ~10 minutes. Increasing concentrations of PAH (0.02 μM – 100 μM) did not appear to affect the initial-rate, or the time to steady-state. There was no appreciable accumulation of PAH in CHO cells that were not stably transfected with OAT1 (data not shown).

4.2 Effect of Time on Transport Kinetics

Next, the kinetics of PAH uptake (zero-*trans*) at initial-rate (15 sec) and approximate steady-state (10 min) was determined in a single representative experiment to see how the time point chosen influences the kinetic parameters, J_{max} and K_m (**Figure 4.2**). The non-linear regression analysis used in Figure 4.2 are competitive inhibition kinetics, where unlabeled substrate competes for transporter-mediated uptake of labeled substrate, which is being measured. Consequently, the intracellular concentration of [^{3}H]-PAH went down

with increasing concentrations of unlabeled PAH. In the absence of unlabeled PAH in the transport buffer, the uptake of [^{3}H]-PAH was ~4 times greater at initial-rate than steady-state. In this experiment the J_{max} value was two-fold lower at steady-state compared to initial-rate (16. 2 vs. 8.1 pmol · min^{-1} · 10^6 cells), and the K_m value was approximately two-fold higher at steady-state (4.2 vs. 7.6 μM). This observation led me to examine in more detail the effect of incubation time on these kinetic parameters. **Figure 4.3** shows the effect of increasing incubation time (15 sec to 45 min) on the J_{max}, K_m and CL_{int} (J_{max}/K_m) values. There was a significant decrease in the J_{max} value with time (**Figure 4.3A** and **Table 4.1**). There was also a significant effect of incubation time on the K_m value ($P < 0.05$, One-Way ANOVA), where it appeared to be higher at longer incubation times (**Figure 4.3B and Table 4.1**). Due to changes in both J_{max} (decrease) and K_m (apparent increase), CL_{int} decreased significantly with increasing time (**Figure 4.3C** and **Table 4.1**). From 15s to 45 min, the CL_{int} ranged 11-fold.

4.3 Equilibrium Exchange Experiments

Equilibrium exchange experiments were conducted at room temperature versus 37^0C to see how equilibrium exchange kinetics differ from zero-*trans* kinetics, and the effect of temperature under equilibrium exchange conditions. **Figure 4.4** shows the effect of temperature (37^0C vs. room temperature) on PAH transport kinetics under equilibrium exchange conditions. In this experiment, the uptake of ^{3}[H]PAH was ~2 times greater at 37^0C than at room temperature. There was a significant effect of temperature on the J_{max} and K_m values. The J_{max} value was approximately four-fold higher at 37^0C compared to

room temperature (54.7 ± 5.8 vs. 15 ± 2.1 pmol· min^{-1} · million $cells^{-1}$, p<0.05, two-tailed unpaired student's t-test), and the K_m value was approximately two-fold higher at 37^0C (7.8 ± 1.2 μM vs. 4.4 ± 0.3 μM; p<0.05, two-tailed unpaired student's t-test). The CL_{int} was two-fold higher at 37^0C compared to room temperature (7.2 ± 0.5 vs. 3.3 ± 0.3 μl · min^{-1} · million $cells^{-1}$; p<0.05, two-tailed unpaired student's t-test). Since zero-*trans* kinetic experiments were done at room temperature, the zero-*trans* kinetic parameters were compared to equilibrium exchange kinetics at room temperature to see how they differ. At approximate initial-rate, there was no significant difference in the kinetic parameters (J_{max} or K_m) determined under zero-*trans* compared to equilibrium exchange conditions. The J_{max} values were 15 ± 2.1 vs. 24. ± 9.9 pmol · min^{-1} · million $cells^{-1}$, and the K_m values were 4.4 ± 0.3 vs. 4.4 ± 0.5 μM, at equilibrium exchange versus zero-*trans* conditions, respectively. Consequently, there was no significant difference in the CL_{int} values determined under equilibrium exchange and zero-*trans* conditions (3.3 ± 0.3 vs. 5.5 ± 1.6 μl · min^{-1} · million $cells^{-1}$, respectively).

4.4 PBPK Model Predictions

To show the impact of changes in transport kinetic parameters on PK predictions, the CL_{int} values obtained at the different incubation time points (zero-*trans*) were used to simulate the plasma concentration-time profile of PAH. Also modeled was the PAH concentration in proximal tubule cells over time. Using the CL_{int} value obtained at 15 sec and parameter estimation of the OAT1 REF value, the predicted and observed clinical

plasma concentration-time profiles agreed reasonably well (**Figure 4.5A**). There was little effect of incubation time on the simulated C_{max} values, with values of ~50 ng · mL^{-1} in all scenarios. In contrast, the simulated plasma $AUC_{0-\infty}$ and plasma clearance were sensitive to changes in CL_{int} (**Figure 4.5A**). The simulated $AUC_{0-\infty}$ ranged from 23.5 mg · L^{-1} · h^{-1} (CL_{int} at 15 sec) to 45.2 mg · L^{-1} · h^{-1} (CL_{int} at 30 min), and the plasma clearance from 31.4 L · h^{-1} (CL_{int} at 15 sec) to 17. 4 L · h^{-1} (CL_{int} at 30 min) – both ~1.8-fold differences in predictions. The predicted C_{max} values for the intracellular concentration of PAH in proximal tubule cells was 710 ng · mL^{-1} (CL_{int} at 15 sec) versus 91 ng · mL^{-1} (at 30 min) – a 7.8-fold difference in predictions (**Figure 4.5B**).

The CL_{int} values obtained under equilibrium exchange conditions (at room temperature and 37ºC) were also used to simulate the plasma concentration-time profile of PAH (**Figure 4.6A**), as well as its concentration in proximal tubule cells over time (**Figure 4.6B**). Temperature had only a modest effect on the plasma $AUC_{0-\infty}$, C_{max} and clearance. The simulated plasma $AUC_{0-\infty}$ under equilibrium exchange conditions at room temperature and 37ºC were 21.3 and 17.2 mg · L^{-1} · h^{-1}, respectively. The simulated plasma C_{max} values at room temperature vs. 37ºC were 53.7 vs. 50.0 ng · mL^{-1}. Temperature had the largest impact on plasma clearance, with values of 35.0 L · h^{-1} (room temperature) and 50.0 L · h^{-1} (37°C) – a 1.4-fold difference. The predicted C_{max} values for the intracellular concentration of PAH in proximal tubule cells at room temperature and 37ºC were 549 and 1039 ng · mL^{-1}, respectively – an approximate 2-fold difference in predictions.

4.5 Effect of Time on Inhibition Potency

Given the significant effect of time on the K_m value, the influence of time on the potency with which five different drugs (probenecid, furosemide, indomethacin, omeprazole, telmisartan) inhibit the 15 sec versus 10 min uptake of PAH by OAT1 was further investigated (**Figure 4.7 and Table 4.2**). Fifteen seconds and 10 min were used as the approximate initial-rate and steady-state time points, respectively. Inhibition potency for omeprazole and furosemide did not change significantly with time. However, inhibition potency for the remaining three drugs was sensitive to incubation time. There was an ~2-fold decrease in inhibition potency for indomethacin at steady-state, whereas inhibition potency of probenecid increased by ~2-fold with the longer incubation time. Telmisartan was ~7-fold more potent when performing uptake at 10 min versus 15 sec.

The relatively large increase in inhibition potency with time caused by telmisartan led to further exploration of the time-dependent nature of inhibition (**Figure 4.8**). In these experiments the CHO-OAT1 cells were pre-incubated with telmisartan at four different concentrations (10 nM, 50 nM, 100 nM or 200 nM) for 1 min, 5 min, 10 min or 30 min, followed by measurement of PAH uptake for 15 sec. There was a significant effect of time on PAH uptake at all four concentrations of telmisartan tested (**Figure 4.8**). The reduction in PAH uptake was significantly different from 1 to 5 min, but there was no significant time-dependent effect thereafter. In order to test the reversibility of telmisartan inhibition after long incubations (e.g., such as 30 min in Figure 4.8), the recovery of PAH transport following the pre-treatment of cells for 30 min with telmisartan (0.5 μM) was investigated in a separate set of experiments. Given the hydrophobicity of telmisartan,

and the drug's high propensity for protein binding, following telmisartan exposure, the cells were rinsed and incubated in WB containing 10% FBS for 2, 5, 10, 20 or 30 min prior to measuring the uptake of PAH for 15 sec. Near-complete recovery of PAH uptake was observed after 20 minutes' recovery following telmisartan exposure (**Figure 4.9**), indicating that the inhibitory effect of telmisartan is reversible, albeit slowly.

To show the potential impact of the relatively large differences in IC_{50} values at initial-rate vs. steady state observed for telmisartan, I used the Mechanistic Kidney model in Simcyp to show the effect of changing an IC_{50} value of a perpetrator drug 7-fold on PAH PK. Here I took advantage of the fact that already contained within Simcyp is a model for the well-known OAT1 inhibitor, probenecid (a uricosuric). Within the probenecid model the K_i value of probenecid against OAT1 is 4.0 μM. I ran a clinical DDI trial with PAH as the victim drug using model parameters from equilibrium exchange done at 37°C (CL_{int} for OAT1 of 7.2 $\mu L \cdot min^{-1} \cdot 10^6$ $cells^{-1}$), with probenecid given I.V. bolus (500 mg), and using IC_{50} values against OAT1 of 4.0 vs. 0.6 μM. **Figure 4.10** shows the simulated plasma concentration-time profile for PAH in the absence vs. presence of probenecid administered simultaneously using the 7-fold difference in K_i values. At 4.0 μM the AUC ratio was predicted to be 1.5-fold higher in the presence vs. absence of probenecid. There was only a modest effect of increasing probenecid inhibition potency 7-fold, where the DDI magnitude went from 1.5-fold to 1.9-fold.

Table 4. 1 Effect of time on OAT1 transport kinetics

Substrate	Incubation Time	J_{max}	K_m	CL_{int}
		pmol. min^{-1}. 10^6 cells^{-1}	*µM*	*µl.min^{-1}. 10^6 cells^{-1}*
PAH	15 sec	24.9 ± 9	4.4 ± 0.6	5.5 ± 1.6
	1 min	21.3 ± 7.7	4.4 ± 0.5	4.8 ± 1.6
	5 min	16 ± 5.1	6.7 ± 0.7	2.4 ± 0.7
	10 min	9.1 ± 1.7	7 ± 0.6	1.4 ± 0.4
	30 min	6.7 ± 4.9	5.3 ± 0.4	1.2 ± 0.07
	45 min	3.9 ± 2.7	6.8 ± 0.3	0.5 ± 0.3

Data are mean ± SEM of four experiments. Significant differences in kinetic parameters determined at different time points (15 sec to 45 min) were determined by One-Way ANOVA, $P < 0.05$, followed by the Tukey's HSD test.

Table 4. 2 The effect of time on potency of OAT1 inhibition.

Inhibitor	IC_{50} against PAH uptake		Fold change
	15 sec	10 min	
	μM		
Omeprazole	9.7 ± 0.8	9.2 ± 0.8	-1.1
Furosemide	19.6 ± 3	15.1 ± 2.2	-1.3
Indomethacin	5.9 ± 0.5	*12.7 ± 1.4	+2.2
Probenecid	9.3 ± 1.3	*5.1 ± 0.6	-1.8
Telmisartan	0.4 ± 0.07	*0.06 ± 0.02	-6.7

Data are mean ± SEM of four experiments. * indicates significant differences in IC_{50} values (between 15 sec and 10 min uptake) determined by unpaired Student's *t* test, $P< 0.05$, + and – indicate an increase and decrease respectively.

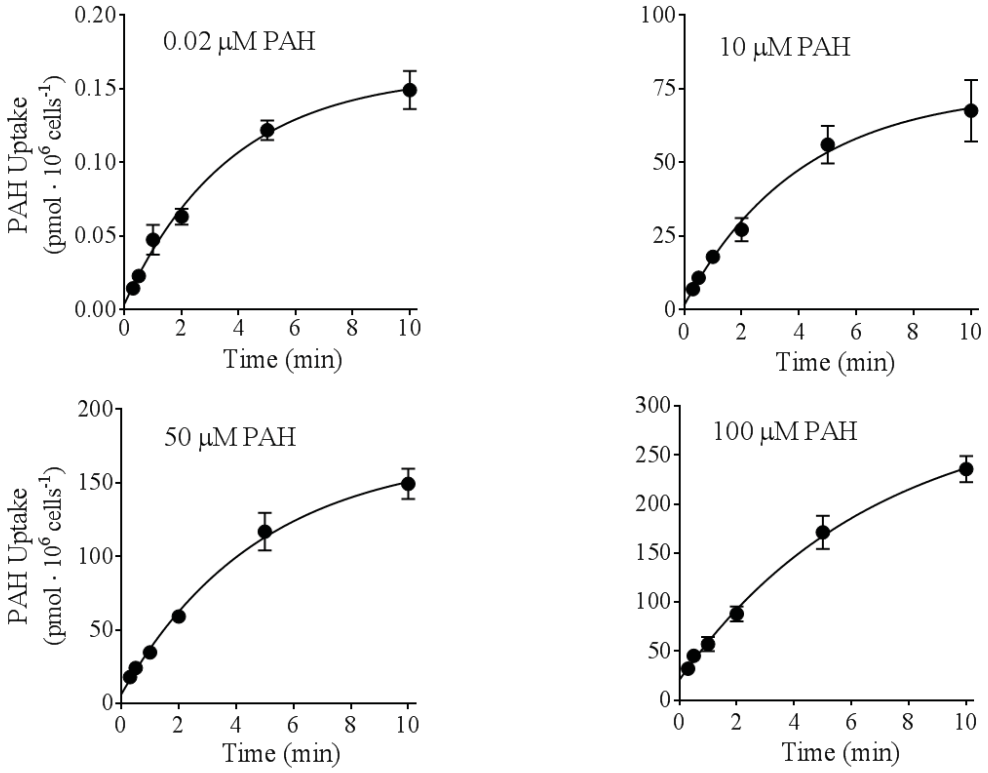

Figure 4. 1 Time course of PAH uptake into CHO-OAT1. To establish initial rate and steady-state time points the time course of PAH uptake at different incubation times was determined using four different concentrations of PAH; 0.02 μM **(A)**, 10 μM **(B)**, 50 μM **(C)** and 100 μM **(D)**. At all four PAH concentrations, uptake was near linear for ~5 minutes, and approached steady-state at ~10 minutes. Data are expressed as mean ± SEM of three observations.

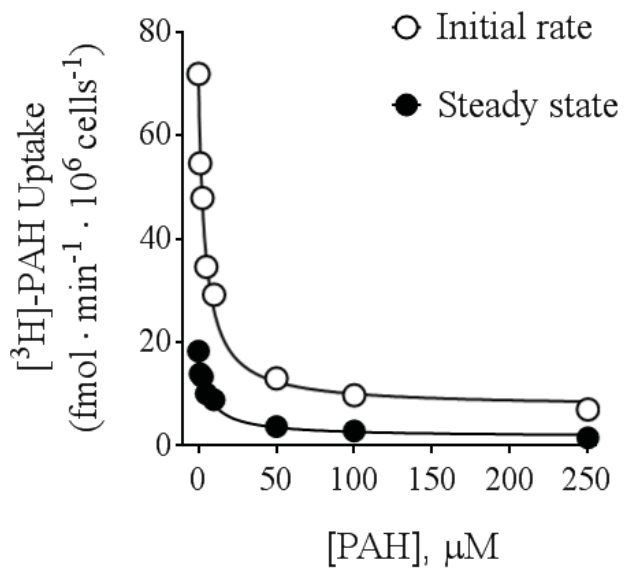

Figure 4. 2 Effect of time on transport kinetics. The kinetics of [^{3}H]-PAH uptake at initial rate (15 sec) and approximate steady-state (10 min) was determined in a single representative experiment. J_{max} value decreased dramatically at steady-state compared to initial-rate, and a modest increase in the K_m value.

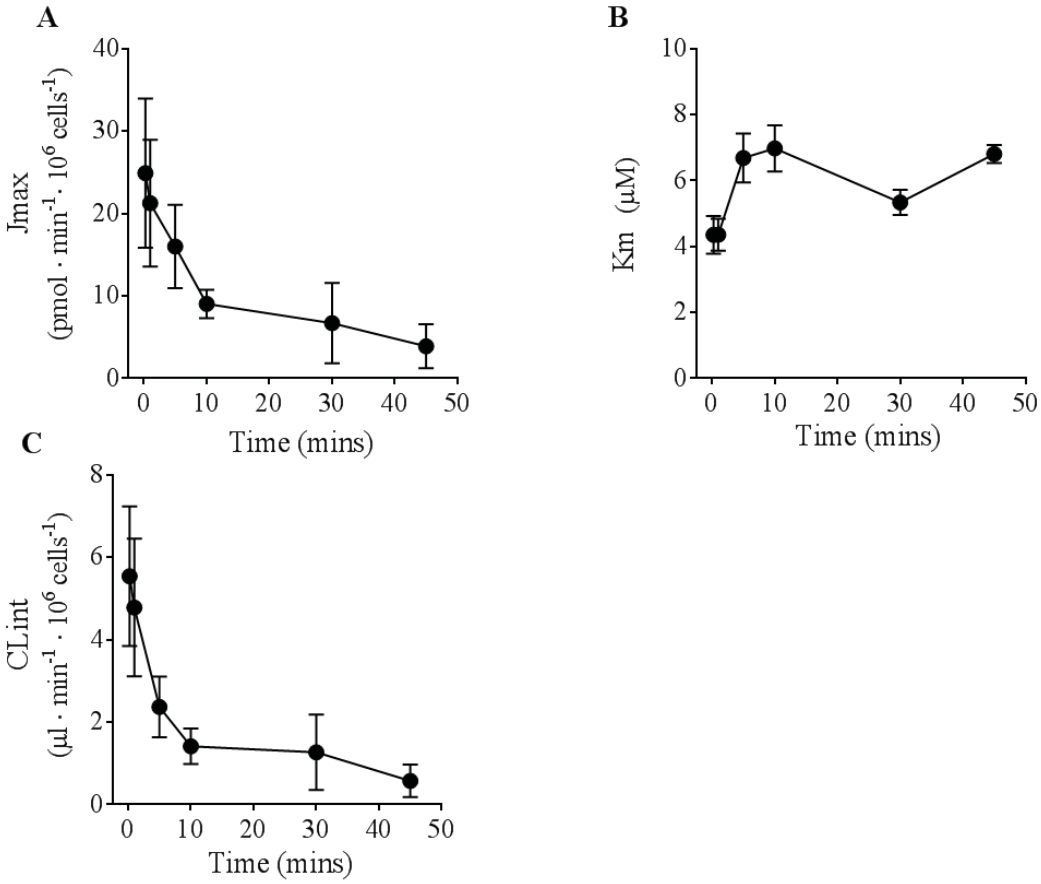

Figure 4. 3 Effect of time on transport kinetics under zero-*trans* conditions. The effect of increasing incubation time on the J_{max}, K_m and CL_{int} (J_{max}/K_m) values was determined. The kinetic constants obtained at each time point are summarized in Table 4.1. Significant differences between kinetic parameters determined at different time points (15 s to 45 min) were determined by one-way ANOVA, $P < 0.05$. There was a significant decrease in the J_{max} value and a significant effect of time on the K_m value. Consequently, the CL_{int} value decreased significantly with time. Data are the mean ± SEM of four experiments.

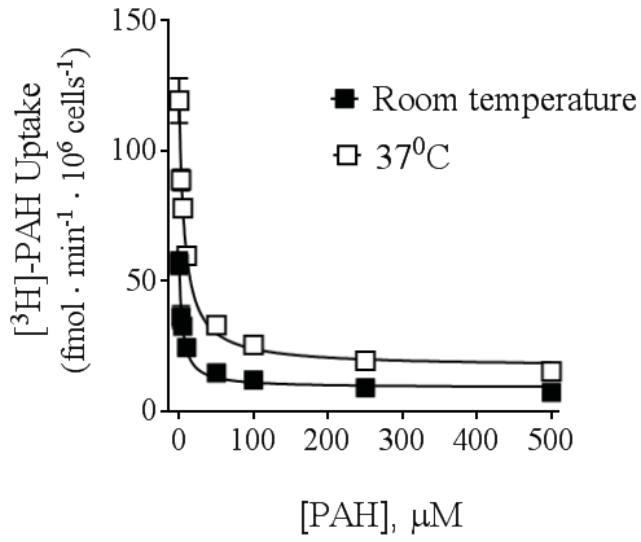

Figure 4. 4 Transport kinetics under equilibrium exchange conditions. CHO-OAT1 cells were pre-exposed for 30 min to increasing concentrations of unlabeled PAH (0-500 μM). The uptake of [^{3}H]-PAH was then determined at either room temperature or 37^{0}C, in the presence of increasing concentrations of unlabeled PAH (0-500 μM). Data are expressed as mean ± SEM of four experiments.

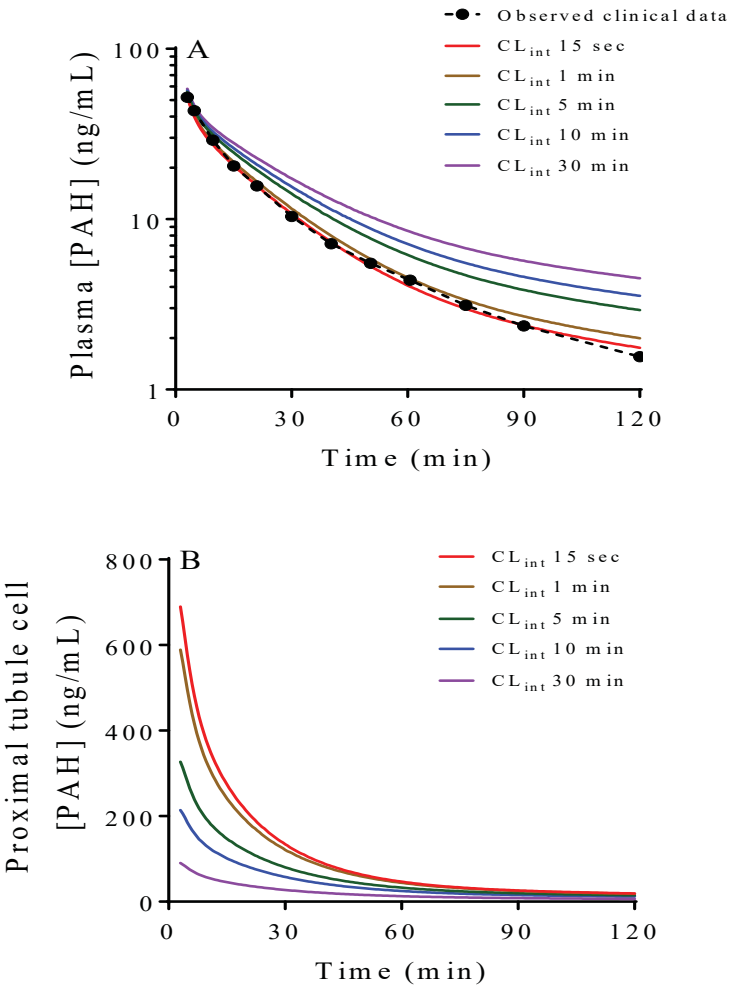

Figure 4. 5 PBPK model predictions under zero-*trans* conditions. CL_{int} values obtained at the different incubation time points were used to simulate the plasma concentration-time profile **(A)**, and intracellular concentrations of PAH in proximal tubule cells over time **(B)**. There was little effect of incubation time on the simulated plasma C_{max} values in all scenarios. There was a 1.8-fold difference in predictions of both the plasma clearance and $AUC_{0-\infty}$, due to changes in CL_{int} (15 sec vs. 30 min). The predicted C_{max} values for the intracellular concentration of PAH in proximal tubule cells showed a 7.8-fold difference in predictions (15 sec vs. 30 min).

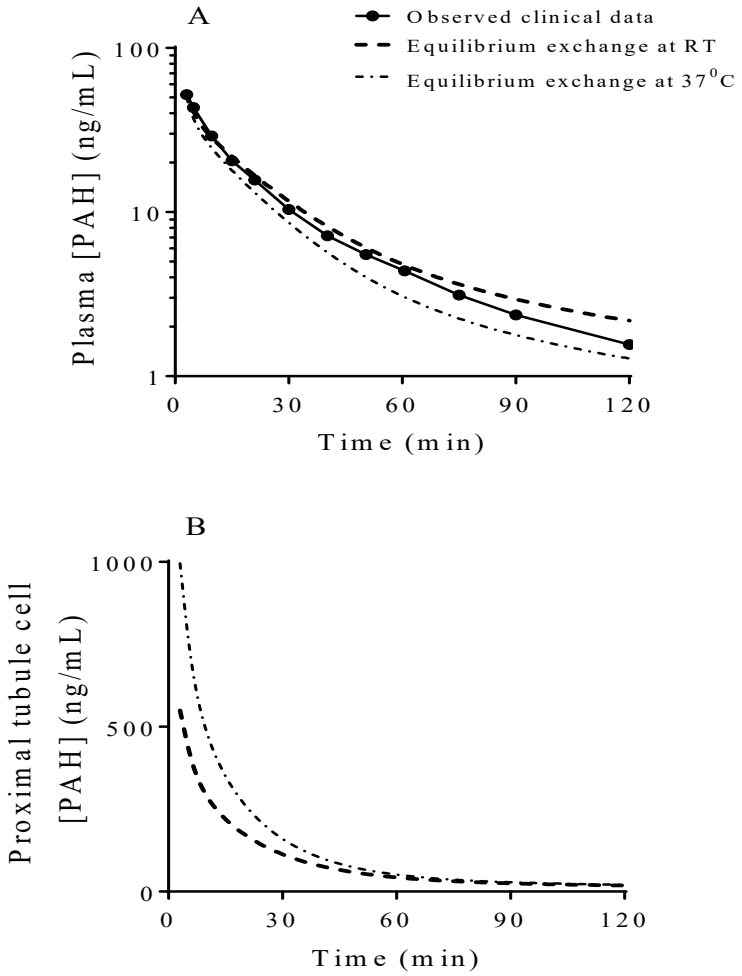

Figure 4. 6 PBPK model predictions under equilibrium exchange conditions. The CL_{int} values obtained at room temperature versus 37^0C under equilibrium exchange conditions were used to simulate the plasma concentration-time profile **(A)**, and intracellular concentrations of PAH in proximal tubule cells over time **(B)**. There was only a modest effect of temperature on the plasma $AUC_{0-\infty}$ and C_{max}. Temperature had the largest impact on the simulated plasma clearance and intracellular concentrations of PAH in the proximal tubule cells; with a 1.4-fold and 2-fold difference in predictions, respectively (37ºC vs. room temperature).

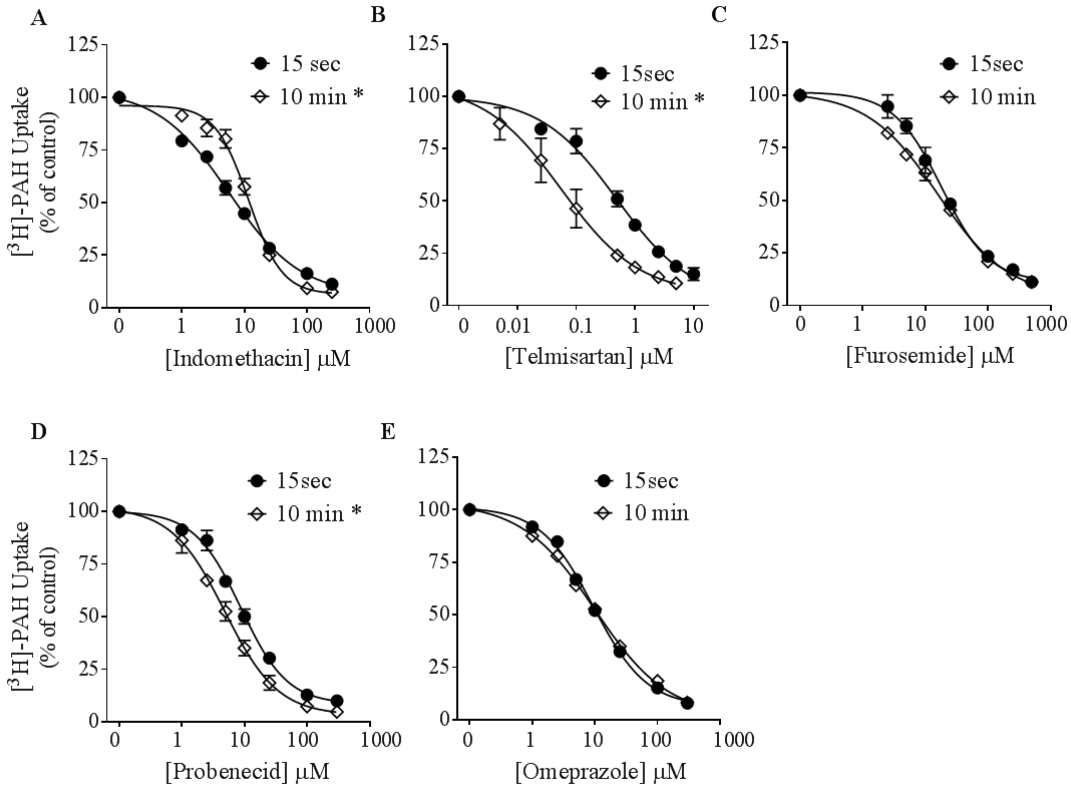

Figure 4. 7 Effect of time on inhibition potency. Inhibition of the 15 sec (approximate initial-rate) versus 10 min (approximate steady-state) uptake of [^{3}H]-PAH into CHO-OAT1 cells was determined in the presence of increasing concentrations of selected OAT1 inhibitors. IC_{50} values are summarized in Table 4.2. Data are the mean ± SEM of four observations and are expressed as a percentage of the control uptake done in the absence of inhibitor. *, indicates significant difference between IC_{50} values at 15 sec vs. 10 min, unpaired Student's *t* test, $P<0.05$.

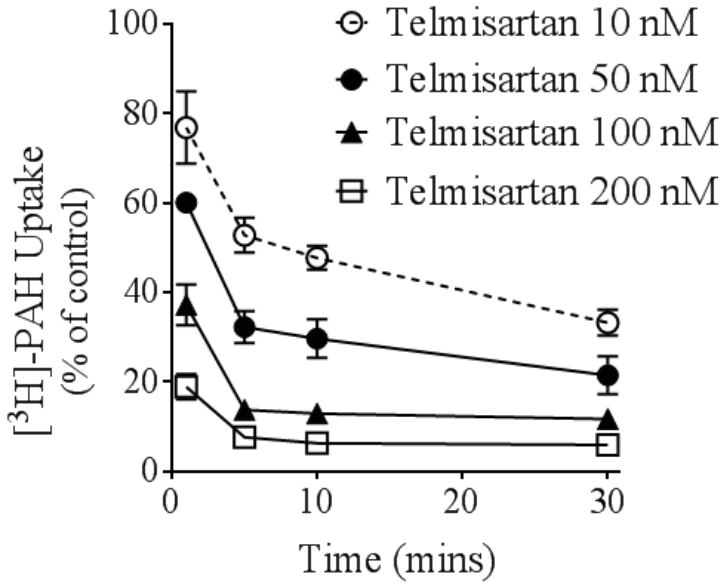

Figure 4. 8 Time-dependent inhibition of OAT1 by telmisartan. CHO-OAT1 cells were pre-incubated with telmisartan at four different concentrations (10 nM, 50 nM, 100 nM or 200 nM) for 1, 5, 10 or 30 minutes, followed by the measurement of PAH uptake for 15 sec. There was a significant effect of time on PAH uptake at all four concentrations tested; One-Way ANOVA, $P<0.05$. The reduction in PAH uptake was significantly different from 1 to 5 min, but there was no significant time-dependent effect from 5 to 30 min; Tukey's HSD test.

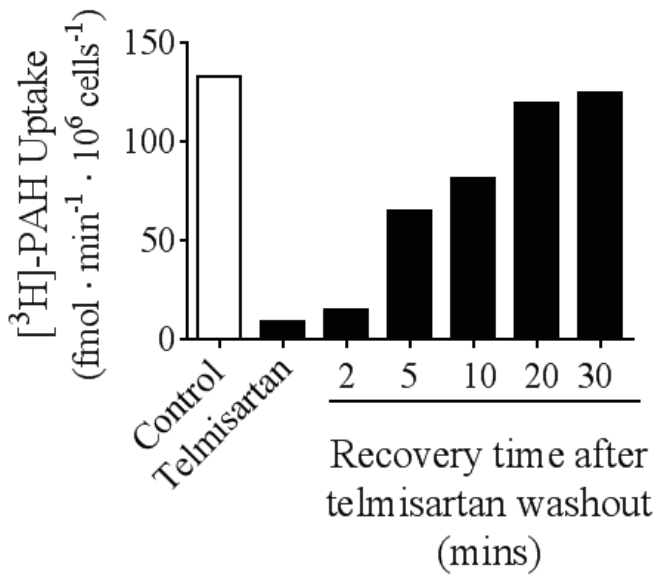

Figure 4. 9 Time course of recovery of OAT1-mediated [^{3}H]-PAH uptake by CHO-OAT1 cells after treatment with telmisartan. In a single experiment, the cells were pre-treated for 30 mins with telmisartan (0.5 μM). or no telmisartan (control). Following telmisartan exposure, the cells were rinsed and incubated in Waymouth buffer containing 10% fetal bovine serum for the time points indicated (recovery time after telmisartan washout) prior to measuring the uptake of PAH for 15 sec. Near-complete recovery of PAH uptake was observed after 20 minutes' recovery following telmisartan exposure.

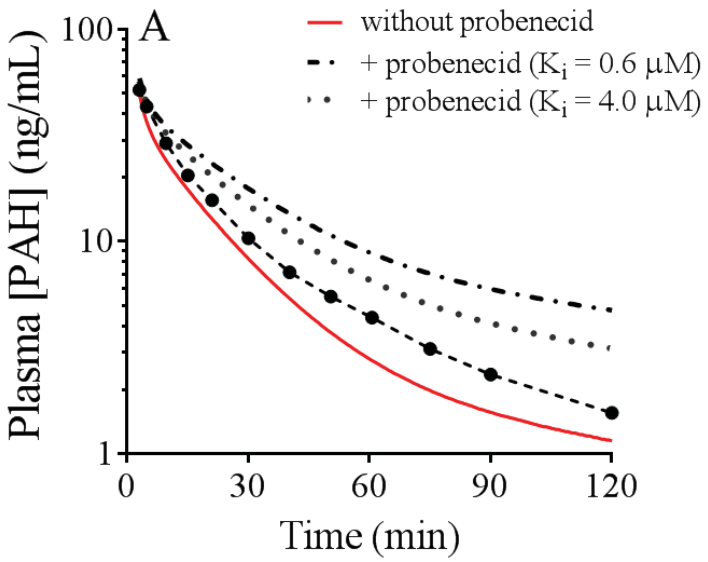

Figure 4. 10 PBPK simulation of the effect of increasing inhibition potency on PAH pharmacokinetics. The plasma concentration-time profile for PAH in the absence vs. presence of probenecid administered simultaneously was simulated using a 7-fold difference in K_i values (4.0 and 0.6 μM). At 4.0 μM, the AUC ratio was predicted to be 1.5-fold higher in the presence vs. absence of probenecid. A 7-fold increase in probenecid inhibition potency (0. 6 μM) increases the DDI magnitude from 1.5-fold to 1.9-fold.

CHAPTER 5 DISCUSSION

5.1 Overview

The present study examined the influence of incubation time on ligand interactions with OAT1 and its influence on PBPK predictions. The kinetic parameters of transport, J_{max} and K_m, which define the *in vitro* intrinsic uptake clearance (CL_{int}) of a drug substrate, are important parameters in the functional assessment and characterization of drug transport, and are essential input parameters required for mechanistic PBPK modeling that is used in drug development (Jones et al., 2012; Rostami-Hodjegan, 2012). Indeed, PBPK predictions are useful in guiding clinical plans for NMEs, and have been used for a variety of predictions in drug development, including first-in-human dose, DDIs, and the impact of renal and hepatic impairment on PK (Poirier et al., 2009; Rostami-Hodjegan, 2012; Zhao et al., 2011). Determination of kinetic parameters for uptake transporters are routinely done *in vitro* using heterologous expression systems, typically under initial-rate conditions, where substrate uptake is linear with time (Zamek Gliszczynski et al., 2013). These conditions are referred to as 'sink' or 'zero-*trans*' conditions, since upon initiation of uptake the substrate concentration inside of the cell is zero (Ginsburg & Ram, 1975). At initial-rate the predominant direction of flux is from extracellular to intracellular, whereas at steady-state the rates of influx and efflux are equal. Since OAT1 is an obligatory exchanger, and PAH has a low passive permeability,

at steady-state PAH flux likely occurs predominantly via translocation on OAT1, with some flux occurring via PAH/PAH self-exchange.

5.2 *In Vitro* Time of Incubation Influences OAT1 Transport Kinetics

It is unclear what effect incubation time has on transport kinetics under initial zero-*trans* conditions. This raised the question of how kinetic parameters of OAT1-mediated transport differ based on the incubation time used. Before performing kinetic experiments, the uptake of PAH was measured at four different concentrations to determine if the time course is influenced by substrate concentration. The concentrations of PAH tested were well below the K_m value (0.02 μM), at the ~K_m value (10 μM), and ~5-fold (50 μM) and ~10-fold (100 μM) above the K_m value. Despite large differences in concentration, the time courses were qualitatively similar, indicating that initial-rate and time to steady-state are equivalent across all substrate concentrations tested in saturation kinetic experiments.

The effect of incubation time (15sec – 45 min) on the kinetics of PAH transport was then examined. As incubation time increased there was a dramatic decrease in the J_{max} value. Maximal transport rate is a function of the number of functional transporters in the plasma membrane and each transport protein's turnover number (i.e., the number of translocation events per unit time). Hotchkiss et al, showed using cell surface biotinylation that OAT1 expression level at the cell surface does not change appreciably over a 60 minute *in vitro* experiment (Hotchkiss et al., 2015), ruling out possible changes

in the number of transporters as a reason for the decrease in J_{max} observed here. Since the units of J_{max} are expressed per unit time it is logical that the J_{max} value decreased as time increased. The reduction in the J_{max} values at longer incubation times can also be rationalized by the decrease with time in the inwardly-directed PAH gradient as steady-state is approached. That is, at steady-state there is bidirectional flux of PAH (i.e., PAH/PAH self-exchange), versus the predominant influx of PAH at initial-rate time points (i.e., PAH/α-ketoglutarate exchange).

There also appeared to be a modest increase in the K_m value at longer incubation times, and as a consequence of the decrease in J_{max} and increase in K_m, the CL_{int} decreased with increasing time as well. CL_{int} is an important input parameter required for mechanistic PBPK modeling. Using the CL_{int} values obtained at the various time points and Simcyp, this study showed a nearly two-fold difference in the predicted plasma $AUC_{0-\infty}$, and an even more dramatic effect of incubation time on the predicted proximal tubular cell C_{max} and $AUC_{0-\infty}$. My results show that the time point chosen for *in vitro* transport experiments influences the predictive capability of mechanistic PBPK modeling, and this most certainly holds for all transporters, not simply OAT1. Importantly, it is recommended to consider proceeding to a clinical DDI study if predictive methods (static or mechanistic modeling) suggests a greater than 2-fold change in exposure (AUC ratio $\geq$2) in the presence of perpetrator drugs (Brouwer et al., 2013). Thus, two-fold differences in predictions, as shown here, could be a factor in deciding the course for clinical development of NMEs.

5.3 Effect of *In Vitro* Time of Incubation on Inhibition Potency against OAT1

The modest apparent increase in the K_m value for PAH transport at longer incubation times led to the speculation that the potency of OAT1 inhibition may be sensitive to incubation time as well. The potency with which five drugs inhibit OAT1 was tested at either initial-rate (15 sec) or approximate steady-state (10 min). Drugs with a variety of inhibition mechanisms were chosen, including competitive (probenecid, indomethacin and furosemide), mixed-type (omeprazole), and non-competitive (telmisartan). IC_{50} values were sensitive to incubation time for some inhibitors, but not all. There was no change in IC_{50} values for omeprazole and furosemide, a decrease for probenecid, and increases for indomethacin and telmisartan. IC_{50} values (or K_i values) are used in both static and dynamic (i.e., PBPK) models to predict transporter-mediated DDI potential and its clinical relevance (US Food Drug Administration, 2017). Importantly, an ~7-fold magnitude difference in IC_{50} value, such as was observed with telmisartan here, could be a deciding factor as to whether or not to conduct a clinical DDI trial. At an 80 mg dose the unbound plasma concentration of telmisartan is ~10 nM (Taylor et al., 2011). Thus, based on the IC_{50} values obtained at 15s (0.4 μM) and 10 min (0.06 μM), telmisartan could cause a DDI if the K_i value *in vivo* is 0.06 μM, based on the static model. That is, the $[I_{u,max}]/K_i$ ratio for telmisartan ranged between 0.025 (at 15 s) and 0.17 (at 10 min), which at 0.06 μM is higher than the ratio of >0.1 that would potentially trigger a clinical DDI study. However, I am unaware of any clinical DDIs between telmisartan and OAT1 substrates, albeit, this requires further investigation. Differences in PK predictions, as illustrated with a simulation of the probenecid-PAH DDI could be important since the

AUC ratio when using a 7-fold lower probenecid K_i value of 0.6 μM is close to what would potentially trigger a clinical DDI study (≥2-fold change in AUC).

There is considerable experimental data to suggest that transport proteins alternate between outward- and inward-facing conformations during substrate translocation (Diallinas, 2014). There is also evidence showing that during translocation there are structural rearrangements in transmembrane helices that lead to alteration in the physical location of amino acids in the ligand binding pocket of transport proteins. For example, multi-targeted molecular dynamic simulations with P-gp show that it goes from an inward-facing to an outward-facing conformation, and that during this transition there are conformational changes in transmembrane helices and in amino acid residues lining the drug-binding pocket (Prajapati & Sangamwar, 2014). With respect to organic anion exchangers, it has been proposed that during substrate translocation OAT1 'switches' between extracellular-facing and intracellular-facing conformations (Kaler et al., 2007). Ultimately, bending or movement of helices during the translocation step of OAT1 could result in a change in the availability of different amino acids for ligand binding. Based on this "switching" hypothesis, I speculate that at initial-rate time points where flux of substrate into the cell is largely from extracellular to intracellular, the ligand interacts predominately with the exchanger in its extracellular-facing conformation. Alternatively, at steady-state, where flux is bidirectional, the ligand interacts with the ligand binding region in both its extracellular- and intracellular-facing conformations (**Figure 5.1**). It is possible that structural rearrangements in helices during translocation influences the amino acids available for interaction with ligand, and that differences in IC_{50} values at initial-rate vs. steady-state reflect differences in binding affinity of the ligand for the

extracellular- vs. intracellular-facing conformations, assuming that IC_{50} values are reflective of K_d values. Indeed, Kimura et al. used frontal affinity chromatography with OAT1 immobilized to a column and showed that while IC_{50} values and dissociation constant (K_d) values differ several fold, there is a significant correlation between the two (Kimura et al., 2007). In cases where IC_{50} values were higher at steady-state (indomethacin), suggests that there is a lower affinity of the ligand for the intracellular-facing conformation, and the reverse is true in cases where the IC_{50} was lower at steady-state (probenecid and telmisartan). Similar IC_{50} values (furosemide and omeprazole) under both conditions suggests similar affinities for ligand binding in the intracellular- and extracellular-facing conformations. For the substrate PAH, there was an apparent increase in its K_m value with increasing time when *in vitro* experiments were conducted under zero-*trans* conditions. These data suggest that PAH has a lower affinity for the ligand binding region in its inward-facing conformation than outward-facing. Although I have not done the experiment, I anticipate examining the potency with which PAH inhibits transport of another OAT1 substrate (e.g., cidofovir) conducted at initial-rate vs. steady-state would be confirmatory.

The influence of the chosen time point on inhibition potency was an interesting observation since it varied from no change to decreased or increased inhibition potency. Previous studies have reported a 5- to 20-fold increase in inhibition potency of cyclosporin A towards OATP1B1 and OATP1B3 following a longer pre-incubation time (30 min to 1 hour) compared to a brief co-incubation time (Amundsen et al., 2010; Gertz et al., 2013). In these studies, it was not known whether the shifts in IC_{50} values were due to a time-dependent inhibition mechanism (mechanism-based inhibition) or some other

mechanism. Previous work with OAT1 showed the ability of transport activity to recover after brief treatment and removal of telmisartan, indicating that binding of telmisartan to OAT1 is reversible, albeit slowly (Hotchkiss et al., 2015), likely ruling out a covalent-type mechanism-based inhibition. However, when classical time-dependent inhibition studies were conducted, as would be done for cytochrome P450s, the effect of incubation time on the extent of OAT1 inhibition by telmisartan was significant, indicating that telmisartan is in fact a time-dependent inhibitor. Perhaps this time-dependent inhibition is due to the time it takes telmisartan to diffuse into the cell and access the OAT1 ligand binding region in its intracellular-facing conformation, where it has greater affinity.

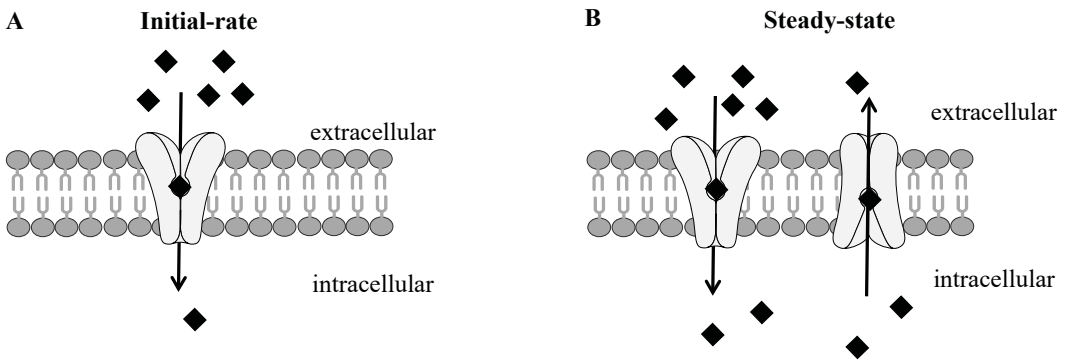

Figure 5. 1 Hypothesis for differences in transport and inhibition kinetic parameters at initial-rate and steady-state time points. During substrate translocation, anion exchangers, like OAT1, alternate between extracellular- and intracellular-facing conformations. At initial-rate time points, where flux of substrate into the cell is predominantly from extracellular to intracellular, the ligand interacts with the exchanger predominately in its extracellular-facing conformation. Alternatively, at steady-state, where flux is bidirectional, the ligand interacts with the ligand binding region in both conformations. Structural rearrangements in helices during translocation likely influence amino acids available for interaction with ligand, and thus, differences in K_m and IC_{50} values at initial-rate versus steady-state reflect differences in binding affinity of the ligand for the extracellular- versus intracellular-facing conformations of the transport protein.

5.4 OAT1 Transport Kinetics Under Equilibrium Exchange Conditions

Following administration, substrates of drug uptake transporters like OAT1 likely equilibrate rapidly across the plasma membrane of cells in which the transport proteins are expressed – in this case, RPT cells. Determination of *in vitro* kinetic parameters using cell-based assays, however, is generally conducted under zero-*trans* conditions where there is no drug in the cell prior to measuring substrate uptake. For the purpose of determining transport kinetic parameters for IVIVE and PBPK modeling, a more physiologically-relevant approach may be to conduct uptake experiments under equilibrium conditions, where drug concentration across the cell is at some equilibrium. Equilibrium exchange experiments have been used to study the kinetic and energetic mechanisms of membrane transport for a variety of inorganic and organic ion transport proteins (Stein, 1986). In these studies, the *in vitro* system (in our case CHO-OAT1 cells) is pre-loaded to steady-state with substrate prior to performing saturation kinetic experiments. To our knowledge, no one has examined transport kinetics for OAT1 under equilibrium conditions. What I found was that when uptake was conducted at room temperature, there was no difference in CL_{int} values when kinetics were conducted at initial-rate time points under *zero*-trans vs. equilibrium exchange conditions. It is important to note that the different buffers (WB vs. Kreb's) used for *zero*-trans vs. equilibrium exchange experiments could impact the comparison. The next condition that was evaluated was the effect on kinetics of increasing temperature of the *in vitro* incubation media from room temperature to 37°C (physiological). Under equilibrium exchange conditions, increasing temperature from 21°C to 37°C led to a 4-fold increase

in the J_{max} value for PAH transport. The Q_{10} effect is the measure of the sensitivity of a physiological process to an increase in temperature by 10°C, where for most physiological processes the reaction rate increases by 2- to 3-fold with every 10°C increase (Schmidt-Nielsen, 1997). The 4-fold increase in the J_{max} value observed here with a 16°C increase in temperature is consistent with the Q_{10} effect, and must be due to an increase in the number of translocation events per unit time, i.e., increase in OAT1 turnover number. Others have shown increased transport activity with increasing temperature (Xie et al., 2000, Bossi, et al., 2012). For example, Xie et al. (Xie et al., 2000) established the role of the dopamine transporter (DAT) in methamphetamine-induced neurotoxicity at higher temperatures compared to lower temperatures. Small physiological increases in temperature increases DAT-mediated accumulation of methamphetamine, and consequently, methamphetamine-induced neurotoxicity in rodents, whereas lower temperatures (hypothermia) ameliorate the toxicity.

While the effect of temperature on the J_{max} value can be explained from the Q_{10} effect, it is more difficult to explain why the K_m value was significantly higher at 37°C (2-fold). One issue to consider when using over-expressing heterologous transporters are the high rates of transport that are achieved, which may lead to unstirred water layers at the cell surface. Ultimately, as the rate of uptake transport increases at the cell surface the substrate concentration at the cell surface (i.e., ligand binding region of the transporter) decreases, which would lead to an apparent increase in the experimentally determined K_m value. Shibayama et al. has shown that there is a positive correlation between J_{max} and K_m values for tetraethylammonium transport by the organic cation transporter 2 (Shibayama et al., 2015). They also showed that rapid shaking during uptake

measurement leads to a subsequent reduction in the K_m value, suggesting that shaking can at least reduce the unstirred water-layer effect. Ultimately, unstirred water layers are a confounding factor for IVIVE of drug transport activity, and have to be considered when using *in vitro* data, IVIVE and PBPK modeling.

5.5 Perspectives

The question remains, what is the most appropriate *in vitro* condition to use for accurate mechanistic PBPK modeling for transporters. As this study shows, we have to consider incubation time for both perpetrators and victims, whether to conduct studies at initial zero-*trans* or equilibrium conditions, and the influence of temperature and unstirred water layers. Another big consideration is the energetics of the transport process itself. With respect to OAT1, it is an obligatory exchanger that uses the energy in the outwardly-directed α-KG gradient to mediate anionic drug uptake, and the α-KG gradient is maintained in part through the activity of Na^+-dicarboxylate co-transport activity (Pelis & Wright, 2011; Pritchard, 1995; Russel et al., 2002). Importantly, cultured cells used for *in vitro* transport studies in drug development lack endogenous expression of Na^+-dicarboxylate co-transporters. On-going studies in the lab are characterizing HEK cells that express only OAT1 (HEK-OAT1) vs. HEK cells that express OAT1 and NaDC3 (HEK-OAT1/NaDC3). I anticipate that expression of NaDC3 in HEK cells will lead to elevation in intracellular α-KG levels thus stimulating OAT1 turnover number (i.e., an increase in J_{max}). There is also the potential for protein-protein interactions between OAT1 and NaDC3 that could influence one another's kinetics. Once we have accurate

REF values for transporters like OAT1, for example by using LC-MS/MS, we can then use PBPK modeling to determine the most physiologically-relevant condition for prospective ('bottom-up') predictions of transporter involvement in PK based on *in vitro* data.

CHAPTER 6 CONCLUSION

In this study we conducted *in vitro* kinetic experiments with OAT1, a renal transporter important for PK and a site of DDIs. Experiments were conducted under two different conditions, initial zero-*trans* vs. equilibrium exchange. The data show that transport kinetics and inhibition potency are both influenced by the *in vitro* incubation time used. The effect of *in vitro* incubation time led to modest to large differences in PBPK predictions in the involvement of OAT1 in PK and DDIs. The data also suggest that during translocation OAT1 transitions from an extracellular- to intracellular-facing conformation, and depending on the conformation, the affinity of ligand binding may differ for some drugs. Future work in our laboratory is directed at determining the most physiologically-relevant *in vitro* conditions for better PBPK modeling of renal transporter involvement in PK and DDIs, and in using LC-MS/MS for quantifying renal transporter abundance for IVIVE of transporter activity.

REFERENCES

Aherne, G. W., Piall, E., Marks, V., Mould, G., & White, W. F. (1978). Prolongation and enhancement of serum methotrexate concentrations by probenecid. *British Medical Journal, 1*(6120), 1097-1099. 10.1136/bmj.1.6120.1097

Ahn, S. Y., & Bhatnagar, V. (2008). Update on the molecular physiology of organic anion transporters. *Current Opinion in Nephrology and Hypertension, 17*(5), 499-505. 10.1097/MNH.0b013e32830b5d5d [doi]

Ahn, S. Y., Eraly, S. A., Tsigelny, I., & Nigam, S. K. (2009). Interaction of organic cations with organic anion transporters. *The Journal of Biological Chemistry, 284*(45), 31422-31430. 10.1074/jbc.M109.024489 [doi]

Amundsen, R., Christensen, H., Zabihyan, B., & Asberg, A. (2010). Cyclosporine A, but not tacrolimus, shows relevant inhibition of organic anion-transporting protein 1B1-mediated transport of atorvastatin. *Drug Metabolism and Disposition, 38*(9), 1499-1504. 10.1124/dmd.110.032268

Aslamkhan, A., Han, Y., Walden, R., Sweet, D., & Pritchard, J. (2003). Stoichiometry of organic anion/dicarboxylate exchange in membrane vesicles from rat renal cortex and hOAT1-expressing cells. *American Journal of Physiology.Renal Physiology, 285*(4), F775-F783. 10.1152/ajprenal.00140.2003

Astorga, B., Wunz, T. M., Morales, M., Wright, S. H., & Pelis, R. M. (2011). Differences in the substrate binding regions of renal organic anion transporters 1 (OAT1) and 3 (OAT3). *American Journal of Physiology.Renal Physiology, 301*(2), F378-86. 10.1152/ajprenal.00735.2010 [doi]

Babu, E., Takeda, M., Narikawa, S., Kobayashi, Y., Enomoto, A., Tojo, A., Endou, H. (2002). Role of human organic anion transporter 4 in the transport of ochratoxin A. *Biochimica Et Biophysica Acta, 1590*(1-3), 64-75. S0167488902001878 [pii]

Badee, J., Achour, B., Rostami-Hodjegan, A., & Galetin, A. (2015). Meta-analysis of expression of hepatic organic anion-transporting polypeptide (OATP) transporters in cellular systems relative to human liver tissue. *Drug Metabolism and Disposition: The Biological Fate of Chemicals, 43*(4), 424-432. 10.1124/dmd.114.062034 [doi]

Balimane, P. V., Han, Y. H., & Chong, S. (2006). Current industrial practices of assessing permeability and P-glycoprotein interaction. *The AAPS Journal, 8*(1), E1-13. 10.1208/aapsj080101 [doi]

Bam, R., Yant, S., & Cihlar, T. (2014). Tenofovir alafenamide is not a substrate for renal organic anion transporters (OATs) and does not exhibit OAT-dependent cytotoxicity. *Antiviral Therapy, 19*(7), 687-692. 10.3851/IMP2770

Bickel, M., Khaykin, P., Stephan, C., Schmidt, K., Buettner, M., Amann, K., Jung, O. (2013). Acute kidney injury caused by tenofovir disoproxil fumarate and diclofenac co-administration. *HIV Medicine, 14*(10), 633-638. 10.1111/hiv.12072 [doi]

Bleasby, K., Castle, J. C., Roberts, C. J., Cheng, C., Bailey, W. J., Sina, J. F., Slatter, J. G. (2006). Expression profiles of 50 xenobiotic transporter genes in humans and pre-clinical species: A resource for investigations into drug disposition. *Xenobiotica, 36*(10-11), 963-988. 10.1080/00498250600861751

Breljak, D., Ljubojevic, M., Hagos, Y., Micek, V., Balen Eror, D., Vrhovac Madunic, I., Sabolic, I. (2016). Distribution of organic anion transporters NaDC3 and OAT1-3 along the human nephron. *American Journal of Physiology.Renal Physiology, 311*(1), F227-38. 10.1152/ajprenal.00113.2016 [doi]

Bossi, E., Cherubino, F., Margheritis, E., Oyadeyi, A. S., Vollero, A., & Peres, A. (2012). Temperature effects on the kinetic properties of the rabbit intestinal oligopeptide cotransporter PepT1. *Pflugers Archiv : European Journal of Physiology, 464*(2), 183-191. 10.1007/s00424-012-1125-8 [doi]

Brouwer, K. L., Aleksunes, L. M., Brandys, B., Giacoia, G. P., Knipp, G., Lukacova, V., Pediatric Transporter Working Group. (2015). Human ontogeny of drug transporters: Review and recommendations of the pediatric transporter working group. *Clinical Pharmacology and Therapeutics, 98*(3), 266-287. 10.1002/cpt.176 [doi]

Brouwer, K. L., Keppler, D., Hoffmaster, K. A., Bow, D. A., Cheng, Y., Lai, Y., International Transporter Consortium. (2013). In vitro methods to support transporter evaluation in drug discovery and development. *Clinical Pharmacology and Therapeutics, 94*(1), 95-112. 10.1038/clpt.2013.81 [doi]

Brown, C. D., Sayer, R., Windass, A. S., Haslam, I. S., De Broe, M. E., D'Haese, P. C., & Verhulst, A. (2008). Characterisation of human tubular cell monolayers as a model of proximal tubular xenobiotic handling. *Toxicology and Applied Pharmacology, 233*(3), 428-438. 10.1016/j.taap.2008.09.018 [doi]

Brzica, H., Breljak, D., Ljubojevic, M., Balen, D., Micek, V., Anzai, N., & Sabolic, I. (2009). Optimal methods of antigen retrieval for organic anion transporters in cryosections of the rat kidney. *Arhiv Za Higijenu Rada i Toksikologiju, 60*(1), 7-17. 10.2478/10004-1254-60-2009-1895 [doi]

Burckhardt, B. C., Wolff, N. A., & Burckhardt, G. (2000). Electrophysiologic characterization of an organic anion transporter cloned from winter flounder kidney (fROAT). *Journal of the American Society of Nephrology, 11*(1), 9-17.

Burckhardt, G., & Burckhardt, B. C. (2011). In vitro and in vivo evidence of the importance of organic anion transporters (OATs) in drug therapy. *Handbook of Experimental Pharmacology, (201):29-104. doi*(201), 29-104. 10.1007/978-3-642-14541-4_2 [doi]

Burckhardt, G. (2012). Drug transport by organic anion transporters (OATs). *Pharmacology & Therapeutics, 136*(1), 106-130. 10.1016/j.pharmthera.2012.07.010

Cesaro, S., Zhou, X., Manzardo, C., Buonfrate, D., Cusinato, R., Tridello, G., . . . Messina, C. (2005). Cidofovir for cytomegalovirus reactivation in pediatric patients after hematopoietic stem cell transplantation. *Journal of Clinical Virology : The Official Publication of the Pan American Society for Clinical Virology, 34*(2), 129-132. S1386-6532(05)00072-7 [pii]

Cha, S. H., Sekine, T., Fukushima, J. I., Kanai, Y., Kobayashi, Y., Goya, T., & Endou, H. (2001). Identification and characterization of human organic anion transporter 3 expressing predominantly in the kidney. *Molecular Pharmacology, 59*(5), 1277-1286.

Chatsudthipong, V., & Dantzler, W. H. (1991). PAH-alpha-KG countertransport stimulates PAH uptake and net secretion in isolated snake renal tubules. *The American Journal of Physiology, 261*(5 Pt 2), F858-67.

Chatsudthipong, V., & Dantzler, W. H. (1992). PAH/alpha-KG countertransport stimulates PAH uptake and net secretion in isolated rabbit renal tubules. *The American Journal of Physiology, 263*(3 Pt 2), F384-91.

Cheng, Y., Vapurcuyan, A., Shahidullah, M., Aleksunes, L., & Pelis, R. (2012). Expression of organic anion transporter 2 in the human kidney and its potential role in the tubular secretion of guanine-containing antiviral drugs. *Drug Metabolism and Disposition, 40*(3), 617-624. 10.1124/dmd.111.042036

Chioukh, R., Noel Hudson, M., Ribes, S., Fournier, N., Becquemont, L., & Verstuyft, C. (2014). Proton pump inhibitors inhibit methotrexate transport by renal basolateral organic anion transporter hOAT3. *Drug Metabolism and Disposition, 42*(12), 2041-2048. 10.1124/dmd.114.058529

Chu, X. Y., Bleasby, K., Yabut, J., Cai, X., Chan, G. H., Hafey, M. J., . . . Evers, R. (2007). Transport of the dipeptidyl peptidase-4 inhibitor sitagliptin by human organic anion transporter 3, organic anion transporting polypeptide 4C1, and multidrug resistance P-glycoprotein. *The Journal of Pharmacology and Experimental Therapeutics, 321*(2), 673-683. jpet.106.116517 [pii]

Colebatch, A., Marks, J., van der Heijde, D. M., & Edwards, C. (2012). Safety of nonsteroidal antiinflammatory drugs and/or paracetamol in people receiving

methotrexate for inflammatory arthritis: A cochrane systematic review. *Journal of Rheumatology.Supplement, 90*, 62-73. 10.3899/jrheum.120345

Cui, Y., Konig, J., Buchholz, J. K., Spring, H., Leier, I., & Keppler, D. (1999). Drug resistance and ATP-dependent conjugate transport mediated by the apical multidrug resistance protein, MRP2, permanently expressed in human and canine cells. *Molecular Pharmacology, 55*(5), 929-937.

Cummings, B. S., & Lash, L. H. (2000). Metabolism and toxicity of trichloroethylene and S-(1,2-dichlorovinyl)-L-cysteine in freshly isolated human proximal tubular cells. *Toxicological Sciences : An Official Journal of the Society of Toxicology, 53*(2), 458-466.

Denk, G. U., Soroka, C. J., Takeyama, Y., Chen, W. S., Schuetz, J. D., & Boyer, J. L. (2004). Multidrug resistance-associated protein 4 is up-regulated in liver but down-regulated in kidney in obstructive cholestasis in the rat. *Journal of Hepatology, 40*(4), 585-591. 10.1016/j.jhep.2003.12.001 [doi]

Diallinas, G. (2014). Understanding transporter specificity and the discrete appearance of channel-like gating domains in transporters. *Frontiers in Pharmacology, 5*, 207-207. 10.3389/fphar.2014.00207

Doyle, L. A., & Ross, D. (2003). Multidrug resistance mediated by the breast cancer resistance protein BCRP (ABCG2). *Oncogene, 22*(47), 7340-7358. 10.1038/sj.onc.1206938

Ekaratanawong, S., Anzai, N., Jutabha, P., Miyazaki, H., Noshiro, R., Takeda, M., Endou, H. (2004). Human organic anion transporter 4 is a renal apical organic anion/dicarboxylate exchanger in the proximal tubules. *Journal of Pharmacological Sciences, 94*(3), 297-304.

El-Sheikh, A. A. K., Greupink, R., Wortelboer, H., van den Heuvel, Jeroen J M W, Schreurs, M., Koenderink, J., . . . Russel, F. G. M. (2013). Interaction of immunosuppressive drugs with human organic anion transporter (OAT) 1 and OAT3, and multidrug resistance-associated protein (MRP) 2 and MRP4. *Translational Research, 162*(6), 398-409. 10.1016/j.trsl.2013.08.003

El-Sheikh, A. A., Masereeuw, R., & Russel, F. G. (2008). Mechanisms of renal anionic drug transport. *European Journal of Pharmacology, 585*(2-3), 245-255. 10.1016/j.ejphar.2008.02.085 [doi]

El-Sheikh, A. A., van den Heuvel, J. J., Koenderink, J. B., & Russel, F. G. (2007). Interaction of nonsteroidal anti-inflammatory drugs with multidrug resistance protein (MRP) 2/ABCC2- and MRP4/ABCC4-mediated methotrexate transport. *The Journal of Pharmacology and Experimental Therapeutics, 320*(1), 229-235. jpet.106.110379 [pii]

Enomoto, A., Takeda, M., Shimoda, M., Narikawa, S., Kobayashi, Y., Kobayashi, Y., Endou, H. (2002). Interaction of human organic anion transporters 2 and 4 with organic anion transport inhibitors. *The Journal of Pharmacology and Experimental Therapeutics, 301*(3), 797-802.

Eraly, S. A., Vallon, V., Vaughn, D. A., Gangoiti, J. A., Richter, K., Nagle, M., . . . Nigam, S. K. (2006). Decreased renal organic anion secretion and plasma accumulation of endogenous organic anions in OAT1 knock-out mice. *The Journal of Biological Chemistry, 281*(8), 5072-5083. M508050200 [pii]

European Medicines Agency (2012). Guideline on the investigation of drug interactions. (CPMP/EWP/560/95/Rev. 1 Corr. 2). *London: Committee for Human Medicinal Products* (CHMP).

Feng, B., Hurst, S., Lu, Y., Varma, M. V., Rotter, C. J., El-Kattan, A., Corrigan, B. (2013). Quantitative prediction of renal transporter-mediated clinical drug-drug interactions. *Molecular Pharmaceutics, 10*(11), 4207-4215. 10.1021/mp400295c [doi]

Feng, B., & Varma, M. (2016). Evaluation and quantitative prediction of renal transporter-mediated drug-drug interactions. *The Journal of Clinical Pharmacology, 56 Suppl 7*, S110-S121. 10.1002/jcph.702

Gallus, J., Juvale, K., & Wiese, M. (2014). Characterization of 3-methoxy flavones for their interaction with ABCG2 as suggested by ATPase activity. *Biochimica Et Biophysica Acta, 1838*(11), 2929-2938. 10.1016/j.bbamem.2014.08.003

George, B., You, D., Joy, M., & Aleksunes, L. (2017). Xenobiotic transporters and kidney injury. *Advanced Drug Delivery Reviews, 116*, 73-91. 10.1016/j.addr.2017.01.005

Gertz, M., Cartwright, C., Hobbs, M., Kenworthy, K., Rowland, M., Houston, J. B., & Galetin, A. (2013). Cyclosporine inhibition of hepatic and intestinal CYP3A4, uptake and efflux transporters: Application of PBPK modeling in the assessment of drug-drug interaction potential. *Pharmaceutical Research, 30*(3), 761-780. 10.1007/s11095-012-0918-y

Giessmann, T., May, K., Modess, C., Wegner, D., Hecker, U., Zschiesche, M., . . . Siegmund, W. (2004). Carbamazepine regulates intestinal P-glycoprotein and multidrug resistance protein MRP2 and influences disposition of talinolol in humans. *Clinical Pharmacology & Therapeutics, 76*(3), 192-200. 10.1016/j.clpt.2004.04.011

Ginsburg, H., & Ram, D. (1975). Zero-trans and equilibrium-exchange efflux and infinite-trans uptake of galactose by human erythrocytes. *Biochimica Et Biophysica Acta, 382*(3), 369-376. 10.1016/0005-2736(75)90278-3

Giri, N., Agarwal, S., Shaik, N., Pan, G., Chen, Y., & Elmquist, W. F. (2009). Substrate-dependent breast cancer resistance protein (Bcrp1/Abcg2)-mediated interactions: Consideration of multiple binding sites in in vitro assay design. *Drug Metabolism and Disposition: The Biological Fate of Chemicals, 37*(3), 560-570. 10.1124/dmd.108.022046 [doi]

Glavinas, H., Kis, E., Pal, A., Kovacs, R., Jani, M., Vagi, E., Krajcsi, P. (2007). ABCG2 (breast cancer resistance protein/mitoxantrone resistance-associated protein) ATPase assay: A useful tool to detect drug-transporter interactions. *Drug Metabolism and Disposition: The Biological Fate of Chemicals, 35*(9), 1533-1542. dmd.106.014605 [pii]

Glavinas, H., Mehn, D., Jani, M., Oosterhuis, B., Heredi-Szabo, K., & Krajcsi, P. (2008). Utilization of membrane vesicle preparations to study drug-ABC transporter interactions. *Expert Opinion on Drug Metabolism & Toxicology, 4*(6), 721-732. 10.1517/17425255.4.6.721 [doi]

Greiner, B., Eichelbaum, M., Fritz, P., Kreichgauer, H. P., von Richter, O., Zundler, J., & Kroemer, H. K. (1999). The role of intestinal P-glycoprotein in the interaction of digoxin and rifampin. *The Journal of Clinical Investigation, 104*(2), 147-153. 10.1172/JCI6663 [doi]

Hagos, Y., Stein, D., Ugele, B., Burckhardt, G., & Bahn, A. (2007). Human renal organic anion transporter 4 operates as an asymmetric urate transporter. *Journal of the American Society of Nephrology. JASN, 18*(2), 430-439. ASN.2006040415 [pii]

Hagos, Y., & Wolff, N. A. (2010). Assessment of the role of renal organic anion transporters in drug-induced nephrotoxicity. *Toxins, 2*(8), 2055-2082. 10.3390/toxins2082055 [doi]

Hasannejad, H., Takeda, M., Taki, K., Shin, H. J., Babu, E., Jutabha, P., .Endou, H. (2004). Interactions of human organic anion transporters with diuretics. *The Journal of Pharmacology and Experimental Therapeutics, 308*(3), 1021-1029. 10.1124/jpet.103.059139 [doi]

He, J., Yu, Y., Prasad, B., Chen, X., & Unadkat, J. D. (2014). Mechanism of an unusual, but clinically significant, digoxin-bupropion drug interaction. *Biopharmaceutics & Drug Disposition, 35*(5), 253-263. 10.1002/bdd.1890 [doi]

Henjakovic, M., Hagos, Y., Krick, W., Burckhardt, G., & Burckhardt, B. (2015). Human organic anion transporter 2 is distinct from organic anion transporters 1 and 3 with respect to transport function. *American Journal of Physiology.Renal Physiology, 309*(10), F843-F851. 10.1152/ajprenal.00140.2015

Herman, G. A., Stevens, C., Van Dyck, K., Bergman, A., Yi, B., De Smet, M., Wagner, J. A. (2005). Pharmacokinetics and pharmacodynamics of sitagliptin, an inhibitor of

dipeptidyl peptidase IV, in healthy subjects: Results from two randomized, double-blind, placebo-controlled studies with single oral doses. *Clinical Pharmacology and Therapeutics, 78*(6), 675-688. S0009-9236(05)00410-8 [pii]

Hilgendorf, C., Ahlin, G., Seithel, A., Artursson, P., Ungell, A. L., & Karlsson, J. (2007). Expression of thirty-six drug transporter genes in human intestine, liver, kidney, and organotypic cell lines. *Drug Metabolism and Disposition: The Biological Fate of Chemicals, 35*(8), 1333-1340. dmd.107.014902 [pii]

Hosoyamada, M., Sekine, T., Kanai, Y., & Endou, H. (1999). Molecular cloning and functional expression of a multispecific organic anion transporter from human kidney. *The American Journal of Physiology, 276*(1 Pt 2), F122-8.

Hotchkiss, A., Gao, T., Khan, U., Berrigan, L., Li, M., Ingraham, L., & Pelis, R. (2015). Organic anion transporter 1 is inhibited by multiple mechanisms and shows a transport mode independent of exchange. *Drug Metabolism and Disposition, 43*(12), 1847-1854. 10.1124/dmd.115.065748

Hsu, V., de L T Vieira, M., Zhao, P., Zhang, L., Zheng, J. H., Nordmark, A., Huang, S. M. (2014). Towards quantitation of the effects of renal impairment and probenecid inhibition on kidney uptake and efflux transporters, using physiologically based pharmacokinetic modelling and simulations. *Clinical Pharmacokinetics, 53*(3), 283-293. 10.1007/s40262-013-0117-y [doi]

Hulot, J., Villard, E., Maguy, A., Morel, V., Mir, L., Tostivint, I., Lechat, P. (2005). A mutation in the drug transporter gene ABCC2 associated with impaired methotrexate elimination. *Pharmacogenetics and Genomics, 15*(5), 277-285. 10.1097/01213011-200505000-00002

Huls, M., Brown, C. D. A., Windass, A. S., Sayer, R., van den Heuvel, J J M W, Heemskerk, S., Masereeuw, R. (2008). The breast cancer resistance protein transporter ABCG2 is expressed in the human kidney proximal tubule apical membrane. *Kidney International, 73*(2), 220-225. 10.1038/sj.ki.5002645

Ingraham, L., Li, M., Renfro, J. L., Parker, S., Vapurcuyan, A., Hanna, I., & Pelis, R. (2014). A plasma concentration of a-ketoglutarate influences the kinetic interaction of ligands with organic anion transporter 1. *Molecular Pharmacology, 86*(1), 86-95. 10.1124/mol.114.091777

Inotsume, N., Nishimura, M., Nakano, M., Fujiyama, S., & Sato, T. (1990). The inhibitory effect of probenecid on renal excretion of famotidine in young, healthy volunteers. *Journal of Clinical Pharmacology, 30*(1), 50-56.

Ito, K., Oleschuk, C. J., Westlake, C., Vasa, M. Z., Deeley, R. G., & Cole, S. P. (2001). Mutation of Trp1254 in the multispecific organic anion transporter, multidrug resistance protein 2 (MRP2) (ABCC2), alters substrate specificity and results in loss

of methotrexate transport activity. *Journal of Biological Chemistry, 276*(41), 38108-38114. 10.1074/jbc.M105160200

Ivanyuk, A., Livio, F., Biollaz, J., & Buclin, T. (2017). Renal drug transporters and drug interactions. *Clinical Pharmacokinetics, 56*(8), 825-892. 10.1007/s40262-017-0506-8 [doi]

Iwaki, M., Shimada, H., Irino, Y., Take, M., & Egashira, S. (2017). Inhibition of methotrexate uptake via organic anion transporters OAT1 and OAT3 by glucuronides of nonsteroidal anti-inflammatory drugs. *Biological & Pharmaceutical Bulletin, 40*(6), 926-931. 10.1248/bpb.b16-00970

Izzedine, H., Hulot, J. S., Villard, E., Goyenvalle, C., Dominguez, S., Ghosn, J., Deray, A. G. (2006). Association between ABCC2 gene haplotypes and tenofovir-induced proximal tubulopathy. *The Journal of Infectious Diseases, 194*(11), 1481-1491. JID36585 [pii]

Izzedine, H., Launay-Vacher, V., & Deray, G. (2005). Antiviral drug-induced nephrotoxicity. *American Journal of Kidney Diseases : The Official Journal of the National Kidney Foundation, 45*(5), 804-817. S0272638605002532 [pii]

Jadhav, P. R., Cook, J., Sinha, V., Zhao, P., Rostami-Hodjegan, A., Sahasrabudhe, V., Powell, J. R. (2015). A proposal for scientific framework enabling specific population drug dosing recommendations. *Journal of Clinical Pharmacology, 55*(10), 1073-1078. 10.1002/jcph.579 [doi]

Jani, M., Ambrus, C., Magnan, R., Jakab, K., Beéry, E., Zolnerciks, J., & Krajcsi, P. (2014). Structure and function of BCRP, a broad specificity transporter of xenobiotics and endobiotics. *Archives of Toxicology.Archiv Für Toxikologie, 88*(6), 1205-1248. 10.1007/s00204-014-1224-8

Jia, Y., Liu, Z., Wang, C., Meng, Q., Huo, X., Liu, Q., Liu, K. (2016). P-gp, MRP2 and OAT1/OAT3 mediate the drug-drug interaction between resveratrol and methotrexate. *Toxicology and Applied Pharmacology, 306*, 27-35. 10.1016/j.taap.2016.06.030

Jin, H., & Di, L. (2008). Permeability--in vitro assays for assessing drug transporter activity. *Current Drug Metabolism, 9*(9), 911-920.

Jones, H., Dickins, M., Youdim, K., Gosset, J., Attkins, N., Hay, T., Gardner, I. (2012). Application of PBPK modelling in drug discovery and development at pfizer. *Xenobiotica, 42*(1), 94-106. 10.3109/00498254.2011.627477

Jones, P., & George, A. (2014). A reciprocating twin-channel model for ABC transporters. *Quarterly Reviews of Biophysics, 47*(3), 189-220. 10.1017/S0033583514000031

Jutabha, P., Anzai, N., Kitamura, K., Taniguchi, A., Kaneko, S., Yan, K., . . . Sakurai, H. (2010). Human sodium phosphate transporter 4 (hNPT4/SLC17A3) as a common renal secretory pathway for drugs and urate. *The Journal of Biological Chemistry, 285*(45), 35123-35132. 10.1074/jbc.M110.121301 [doi]

Jutabha, P., Kanai, Y., Hosoyamada, M., Chairoungdua, A., Kim, D. K., Iribe, Y.,. Endou, H. (2003). Identification of a novel voltage-driven organic anion transporter present at apical membrane of renal proximal tubule. *The Journal of Biological Chemistry, 278*(30), 27930-27938. 10.1074/jbc.M303210200 [doi]

K, P. A., Meda, V. S., Kucherlapati, V. S., Dubala, A., M, D., P, R. A. V., B, S. (2012). Pharmacokinetic drug interaction between gemfibrozil and sitagliptin in healthy indian male volunteers. *European Journal of Clinical Pharmacology, 68*(5), 709-714. 10.1007/s00228-011-1177-2 [doi]

Kaler, G., Truong, D., Khandelwal, A., Nagle, M., Eraly, S., Swaan, P., & Nigam, S. (2007). Structural variation governs substrate specificity for organic anion transporter (OAT) homologs. potential remote sensing by OAT family members. *Journal of Biological Chemistry, 282*(33), 23841-23853. 10.1074/jbc.M703467200

Kaufhold, M., Schulz, K., Breljak, D., Gupta, S., Henjakovic, M., Krick, W., . . . Burckhardt, G. (2011). Differential interaction of dicarboxylates with human sodium-dicarboxylate cotransporter 3 and organic anion transporters 1 and 3. *American Journal of Physiology.Renal Physiology, 301*(5), F1026-34. 10.1152/ajprenal.00169.2011 [doi]

Keskitalo, J. E., Pasanen, M. K., Neuvonen, P. J., & Niemi, M. (2009). Different effects of the ABCG2 c.421C>A SNP on the pharmacokinetics of fluvastatin, pravastatin and simvastatin. *Pharmacogenomics, 10*(10), 1617-1624. 10.2217/pgs.09.85 [doi]

Kidron, H., Wissel, G., Manevski, N., Hakli, M., Ketola, R. A., Finel, M., . . . Urtti, A. (2012). Impact of probe compound in MRP2 vesicular transport assays. *European Journal of Pharmaceutical Sciences : Official Journal of the European Federation for Pharmaceutical Sciences, 46*(1-2), 100-105. 10.1016/j.ejps.2012.02.016 [doi]

Kimura, T., Perry, J., Anzai, N., Pritchard, J. B., & Moaddel, R. (2007). Development and characterization of immobilized human organic anion transporter-based liquid chromatographic stationary phase: HOAT1 and hOAT2. *Journal of Chromatography.B, 859*(2), 267-271. 10.1016/j.jchromb.2007.09.039

Kirby, B. J., Collier, A. C., Kharasch, E. D., Whittington, D., Thummel, K. E., & Unadkat, J. D. (2012). Complex drug interactions of the HIV protease inhibitors 3: Effect of simultaneous or staggered dosing of digoxin and ritonavir, nelfinavir, rifampin, or bupropion. *Drug Metabolism and Disposition: The Biological Fate of Chemicals, 40*(3), 610-616. 10.1124/dmd.111.042705 [doi]

Kis, O., Robillard, K., Chan, G. N., & Bendayan, R. (2010). The complexities of antiretroviral drug-drug interactions: Role of ABC and SLC transporters. *Trends in Pharmacological Sciences, 31*(1), 22-35. 10.1016/j.tips.2009.10.001 [doi]

Kobayashi, Y., Ohshiro, N., Sakai, R., Ohbayashi, M., Kohyama, N., & Yamamoto, T. (2005). Transport mechanism and substrate specificity of human organic anion transporter 2 (hOat2 [SLC22A7]). *Journal of Pharmacy and Pharmacology, 57*(5), 573-578. 10.1211/0022357055966

Konig, J., Muller, F., & Fromm, M. F. (2013). Transporters and drug-drug interactions: Important determinants of drug disposition and effects. *Pharmacological Reviews, 65*(3), 944-966. 10.1124/pr.113.007518 [doi]

Konig, J., Nies, A. T., Cui, Y., Leier, I., & Keppler, D. (1999). Conjugate export pumps of the multidrug resistance protein (MRP) family: Localization, substrate specificity, and MRP2-mediated drug resistance. *Biochimica Et Biophysica Acta, 1461*(2), 377-394. S0005-2736(99)00169-8 [pii]

Kremer, J. M., & Hamilton, R. A. (1995). The effects of nonsteroidal antiinflammatory drugs on methotrexate (MTX) pharmacokinetics: Impairment of renal clearance of MTX at weekly maintenance doses but not at 7.5 mg. *The Journal of Rheumatology, 22*(11), 2072-2077.

Kubinova, L., & Janacek, J. (2015). Confocal stereology: An efficient tool for measurement of microscopic structures. *Cell and Tissue Research, 360*(1), 13-28. 10.1007/s00441-015-2138-3 [doi]

Kuo, K., Zhu, H., McNamara, P., & Leggas, M. (2012). Localization and functional characterization of the rat Oatp4c1 transporter in an in vitro cell system and rat tissues. *PLoS One, 7*(6), e39641-e39641. 10.1371/journal.pone.0039641

Kwak, J., Lee, S., Lee, G., Kim, M., Ahn, Y., Lee, J., Lee, M. (2010). Selective inhibition of MDR1 (ABCB1) by HM30181 increases oral bioavailability and therapeutic efficacy of paclitaxel. *European Journal of Pharmacology, 627*(1-3), 92-98. 10.1016/j.ejphar.2009.11.008

Kyrklund, C., Backman, J., Neuvonen, M., & Neuvonen, P. (2003). Gemfibrozil increases plasma pravastatin concentrations and reduces pravastatin renal clearance. *Clinical Pharmacology & Therapeutics, 73*(6), 538-544. 10.1016/S0009-9236(03)00052-3

Lash, L. H., Putt, D. A., & Cai, H. (2006). Membrane transport function in primary cultures of human proximal tubular cells. *Toxicology, 228*(2-3), 200-218. S0300-483X(06)00547-6 [pii]

Leier, I., Hummel-Eisenbeiss, J., Cui, Y., & Keppler, D. (2000). ATP-dependent para-aminohippurate transport by apical multidrug resistance protein MRP2. *Kidney International, 57*(4), 1636-1642. S0085-2538(15)46912-1 [pii]

Lepist, E. I., & Ray, A. S. (2012). Renal drug-drug interactions: What we have learned and where we are going. *Expert Opinion on Drug Metabolism & Toxicology, 8*(4), 433-448. 10.1517/17425255.2012.667401 [doi]

Lepist, E. I., Zhang, X., Hao, J., Huang, J., Kosaka, A., Birkus, G., Ray, A. S. (2014). Contribution of the organic anion transporter OAT2 to the renal active tubular secretion of creatinine and mechanism for serum creatinine elevations caused by cobicistat. *Kidney International, 86*(2), 350-357. 10.1038/ki.2014.66 [doi]

Leuthold, S., Hagenbuch, B., Mohebbi, N., Wagner, C. A., Meier, P. J., & Stieger, B. (2009). Mechanisms of pH-gradient driven transport mediated by organic anion polypeptide transporters. *American Journal of Physiology.Cell Physiology, 296*(3), C570-82. 10.1152/ajpcell.00436.2008 [doi]

Lin, J. H., Los, L. E., Ulm, E. H., & Duggan, D. E. (1988). Kinetic studies on the competition between famotidine and cimetidine in rats. evidence of multiple renal secretory systems for organic cations. *Drug Metabolism and Disposition: The Biological Fate of Chemicals, 16*(1), 52-56.

Linton, K., & Higgins, C. (2007). Structure and function of ABC transporters: The ATP switch provides flexible control. *Pflügers Archiv - European Journal of Physiology, 453*(5), 555-567. 10.1007/s00424-006-0126-x

Ljubojevic, M., Balen, D., Breljak, D., Kusan, M., Anzai, N., Bahn, A., Sabolic, I. (2007). Renal expression of organic anion transporter OAT2 in rats and mice is regulated by sex hormones. *American Journal of Physiology.Renal Physiology, 292*(1), F361-72. 00207.2006 [pii]

Maeda, K., Tian, Y., Fujita, T., Ikeda, Y., Kumagai, Y., Kondo, T., Sugiyama, Y. (2014). Inhibitory effects of p-aminohippurate and probenecid on the renal clearance of adefovir and benzylpenicillin as probe drugs for organic anion transporter (OAT) 1 and OAT3 in humans. *European Journal of Pharmaceutical Sciences, 59*, 94-103. 10.1016/j.ejps.2014.04.004

Maliepaard, M., Scheffer, G. L., Faneyte, I. F., van Gastelen, M. A., Pijnenborg, A. C., Schinkel, A. H., Schellens, J. H. (2001). Subcellular localization and distribution of the breast cancer resistance protein transporter in normal human tissues. *Cancer Research, 61*(8), 3458-3464.

Mao, Q., & Unadkat, J. D. (2015). Role of the breast cancer resistance protein (BCRP/ABCG2) in drug transport--an update. *The AAPS Journal, 17*(1), 65-82. 10.1208/s12248-014-9668-6 [doi]

Marty, F., Winston, D., Rowley, S., Vance, E., Papanicolaou, G., Mullane, K., . . . Boeckh, M. (2013). CMX001 to prevent cytomegalovirus disease in hematopoietic-cell transplantation. *The New England Journal of Medicine, 369*(13), 1227-1236. 10.1056/NEJMoa1303688

Merino, G., Alvarez, A. I., Pulido, M. M., Molina, A. J., Schinkel, A. H., & Prieto, J. G. (2006). Breast cancer resistance protein (BCRP/ABCG2) transports fluoroquinolone antibiotics and affects their oral availability, pharmacokinetics, and milk secretion. *Drug Metabolism and Disposition: The Biological Fate of Chemicals, 34*(4), 690-695. dmd.105.008219 [pii]

Mikkaichi, T., Suzuki, T., Onogawa, T., Tanemoto, M., Mizutamari, H., Okada, M.,. . . Abe, T. (2004). Isolation and characterization of a digoxin transporter and its rat homologue expressed in the kidney. *Proceedings of the National Academy of Sciences of the United States of America, 101*(10), 3569-3574. 10.1073/pnas.0304987101

Miroševic Skvrce, N., Božina, N., Zibar, L., Barišic, I., Pejnovic, L., & Macolic Šarinic, V. (2013). CYP2C9 and ABCG2 polymorphisms as risk factors for developing adverse drug reactions in renal transplant patients taking fluvastatin: A case-control study. *Pharmacogenomics, 14*(12), 1419-1431. 10.2217/pgs.13.135

Mizuarai, S., Aozasa, N., & Kotani, H. (2004). Single nucleotide polymorphisms result in impaired membrane localization and reduced atpase activity in multidrug transporter ABCG2. *International Journal of Cancer, 109*(2), 238-246. 10.1002/ijc.11669

Moller, J. V., & Sheikh, M. I. (1982). Renal organic anion transport system: Pharmacological, physiological, and biochemical aspects. *Pharmacological Reviews, 34*(4), 315-358.

Morrissey, K. M., Stocker, S. L., Wittwer, M. B., Xu, L., & Giacomini, K. M. (2013). Renal transporters in drug development. *Annual Review of Pharmacology and Toxicology, 53*, 503-529. 10.1146/annurev-pharmtox-011112-140317 [doi]

Motohashi, H., Sakurai, Y., Saito, H., Masuda, S., Urakami, Y., Goto, M., Inui, K. (2002). Gene expression levels and immunolocalization of organic ion transporters in the human kidney. *Journal of the American Society of Nephrology : JASN, 13*(4), 866-874.

Muller, F., & Fromm, M. F. (2011). Transporter-mediated drug-drug interactions. *Pharmacogenomics, 12*(7), 1017-1037. 10.2217/pgs.11.44 [doi]

Nakagomi Hagihara, R., Nakai, D., & Tokui, T. (2007). Inhibition of human organic anion transporter 3 mediated pravastatin transport by gemfibrozil and the metabolites in humans. *Xenobiotica, 37*(4), 416-426. 10.1080/00498250601188808

Nakamura, K., Hirayama-Kurogi, M., Ito, S., Kuno, T., Yoneyama, T., Obuchi, W., Ohtsuki, S. (2016). Large-scale multiplex absolute protein quantification of drug-metabolizing enzymes and transporters in human intestine, liver, and kidney microsomes by SWATH-MS: Comparison with MRM/SRM and HR-MRM/PRM. *Proteomics, 16*(15-16), 2106-2117. 10.1002/pmic.201500433 [doi]

Nigam, S. K., Bush, K. T., Martovetsky, G., Ahn, S. Y., Liu, H. C., Richard, E., . . . Wu, W. (2015). The organic anion transporter (OAT) family: A systems biology perspective. *Physiological Reviews, 95*(1), 83-123. 10.1152/physrev.00025.2013 [doi]

Nozaki, Y., Kusuhara, H., Kondo, T., Hasegawa, M., Shiroyanagi, Y., Nakazawa, H., . . . Sugiyama, Y. (2007). Characterization of the uptake of organic anion transporter (OAT) 1 and OAT3 substrates by human kidney slices. *The Journal of Pharmacology and Experimental Therapeutics, 321*(1), 362-369. jpet.106.113076 [pii]

Nyengaard, J. R., Flyvbjerg, A., & Rasch, R. (1993). The impact of renal growth, regression and regrowth in experimental diabetes mellitus on number and size of proximal and distal tubular cells in the rat kidney. *Diabetologia, 36*(11), 1126-1131.

Ortiz, A., Justo, P., Sanz, A., Melero, R., Caramelo, C., Guerrero, M. F., . . . Egido, J. (2005). Tubular cell apoptosis and cidofovir-induced acute renal failure. *Antiviral Therapy, 10*(1), 185-190.

Otani, N., Ouchi, M., Hayashi, K., Jutabha, P., & Anzai, N. (2017). Roles of organic anion transporters (OATs) in renal proximal tubules and their localization. *Anatomical Science International, 92*(2), 200-206. 10.1007/s12565-016-0369-3 [doi]

Pelis, R. M., & Wright, S. H. (2011). Renal transport of organic anions and cations. *Comprehensive Physiology, 1*(4), 1795-1835. 10.1002/cphy.c100084 [doi]

Pelis, R. M., & Wright, S. H. (2014). SLC22, SLC44, and SLC47 transporters--organic anion and cation transporters: Molecular and cellular properties. *Current Topics in Membranes, 73*, 233-261. 10.1016/B978-0-12-800223-0.00006-2 [doi]

Perry, J., Dembla Rajpal, N., Hall, L., & Pritchard, J. (2006). A three-dimensional model of human organic anion transporter 1: Aromatic amino acids required for substrate transport. *Journal of Biological Chemistry, 281*(49), 38071-38079. 10.1074/jbc.M608834200

Poirier, A., Funk, C., Scherrmann, J., & Lavé, T. (2009). Mechanistic modeling of hepatic transport from cells to whole body: Application to napsagatran and fexofenadine. *Molecular Pharmaceutics, 6*(6), 1716-1733. 10.1021/mp8002495

Poirier, A., Portmann, R., Cascais, A. C., Bader, U., Walter, I., Ullah, M., & Funk, C. (2014). The need for human breast cancer resistance protein substrate and inhibition evaluation in drug discovery and development: Why, when, and how? *Drug Metabolism and Disposition: The Biological Fate of Chemicals, 42*(9), 1466-1477. 10.1124/dmd.114.058248 [doi]

Pollex, E., Anger, G., Hutson, J., Koren, G., & Piquette Miller, M. (2010). Breast cancer resistance protein (BCRP)-mediated glyburide transport: Effect of the C421A/Q141K BCRP single-nucleotide polymorphism. *Drug Metabolism and Disposition, 38*(5), 740-744. 10.1124/dmd.109.030791

Posada, M. M., Bacon, J. A., Schneck, K. B., Tirona, R. G., Kim, R. B., Higgins, J. W., Hillgren, K. M. (2015). Prediction of renal transporter mediated drug-drug interactions for pemetrexed using physiologically based pharmacokinetic modeling. *Drug Metabolism and Disposition: The Biological Fate of Chemicals, 43*(3), 325-334. 10.1124/dmd.114.059618 [doi]

Prajapati, R., & Sangamwar, A. T. (2014). Translocation mechanism of P-glycoprotein and conformational changes occurring at drug-binding site: Insights from multi-targeted molecular dynamics. *Biochimica Et Biophysica Acta, 1838*(11), 2882-2898. 10.1016/j.bbamem.2014.07.018 [doi]

Prescott, L. F., Freestone, S., & McAuslane, J. A. (1993). The concentration-dependent disposition of intravenous p-aminohippurate in subjects with normal and impaired renal function. *British Journal of Clinical Pharmacology, 35*(1), 20-29.

Pritchard, J. B. (1988). Coupled transport of p-aminohippurate by rat kidney basolateral membrane vesicles. *The American Journal of Physiology, 255*(4 Pt 2), F597-604.

Pritchard, J. B. (1995). Intracellular alpha-ketoglutarate controls the efficacy of renal organic anion transport. *The Journal of Pharmacology and Experimental Therapeutics, 274*(3), 1278-1284.

Pritchard, J. B., & Miller, D. S. (1993). Mechanisms mediating renal secretion of organic anions and cations. *Physiological Reviews, 73*(4), 765-796.

Rau, T., Erney, B., Göres, R., Eschenhagen, T., Beck, J., & Langer, T. (2006). High-dose methotrexate in pediatric acute lymphoblastic leukemia: Impact of ABCC2 polymorphisms on plasma concentrations. *Clinical Pharmacology & Therapeutics, 80*(5), 468-476. 10.1016/j.clpt.2006.08.012

Ray, A. S., Cihlar, T., Robinson, K. L., Tong, L., Vela, J. E., Fuller, M. D., Rhodes, G. R. (2006). Mechanism of active renal tubular efflux of tenofovir. *Antimicrobial Agents and Chemotherapy, 50*(10), 3297-3304. 50/10/3297 [pii]

Rizwan, A. N., & Burckhardt, G. (2007). Organic anion transporters of the SLC22 family: Biopharmaceutical, physiological, and pathological roles. *Pharmaceutical Research, 24*(3), 450-470. 10.1007/s11095-006-9181-4 [doi]

Robertson, E. E., & Rankin, G. O. (2006). Human renal organic anion transporters: Characteristics and contributions to drug and drug metabolite excretion. *Pharmacology & Therapeutics, 109*(3), 399-412. S0163-7258(05)00174-9 [pii]

Robey, R. W., Lin, B., Qiu, J., Chan, L. L., & Bates, S. E. (2011). Rapid detection of ABC transporter interaction: Potential utility in pharmacology. *Journal of Pharmacological and Toxicological Methods, 63*(3), 217-222. 10.1016/j.vascn.2010.11.003 [doi]

Rodgers, T., & Rowland, M. (2007). Mechanistic approaches to volume of distribution predictions: Understanding the processes. *Pharmaceutical Research, 24*(5), 918-933. 10.1007/s11095-006-9210-3

Rodriguez-Novoa, S., Labarga, P., Soriano, V., Egan, D., Albalater, M., Morello, J., . . . Owen, A. (2009). Predictors of kidney tubular dysfunction in HIV-infected patients treated with tenofovir: A pharmacogenetic study. *Clinical Infectious Diseases : An Official Publication of the Infectious Diseases Society of America, 48*(11), e108-16. 10.1086/598507 [doi]

Rostami-Hodjegan, A. (2012). Physiologically based pharmacokinetics joined with in vitro-in vivo extrapolation of ADME: A marriage under the arch of systems pharmacology. *Clinical Pharmacology and Therapeutics, 92*(1), 50-61. 10.1038/clpt.2012.65 [doi]

Rowland, M., Peck, C., & Tucker, G. (2011). Physiologically-based pharmacokinetics in drug development and regulatory science. *Annual Review of Pharmacology and Toxicology, 51*, 45-73. 10.1146/annurev-pharmtox-010510-100540 [doi]

Russel, F. G., Masereeuw, R., & van Aubel, R. A. (2002). Molecular aspects of renal anionic drug transport. *Annual Review of Physiology, 64*, 563-594. 10.1146/annurev.physiol.64.081501.155913 [doi]

Sager, J., Yu, J., Ragueneau Majlessi, I., & Isoherranen, N. (2015). Physiologically based pharmacokinetic (PBPK) modeling and simulation approaches: A systematic review of published models, applications, and model verification. *Drug Metabolism and Disposition, 43*(11), 1823-1837. 10.1124/dmd.115.065920

Santucci, R., Levêque, D., Lescoute, A., Kemmel, V., & Herbrecht, R. (2010). Delayed elimination of methotrexate associated with co-administration of proton pump inhibitors. *Anticancer Research, 30*(9), 3807-3810.

Sarkadi, B., Price, E. M., Boucher, R. C., Germann, U. A., & Scarborough, G. A. (1992). Expression of the human multidrug resistance cDNA in insect cells generates a high activity drug-stimulated membrane ATPase. *The Journal of Biological Chemistry, 267*(7), 4854-4858.

Sayama, H., Takubo, H., Komura, H., Kogayu, M., & Iwaki, M. (2014). Application of a physiologically based pharmacokinetic model informed by a top-down approach for the prediction of pharmacokinetics in chronic kidney disease patients. *The AAPS Journal, 16*(5), 1018-1028. 10.1208/s12248-014-9626-3 [doi]

Scheen, A. J. (2007). Drug-drug and food-drug pharmacokinetic interactions with new insulinotropic agents repaglinide and nateglinide. *Clinical Pharmacokinetics, 46*(2), 93-108. 4621 [pii]

Schmidt-Nielsen, K. (1997). Animal physiology: adaptation and environment. *Cambridge University Press, 4th ed.*

Schophuizen, C. M., Wilmer, M. J., Jansen, J., Gustavsson, L., Hilgendorf, C., Hoenderop, J. G., . . . Masereeuw, R. (2013). Cationic uremic toxins affect human renal proximal tubule cell functioning through interaction with the organic cation transporter. *Pflugers Archiv : European Journal of Physiology, 465*(12), 1701-1714. 10.1007/s00424-013-1307-z [doi]

Scotcher, D., Jones, C., Posada, M., Rostami-Hodjegan, A., & Galetin, A. (2016). Key to opening kidney for in vitro-in vivo extrapolation entrance in health and disease: Part I: In vitro systems and physiological data. *The AAPS Journal, 18*(5), 1067-1081. 10.1208/s12248-016-9942-x [doi]

Sekine, T., Watanabe, N., Hosoyamada, M., Kanai, Y., & Endou, H. (1997). Expression cloning and characterization of a novel multispecific organic anion transporter. *The Journal of Biological Chemistry, 272*(30), 18526-18529.

Shardlow, C. E., Generaux, G. T., Patel, A. H., Tai, G., Tran, T., & Bloomer, J. C. (2013). Impact of physiologically based pharmacokinetic modeling and simulation in drug development. *Drug Metabolism and Disposition: The Biological Fate of Chemicals, 41*(12), 1994-2003. 10.1124/dmd.113.052803 [doi]

Shen, H., Liu, T., Morse, B. L., Zhao, Y., Zhang, Y., Qiu, X., Lai, Y. (2015). Characterization of organic anion transporter 2 (SLC22A7): A highly efficient transporter for creatinine and species-dependent renal tubular expression. *Drug Metabolism and Disposition: The Biological Fate of Chemicals, 43*(7), 984-993. 10.1124/dmd.114.062364 [doi]

Shikano, N., Kanai, Y., Kawai, K., Ishikawa, N., & Endou, H. (2004). Transport of 99mTc-MAG3 via rat renal organic anion transporter 1. *Journal of Nuclear Medicine : Official Publication, Society of Nuclear Medicine, 45*(1), 80-85.

Shin, H. J., Lee, C. H., Park, S. J., Shin, J. G., & Song, I. S. (2010). Establishment and characterization of mardin-darby canine kidney cells stably expressing human organic anion transporters. *Archives of Pharmacal Research, 33*(5), 709-716. 10.1007/s12272-010-0510-0 [doi]

Shirasaka, Y., Onishi, Y., Sakurai, A., Nakagawa, H., Ishikawa, T., & Yamashita, S. (2006). Evaluation of human P-glycoprotein (MDR1/ABCB1) ATPase activity assay method by comparing with in vitro transport measurements: Michaelis-menten kinetic analysis to estimate the affinity of P-glycoprotein to drugs. *Biological & Pharmaceutical Bulletin, 29*(12), 2465-2471. JST.JSTAGE/bpb/29.2465 [pii]

Slot, A. J., Molinski, S. V., & Cole, S. P. (2011). Mammalian multidrug-resistance proteins (MRPs). *Essays in Biochemistry, 50*(1), 179-207. 10.1042/bse0500179 [doi]

Smeets, P. H., van Aubel, R. A., Wouterse, A. C., van den Heuvel, J. J., & Russel, F. G. (2004). Contribution of multidrug resistance protein 2 (MRP2/ABCC2) to the renal excretion of p-aminohippurate (PAH) and identification of MRP4 (ABCC4) as a novel PAH transporter. *Journal of the American Society of Nephrology : JASN, 15*(11), 2828-2835. 15/11/2828 [pii]

Smith, H. W., Finkelstein, N., Aliminosa, L., Crawford, B., & Graber, M. (1945). The renal clearances of substituted hippuric acid derivatives and other aromatic acids in dog and man. *Journal of Clinical Investigation, 24*(3), 388-404. 10.1172/JCI101618

Soars, M. G., Barton, P., Elkin, L. L., Mosure, K. W., Sproston, J. L., & Riley, R. J. (2014). Application of an in vitro OAT assay in drug design and optimization of renal clearance. *Xenobiotica; the Fate of Foreign Compounds in Biological Systems, 44*(7), 657-665. 10.3109/00498254.2013.879625 [doi]

Stein, W. D. (1986). Transport and diffusion across cell membranes. *Academic Press*. . . pp 704

Sweet, D. H., Chan, L. M., Walden, R., Yang, X. P., Miller, D. S., & Pritchard, J. B. (2003). Organic anion transporter 3 (Slc22a8) is a dicarboxylate exchanger indirectly coupled to the na+ gradient. *American Journal of Physiology.Renal Physiology, 284*(4), F763-9. 10.1152/ajprenal.00405.2002 [doi]

Tahara, H., Kusuhara, H., Endou, H., Koepsell, H., Imaoka, T., Fuse, E., & Sugiyama, Y. (2005). A species difference in the transport activities of H2 receptor antagonists by rat and human renal organic anion and cation transporters. *The Journal of Pharmacology and Experimental Therapeutics, 315*(1), 337-345. 10.1124/jpet.105.088104

Takahara, N., Saga, T., Inubushi, M., Kusuhara, H., Seki, C., Ito, S., Fujibayashi, Y. (2013). Drugs interacting with organic anion transporter-1 affect uptake of tc-99m-mercaptoacetyl-triglycine (MAG3) in the human kidney: Therapeutic drug

interaction in tc-99m-MAG3 diagnosis of renal function and possible application of tc-99m-MAG3 for drug development. *Nuclear Medicine and Biology, 40*(5), 643-650. 10.1016/j.nucmedbio.2013.03.006

Taylor, A., Siragy, H., & Nesbitt, S. (2011). Angiotensin receptor blockers: Pharmacology, efficacy, and safety. *Journal of Clinical Hypertension, 13*(9), 677-686. 10.1111/j.1751-7176.2011.00518.x

Te Brake, L. H., Russel, F. G., van den Heuvel, J. J., de Knegt, G. J., de Steenwinkel, J. E., Burger, D. M., Koenderink, J. B. (2016). Inhibitory potential of tuberculosis drugs on ATP-binding cassette drug transporters. *Tuberculosis (Edinburgh, Scotland), 96*, 150-157. 10.1016/j.tube.2015.08.004 [doi]

Tippin, T., Morrison, M., Brundage, T., & Momméja Marin, H. (2016). Brincidofovir is not A substrate for the human organic anion transporter 1 (Oat1): A mechanistic explanation for the lack of nephrotoxicity observed in clinical studies. *Therapeutic Drug Monitoring,* 10.1097/FTD.0000000000000353

Tirona, R. G. (2011). Molecular mechanisms of drug transporter regulation. *Handbook of Experimental Pharmacology, (201):373-402. doi*(201), 373-402. 10.1007/978-3-642-14541-4_10 [doi]

Toyohara, T., Suzuki, T., Morimoto, R., Akiyama, Y., Souma, T., Shiwaku, H., Abe, T. (2009). SLCO4C1 transporter eliminates uremic toxins and attenuates hypertension and renal inflammation. *Journal of the American Society of Nephrology, 20*(12), 2546-2555. 10.1681/ASN.2009070696

Tsamandouras, N., Rostami-Hodjegan, A., & Aarons, L. (2015). Combining the 'bottom up' and 'top down' approaches in pharmacokinetic modelling: Fitting PBPK models to observed clinical data. *British Journal of Clinical Pharmacology, 79*(1), 48-55. 10.1111/bcp.12234 [doi]

Tucker, Theodora G H A, Milne, A., Fournel Gigleux, S., Fenner, K., & Coughtrie, M. W. H. (2012). Absolute immunoquantification of the expression of ABC transporters P-glycoprotein, breast cancer resistance protein and multidrug resistance-associated protein 2 in human liver and duodenum. *Biochemical Pharmacology, 83*(2), 279-285. 10.1016/j.bcp.2011.10.017

Tweedie, D., Polli, J. W., Berglund, E. G., Huang, S. M., Zhang, L., Poirier, A., Feng, B. (2013). Transporter studies in drug development: Experience to date and follow-up on decision trees from the international transporter consortium. *Clinical Pharmacology & Therapeutics, 94*(1), 113-125. 10.1038/clpt.2013.77

Uchino, H., Tamai, I., Yamashita, K., Minemoto, Y., Sai, Y., Yabuuchi, H., Tsuji, A. (2000). p-aminohippuric acid transport at renal apical membrane mediated by human

inorganic phosphate transporter NPT1. *Biochemical and Biophysical Research Communications, 270*(1), 254-259. 10.1006/bbrc.2000.2407

US Food and Drug Administration (2017). In vitro metabolism- and transporter-mediated drug interaction studies—Guidance for industry. *Silver Spring: Center for Drug Evaluation and Research, Food and Drug Administration.*

Uwai, Y., Ida, H., Tsuji, Y., Katsura, T., & Inui, K. (2007). Renal transport of adefovir, cidofovir, and tenofovir by SLC22A family members (hOAT1, hOAT3, and hOCT2). *Pharmaceutical Research, 24*(4), 811-815. 10.1007/s11095-006-9196-x [doi]

Vallon, V., Eraly, S. A., Rao, S. R., Gerasimova, M., Rose, M., Nagle, M., . . . Rieg, T. (2012). A role for the organic anion transporter OAT3 in renal creatinine secretion in mice. *American Journal of Physiology.Renal Physiology, 302*(10), F1293-9. 10.1152/ajprenal.00013.2012 [doi]

Vallon, V., Rieg, T., Ahn, S. Y., Wu, W., Eraly, S. A., & Nigam, S. K. (2008). Overlapping in vitro and in vivo specificities of the organic anion transporters OAT1 and OAT3 for loop and thiazide diuretics. *American Journal of Physiology.Renal Physiology, 294*(4), F867-73. 10.1152/ajprenal.00528.2007 [doi]

van Aubel, R. A., Smeets, P. H., Peters, J. G., Bindels, R. J., & Russel, F. G. (2002). The MRP4/ABCC4 gene encodes a novel apical organic anion transporter in human kidney proximal tubules: Putative efflux pump for urinary cAMP and cGMP. *Journal of the American Society of Nephrology : JASN, 13*(3), 595-603.

van de Water, F. M., Masereeuw, R., & Russel, F. G. (2005). Function and regulation of multidrug resistance proteins (MRPs) in the renal elimination of organic anions. *Drug Metabolism Reviews, 37*(3), 443-471. N5630130Q6624P01 [pii]

van der Sandt, I. C., Blom-Roosemalen, M. C., de Boer, A. G., & Breimer, D. D. (2000). Specificity of doxorubicin versus rhodamine-123 in assessing P-glycoprotein functionality in the LLC-PK1, LLC-PK1:MDR1 and caco-2 cell lines. *European Journal of Pharmaceutical Sciences : Official Journal of the European Federation for Pharmaceutical Sciences, 11*(3), 207-214. S0928-0987(00)00097-X [pii]

Vanwert, A. L., Bailey, R. M., & Sweet, D. H. (2007). Organic anion transporter 3 (Oat3/Slc22a8) knockout mice exhibit altered clearance and distribution of penicillin G. *American Journal of Physiology.Renal Physiology, 293*(4), F1332-41. 00319.2007 [pii]

Vanwert, A. L., Srimaroeng, C., & Sweet, D. H. (2008). Organic anion transporter 3 (oat3/slc22a8) interacts with carboxyfluoroquinolones, and deletion increases systemic exposure to ciprofloxacin. *Molecular Pharmacology, 74*(1), 122-131. 10.1124/mol.107.042853 [doi]

VanWert, A. L., & Sweet, D. H. (2008). Impaired clearance of methotrexate in organic anion transporter 3 (Slc22a8) knockout mice: A gender specific impact of reduced folates. *Pharmaceutical Research, 25*(2), 453-462. 10.1007/s11095-007-9407-0 [doi]

Varma, M. V., Lai, Y., & El-Kattan, A. F. (2017). Molecular properties associated with transporter-mediated drug disposition. *Advanced Drug Delivery Reviews, 116*, 92-99. S0169-409X(17)30070-4 [pii]

Varma, M. V., Pang, K. S., Isoherranen, N., & Zhao, P. (2015). Dealing with the complex drug-drug interactions: Towards mechanistic models. *Biopharmaceutics & Drug Disposition, 36*(2), 71-92. 10.1002/bdd.1934 [doi]

Vinks, A. A. (2013). The future of physiologically based pharmacokinetic modeling to predict drug exposure in pregnant women. *CPT: Pharmacometrics & Systems Pharmacology, 2*, e33. 10.1038/psp.2013.9 [doi]

Volpe, D. A. (2011). Drug-permeability and transporter assays in caco-2 and MDCK cell lines. *Future Medicinal Chemistry, 3*(16), 2063-2077. 10.4155/fmc.11.149 [doi]

Volpe, D. A. (2016). Transporter assays as useful in vitro tools in drug discovery and development. *Expert Opinion on Drug Discovery, 11*(1), 91-103. 10.1517/17460441.2016.1101064 [doi]

Vormfelde, S., Schirmer, M., Hagos, Y., Toliat, M., Engelhardt, S., Meineke, I., Brockmöller, J. (2006). Torsemide renal clearance and genetic variation in luminal and basolateral organic anion transporters. *British Journal of Clinical Pharmacology, 62*(3), 323-335. 10.1111/j.1365-2125.2006.02655.x

Wagner, C., Zhao, P., Pan, Y., Hsu, V., Grillo, J., Huang, S. M., & Sinha, V. (2015). Application of physiologically based pharmacokinetic (PBPK) modeling to support dose selection: Report of an FDA public workshop on PBPK. *CPT: Pharmacometrics & Systems Pharmacology, 4*(4), 226-230. 10.1002/psp4.33 [doi]

Watanabe, T., Maeda, K., Kondo, T., Nakayama, H., Horita, S., Kusuhara, H., & Sugiyama, Y. (2009). Prediction of the hepatic and renal clearance of transporter substrates in rats using in vitro uptake experiments. *Drug Metabolism and Disposition, 37*(7), 1471-1479. 10.1124/dmd.108.026062

Weibel, E. R. (1981). Stereological methods in cell biology: Where are we-- where are we going? *The Journal of Histochemistry and Cytochemistry, 29*(9), 1043-1052. 10.1177/29.9.7026667

Wilmer, M. J., Saleem, M. A., Masereeuw, R., Ni, L., van der Velden, T. J., Russel, F. G., Levtchenko, E. N. (2010). Novel conditionally immortalized human proximal

tubule cell line expressing functional influx and efflux transporters. *Cell and Tissue Research, 339*(2), 449-457. 10.1007/s00441-009-0882-y [doi]

Wright, S. H., & Dantzler, W. H. (2004). Molecular and cellular physiology of renal organic cation and anion transport. *Physiological Reviews, 84*(3), 987-1049. 10.1152/physrev.00040.2003 [doi]

Xia, C. Q., Milton, M. N., & Gan, L. S. (2007). Evaluation of drug-transporter interactions using in vitro and in vivo models. *Current Drug Metabolism, 8*(4), 341-363.

Xie, T., McCann, U. D., Kim, S., Yuan, J., & Ricaurte, G. A. (2000). Effect of temperature on dopamine transporter function and intracellular accumulation of methamphetamine: Implications for methamphetamine-induced dopaminergic neurotoxicity. *The Journal of Neuroscience, 20*(20), 7838-7845.

Yamaguchi, H., Sugie, M., Okada, M., Mikkaichi, T., Toyohara, T., Abe, T., Mano, N. (2010). Transport of estrone 3-sulfate mediated by organic anion transporter OATP4C1: Estrone 3-sulfate binds to the different recognition site for digoxin in OATP4C1. *DRUG METABOLISM AND PHARMACOKINETICS, 25*(3), 314-317. 10.2133/dmpk.25.314

You, G. (2008). Membrane transporters in drug disposition. *Pharmaceutical Research, 25*(2), 441-443. 10.1007/s11095-007-9437-7 [doi]

Yusuf, U., Hale, G. A., Carr, J., Gu, Z., Benaim, E., Woodard, P., Hayden, R. T. (2006). Cidofovir for the treatment of adenoviral infection in pediatric hematopoietic stem cell transplant patients. *Transplantation, 81*(10), 1398-1404. 10.1097/01.tp.0000209195.95115.8e [doi]

Zamek Gliszczynski, M. J., Lee, C. A., Poirier, A., Bentz, J., Chu, X., Ellens, H.,. Galetin, A. (2013). ITC recommendations for transporter kinetic parameter estimation and translational modeling of transport-mediated PK and DDIs in humans. *Clinical Pharmacology & Therapeutics, 94*(1), 64-79. 10.1038/clpt.2013.45

Zelcer, N., Huisman, M., Reid, G., Wielinga, P., Breedveld, P., Kuil, A., Borst, P. (2003). Evidence for two interacting ligand binding sites in human multidrug resistance protein 2 (ATP binding cassette C2). *Journal of Biological Chemistry, 278*(26), 23538-23544. 10.1074/jbc.M303504200

Zhang, X., Groves, C. E., Bahn, A., Barendt, W. M., Prado, M. D., Rodiger, M., Wright, S. H. (2004). Relative contribution of OAT and OCT transporters to organic electrolyte transport in rabbit proximal tubule. *American Journal of Physiology.Renal Physiology, 287*(5), F999-1010. 10.1152/ajprenal.00156.2004 [doi]

Zhao, P., Zhang, L., Grillo, J. A., Liu, Q., Bullock, J. M., Moon, Y. J., Huang, S. (2011). Applications of physiologically based pharmacokinetic (PBPK) modeling and simulation during regulatory review. *Clinical Pharmacology & Therapeutics, 89*(2), 259-267. 10.1038/clpt.2010.298